(NASA-CR-169856) INVESTIGATION OF SEMICONDUCTOR CLAD OPTICAL WAVEGUIDES Annual Status Report, 31 Jul. 1981 - 1 Aug. 1982 (Virginia Univ.) 76 p HC A05/MF A01 CSCL 20F G3/74

N83-18484

Unclas 02726

Annual Status Report

NASA Grant No. NAG-1-177-02

Investigation of Semiconductor Clad Optical Waveguides

Submitted to:

National Aeronautics and Space Administration
Langley Research Center
Hampton, Virginia 23665

Submitted by:

T.E. Batchman
Associate Professor

G.M. McWright
Graduate Student Participant

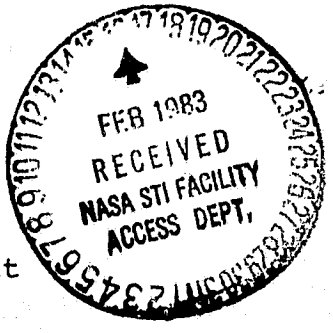

Report No. UVA/528207/EE82/
Report Period: 7/31/81 to 8/1/82

Table of Contents

I. Introduction

Integrated optical device technology is still relatively undeveloped after more than a decade of research. No common substrate or waveguide material has emerged as being a superior device fabrication candidate such as silicon did in the integrated circuit industry. There are a number of research programs attempting to fabricate integrated optical devices on GaAs since this is an ideal material on which to grow laser diodes which operate in the near infrared region of the spectrum. Another common technology uses the class of electro-optic materials such as lithium niobate. While these materials are not restricted in their use to only infrared wavelengths, they do not provide a useful substrate for fabricating lasers.

The third class of substrate and waveguide materials is various types of glass. This has been used because it is relatively easy to fabricate waveguides on glass substrates by a technique known as ion exchange. While it is conceptually possible to construct LED pumped lasers in glass (Nd:glass), it has yet to receive much attention from the research community [1]. This study makes extensive use of glass waveguides because of the ease and economy of fabricating devices in glass. It should be realized that although all calculations in this research program are based on the assumption of a glass guide and substrate, the effects being studied will occur on either of the other materials if the proper refractive indices are used in the calculations.

This study has been based on investigating the effects of a lossy cladding material on a lossless planar dielectric waveguide. The relative permittivity of a lossy material is given by

$$\hat{\varepsilon}_r = \varepsilon_r' - j\varepsilon_r'' = \varepsilon_r' - j\frac{\sigma}{\omega\varepsilon_0} \tag{1}$$

where σ is the conductivity of the material at the frequency of interest (ω). In this study the lossy material is a semiconductor since the properties of such materials can be changed by doping, electric fields and incident photons. Refractive index and permittivity are related through the following equation.

$$\hat{n} = \hat{\varepsilon}_r^{1/2} = n_0 - jk \tag{2}$$

where n_0 and k are the real and imaginary parts of the refractive index, respectively.

Of particular interest in this study is the absorption coefficient, α, which may be related to the imaginary portion of the refractive index by the expression $\alpha = \frac{2\omega k}{c}$. Detailed classical and quantum mechanical analyses of the absorption of energy in semiconductors have been covered by several authors [2, 3, 4]. Section II of this report will review some of the more important concepts of the changes in the absorption coefficient α, (and thus complex permittivity) due to the incident radiation.

Much of the background investigation and computer predictions for using semiconductor clad waveguides as modulators and switches is summarized in Section III. Section IV explains the

oscillatory effect previously observed in terms of a periodic coupling between the guided modes of the dielectric waveguide and the lossy modes of the semiconductor cladding. Frequency filtering properties of silicon-clad waveguides are also examined.

The experimental investigation of the predicted modulation and filtering effects are described in Section V. Due to the problems with fluorescence in the waveguides an analysis of the cause of such light emission was undertaken and new substrate materials were selected for waveguide fabrication.

II. Complex Permittivity Near the Band Edge

Two main properties of semiconductors near the absorption band edge have been investigated in this study; electro-absorption and optical propagation near the band edge. Both of these properties are of interest for development of optical modulators for optical waveguides. Figure 1 shows a typical absorption characteristic for amorphous and crystalline silicon. Since both amorphous and single crystal silicon samples are being used in this study, it should be noted that the band edge does not change significantly with the crystalline structure nor does the relative change in absorption coefficient magnitude.

The electro-absorption effect is based on the ability to control the absorption band edge by application of an electric field of sufficient strength to the semiconductor. This is often known as the Franz-Keldysh effect [5] and is given by an equation of the form

$$\alpha_F = \frac{CE}{E_g - h\nu} \exp\left(-\frac{D(E_g - h\nu)^{3/2}}{E}\right) \qquad (3)$$

where E is the electric field strength, E_g is the gap energy and C and D are material constants. This equation applies for $h\nu < E_g$ in direct semiconductors and basically predicts the presence of an exponential tail on the absorption curve as shown in Figure 2. This effect has been observed in a number of semiconductors including silicon and GaAs and the observed changes in absorption agree well with calculated values on the long-wave side.

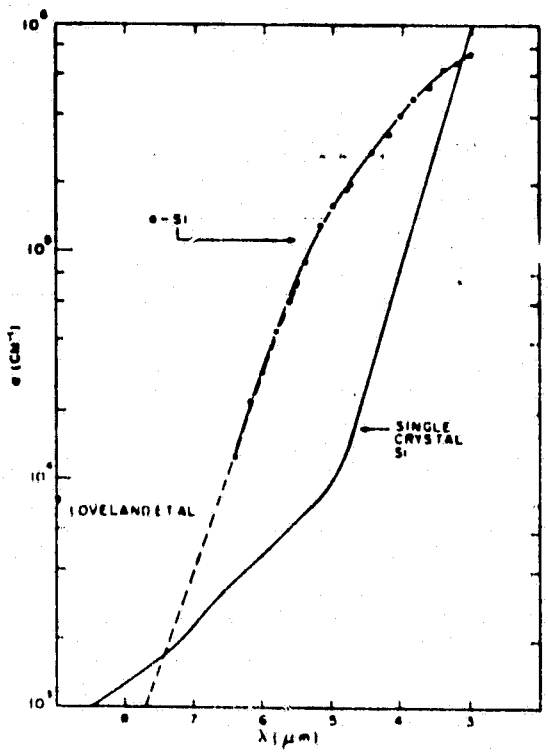

Figure 1. The optical absorption coefficient as a function of wavelength for a-Si and single crystal Si. (From (34))

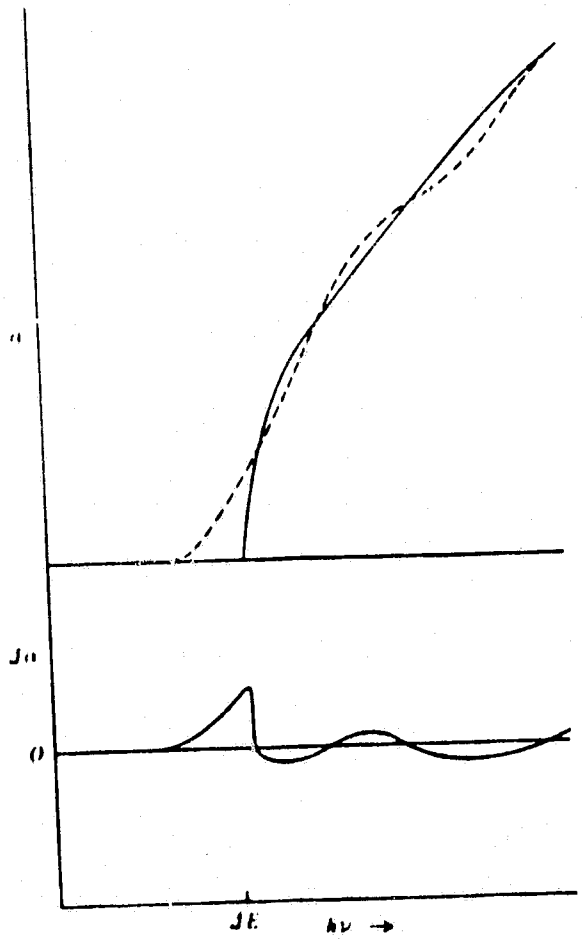

Figure 2. Effect of electric field on absorption near fundamental edge due to direct transition. The broken curve shows absorption coefficient with field on. The lower graph shows the difference ($\Delta\alpha$) between the field-on and the field-off absorption coefficients. (From (5))

The primary prediction of the Franz-Keldysh theory, that the optical absorption edge will broaden and shift toward lower energy in an electric field has been experimentally verified (9); the magnitude of the effect is only appreciable in direct band gap materials, and thus application has been limited primarily to GaAs and GaAs related compounds. For example, an intensity modulator using GaAlAs double heterostructures has been fabricated with band edges close to the light to be modulated [10]. With 8v applied across the active region, (0.4 μm thick) it is possible to obtain fields close to breakdown (300,000 V/cm). The change in absorption for the modulator was two orders of magnitude for only 8v applied.

An electro-absorption detector has also been demonstrated using reverse-biased pn junction double heterostructures [10]. Without an applied field, the semiconductor has a band gap of 0.84 μm; however, light of wavelength 1.06 μm was guided in the heterostructure and subsequently detected with only 16v reverse bias applied.

The second effect of interest in this study also considers propagation of a wave in the dielectric guide near the band gap of the semiconductor cladding. In this case it is assumed that no electric field is applied to the semiconductor, but that the semiconductor is illuminated by photons with energy sufficiently above the band gap to produce electron-hole pairs (although, perhaps, an applied electric field may enhance the photon-induced change in the optical conductivity).

A brief review of the absorption processes in semiconductors will be presented in this section following the analysis of Omar [2]. His discussion will then be extended to include the case of photon-induced changes in the absorption coefficient. Two different absorption processes may be distinguished. They are

1) free carrier (a classical analysis, with $\nu \leq E_g/h$)
2) fundamental (a quantum-mechanical analysis, with $\nu \geq Eg/h$) where ν is the frequency of light, E_g is the semiconductor band gap energy, and h is Planck's constant.

The region at the band gap edge ($\nu \approx Eg/h$) is of particular interest in this study; unfortunately, the exact shape of the band tailing has not been accurately determined, and original calculations are presented here.

Free carrier absorption, in which electrons and holes absorb radiation without becoming excited to another band, has been treated using the Drude theory. The real and imaginary parts of the dielectric constant are

$$\varepsilon_r' = \varepsilon_{L,r} - \frac{\sigma_0 \tau}{\varepsilon_0 (1+\omega^2\tau^2)} = n_0^2 - k^2$$

$$\varepsilon_r'' = \frac{\sigma_0}{\varepsilon_0 \omega (1+\omega^2\tau^2)} = 2n_0 k$$

where

ε_0 is the free-space permittivity,

ω is the angular frequency of the propagating wave,

τ is the collision time between electrons in the semiconductors,

σ_0 is the familiar dc conductivity, and

$\varepsilon_{L,r}$ is the relative permittivity of the ion core.

Lee et al [4] and Gibson [11] have considered the case of infrared or microwave signal ($\nu < Eg/h$) propagation and modulation using free-carrier generation in semiconductors. When an incident light beam with energy greater than the band gap impinges upon a semiconductor, the dc conductivity may be changed by the creation of a number of electron-hole pairs $\Delta n = \Delta p$ such that

$$\sigma_0' = \sigma_0 + e\Delta n(\mu_e + \mu_n) = \sigma_0 + \Delta\sigma_0$$

where μ_e and μ_n are the electron and hole mobilities, respectively. The relevant equations for signal propagation below the band gap (with electron-hole pair generation via a second beam) become

$$\varepsilon_r' = \varepsilon_{L,\nu} - \frac{\sigma_0\tau}{\varepsilon_0(1+\omega^2\tau^2)} + \frac{\Delta\sigma_0\tau}{\varepsilon_0(1+\omega^2\tau^2)}$$

$$\varepsilon_r'' = \frac{\sigma_0}{\varepsilon_0\omega(1+\omega^2\tau^2)} + \frac{\Delta\sigma_0}{\varepsilon_0\omega(1+\omega^2\tau^2)}$$

and the real and imaginary parts of the permittivity are thus changed. Note that $\tau \approx 10^{-13}$ sec and the majority of the permittivity shift appears in the imaginary portion. This study has focused upon semiconductor-clad waveguides and, in particular,

silicon-clad structures. For signal propagation slightly below the silicon band gap edge ($\lambda = 1.15\ \mu m$), the free-carrier contribution to the imaginary portion of the permittivity is

$$\varepsilon_r'' = \frac{\sigma_0}{\varepsilon_0 \omega (1+\omega^2\tau^2)} = \frac{ne^2\tau}{\omega\varepsilon_0 m^* (1+\omega^2\tau^2)} = 1.46 \times 10^{-12}$$

where

n is the electron density and m* is the effective mass of the electron.

Values used in the above calculation are from Lee et al [4]. The above calculated Drude theory value compares to the experimentally measured value by Pierce and Spicer [21] of 0.4; the twelve orders of magnitude difference indicates that the free-carrier contribution to the imaginary part of the permittivity is negligible at frequencies near the band gap edge; we calculate, however, the necessary incident laser ($\lambda = 0.5\ \mu m$) power density required to generate enough electron-hole pairs to change the imaginary portion of the permittivity from 0.4 to 1.0. The resultant power density is [1.95 W/(10 μm x 10 μm)], which is feasible with the currently available experimental arrangement.

In fundamental absorption, the electron absorbs a photon (from the incident beam) and jumps from the valence to the conduction band. Using quantum perturbation theory, one finds that the absorption coefficient for direct band gap semiconductors (GaAs) is (aside from the additional contributions from multi-photon absorption, free carrier absorption, and intraband transistions)

$$\alpha_d = A(h\nu - Eg)^{1/2}, \quad h\nu > Eg$$

where A is a constant involving the properties of the bands [12]

In indirect band gap transistions (Si, Ge), the absorption coefficient is

$$\alpha_i = A'(T)(h\nu - Eg)^2, \quad h\nu > Eg$$

where A'(T) is a constant pertaining to the bands and temperature

Again, we neglect contributions from multi-photon absorption, free-carrier absorption, and intraband transistions.

We have calculated, above, using the classical Drude theory, the power density required to change the imaginary portion of the permittivity from 0.4 to 1.0. This analysis, however, may not be precisely correct for propagation near the band gap edge. Using a quantum mechanical approach, several authors have calculated the influence of injected carriers on the absorption coefficient [13, 14]; their results indicate that the required power density may not be nearly as high as that calculated using the Drude theory [1.95 W/(10 μm x 10 μm)]. It should be noted that the quantum mechanical analysis has been performed only on a direct band gap semiconductor (GaAs) and signal propagation must be near the band gap edge to achieve sufficient change in the absorption coefficient with injected carrier density (Fig. 3). For frequencies sufficiently above the band gap edge, the absorption coefficient is very nearly independent of injected carrier density.

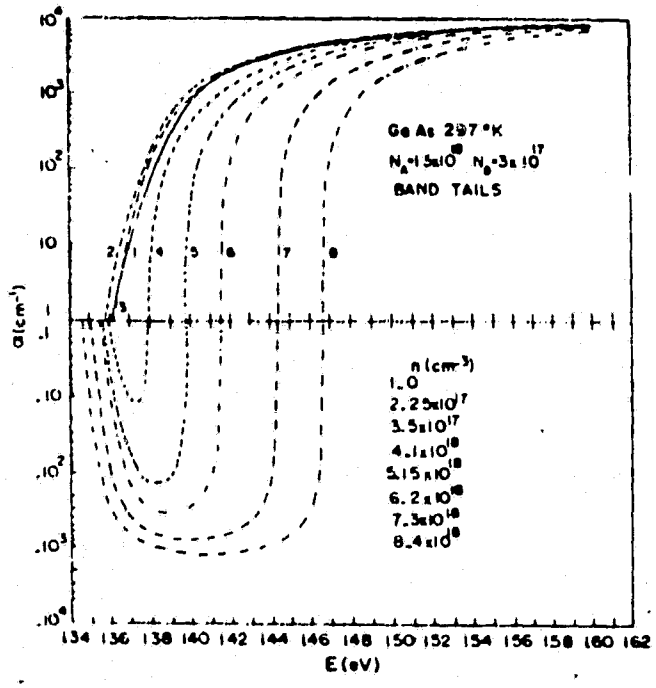

Figure 3. Absorption coefficient vs. photon energy as calculated by using a band tail model for different injected carrier densities in the range n:0 - 4 x 10^{18}cm^{-3}. (From (13))

III. Semiconductor-Clad Dielectric Waveguides: Summary of Previous Research

In this research, a planar waveguide configuration has been used for all computer modeling and fabrication. The four-layer planar waveguide structure under consideration is shown in Figure 4 where the guided light is propagating in the z-direction in the dielectric (N_3), and it is assumed there is no variation in the y-direction. All materials are lossless except for the semiconductor (N_2). The dispersion relations for this structure are well known, and two methods of solution for the complex mode propagation constant ($\alpha + j\beta$) have been described previously [15, 16].

The waveguide consists of a semi-infinite glass substrate, a dielectric core of thickness 1 μm, a semiconductor cladding varying from 0.01 to 10 μm in thickness, and a semi-infinite layer of air. A free-space wavelength of 632.8 nm was assumed, unless otherwise stated, and all material parameters shown in Figure 3 are for this wavelength. The three most common semiconductors, silicon, gallium arsenide, and germanium, were used as the cladding layer, and relative permittivity values are summarized in Table 1. Bulk values have been used where data were not available for thin films. The refractive index of thin amorphous semiconductor films will depend on the method of deposition and any impurities deliberately or accidentally added to the semiconductor [17].

Table I

Semiconductor Parameters at λ = 632.8 nm

Material	Relative Permittivity ε_r'	ε_r''	Refractive Index n	k
Silicon*	16.76	1.75	4.1	0.213
Gallium Arsenide	14.3	1.21	3.79	0.16
Germanium*	14.43	19.54	4.4	2.22

*values for amorphous thin films

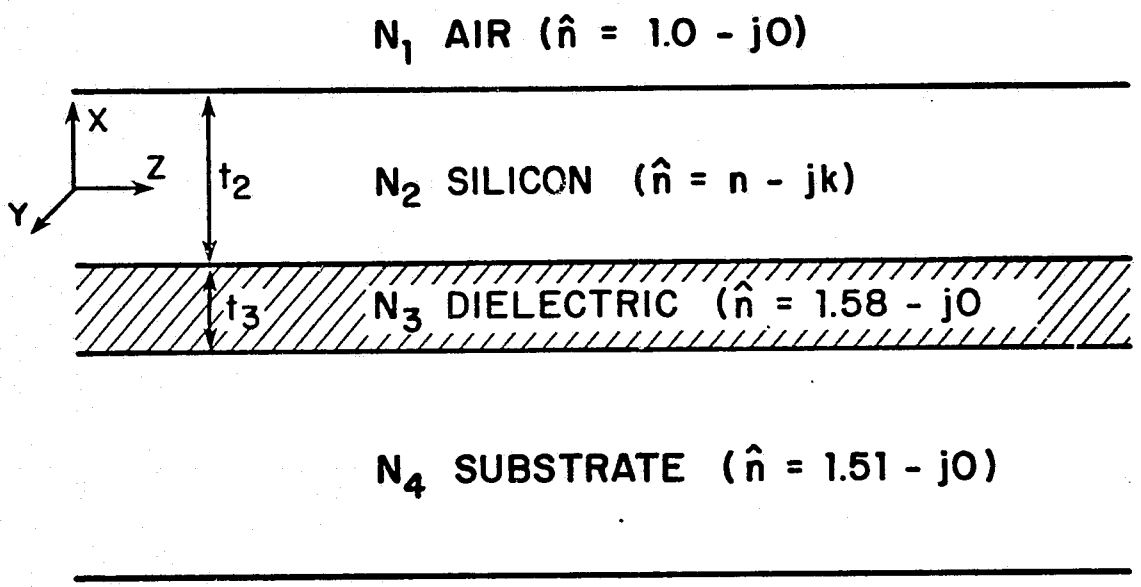

Figure 4. Four-layer planar waveguide structure.

Silicon was selected as the first semiconductor cladding material to be investigated, and the attenuation and phase constant curves of Figures 5 and 6 were generated by varying the cladding thickness from 0.01 to 10 μm. (The phase constant β has been normalized by $k_0 = 2\pi/\lambda_0$ so that all curves show the mode index.) All other parameters were held constant in these calculations and results were confirmed by using both computer solution techniques [15], [16]. It was initially expected that decreasing the lossy cladding thickness to 0.01 μm would reduce the attenuation to zero in a well-behaved manner; however, the results were not as expected below a silicon thickness of 1.0 μm. The curves are similar to exponentially damped sinusoids, with extreme values of the mode index (β/k_0) curves corresponding to the median values (maximum slope) in the attenuation (α) curves. Extreme values of the α curve correspond to median values in the β/k_0 curves and the oscillations in both curves approach the median value at 1.0 μm.

Gallium arsenide, which has a complex permittivity that is nearly the same as silicon, was used for the next series of calculations. The attenuation and phase characteristics were almost identical to those of silicon, and varying the dielectric waveguide thickness t_3 to 0.8 μm had little effect on the characteristics.

Before beginning work on this grant, it was noted that the attenuation and mode index are significantly altered by conductivity changes in the semiconductor cladding [18], [19]. The calculated percentage change in attenuation and relative

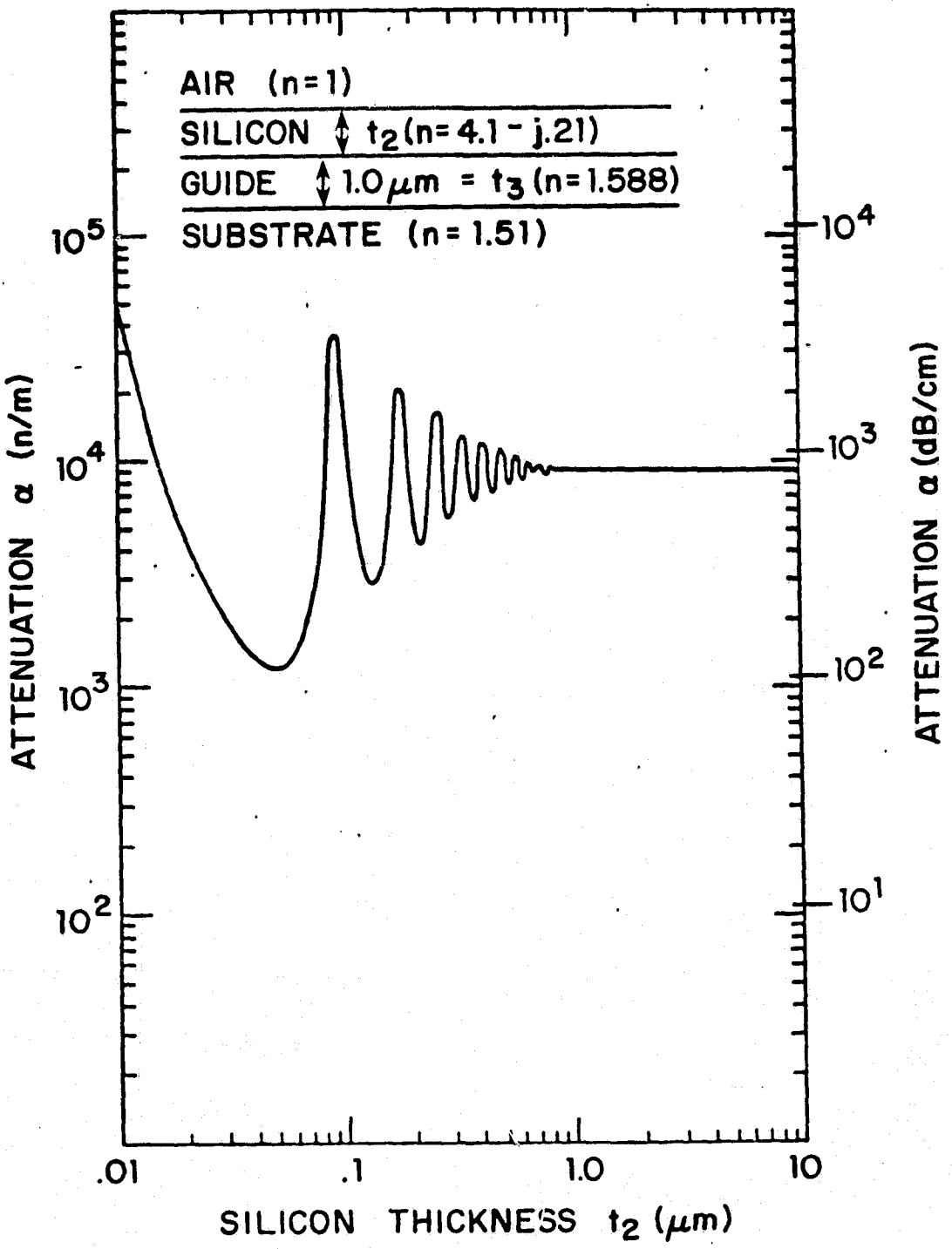

Figure 5. Attenuation characteristics of silicon-clad waveguide (TE_0 mode, normal conductivity).

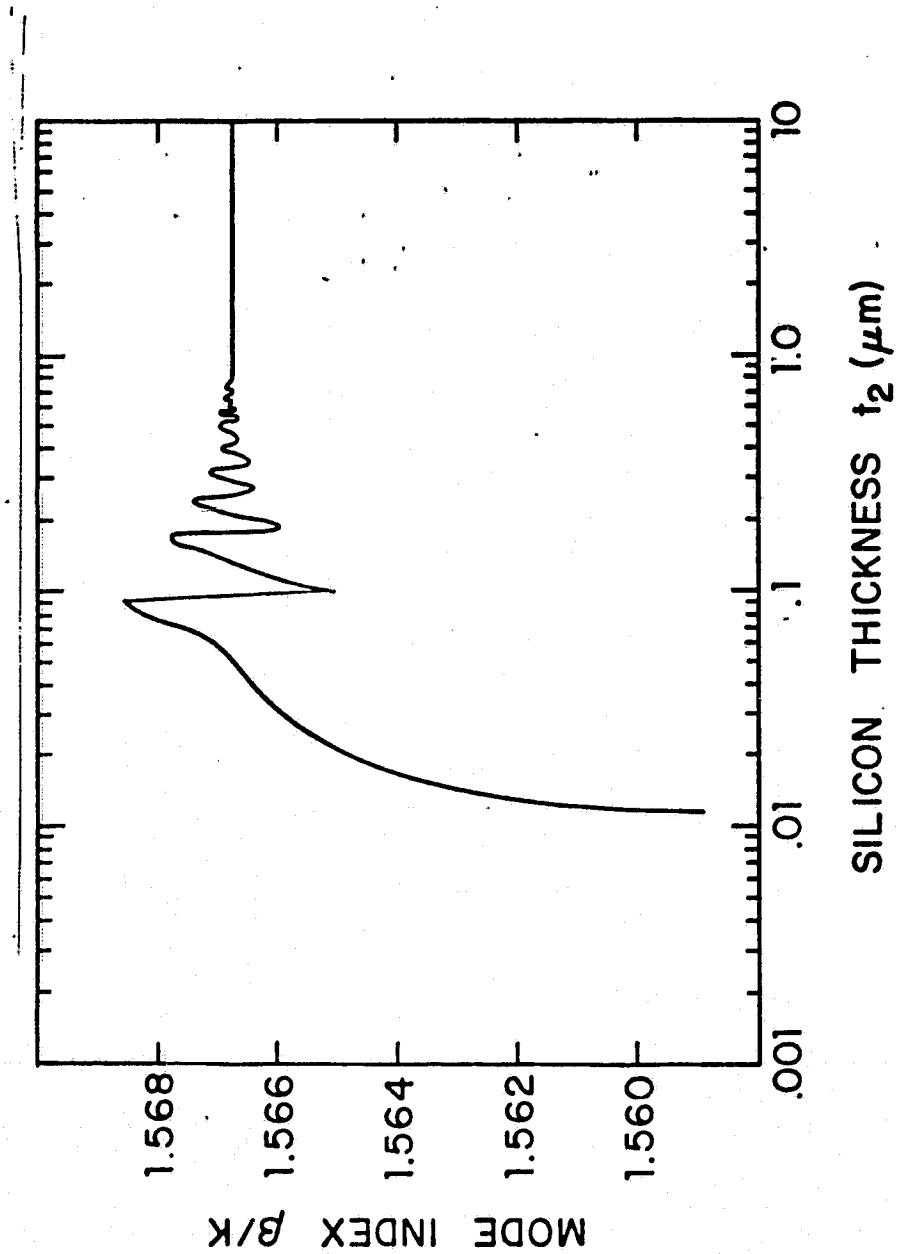

Figure 6. Mode index characteristics of silicon-clad waveguide (TE_0 mode, normal conductivity).

phase shift with conductivity as a parameter is shown in Figures 7 and 8 for a silicon-clad waveguide. Both changes are large enough to be readily measured and useful for device application, such as amplitude or phase modulation.

The remainder of this work describes a theoretical and experimental investigation into the damped oscillatory behavior of the curves of Figures 5 and 6 and the resulting modulation effects. Frequency filtering with the semiconductor-clad guides is also discussed.

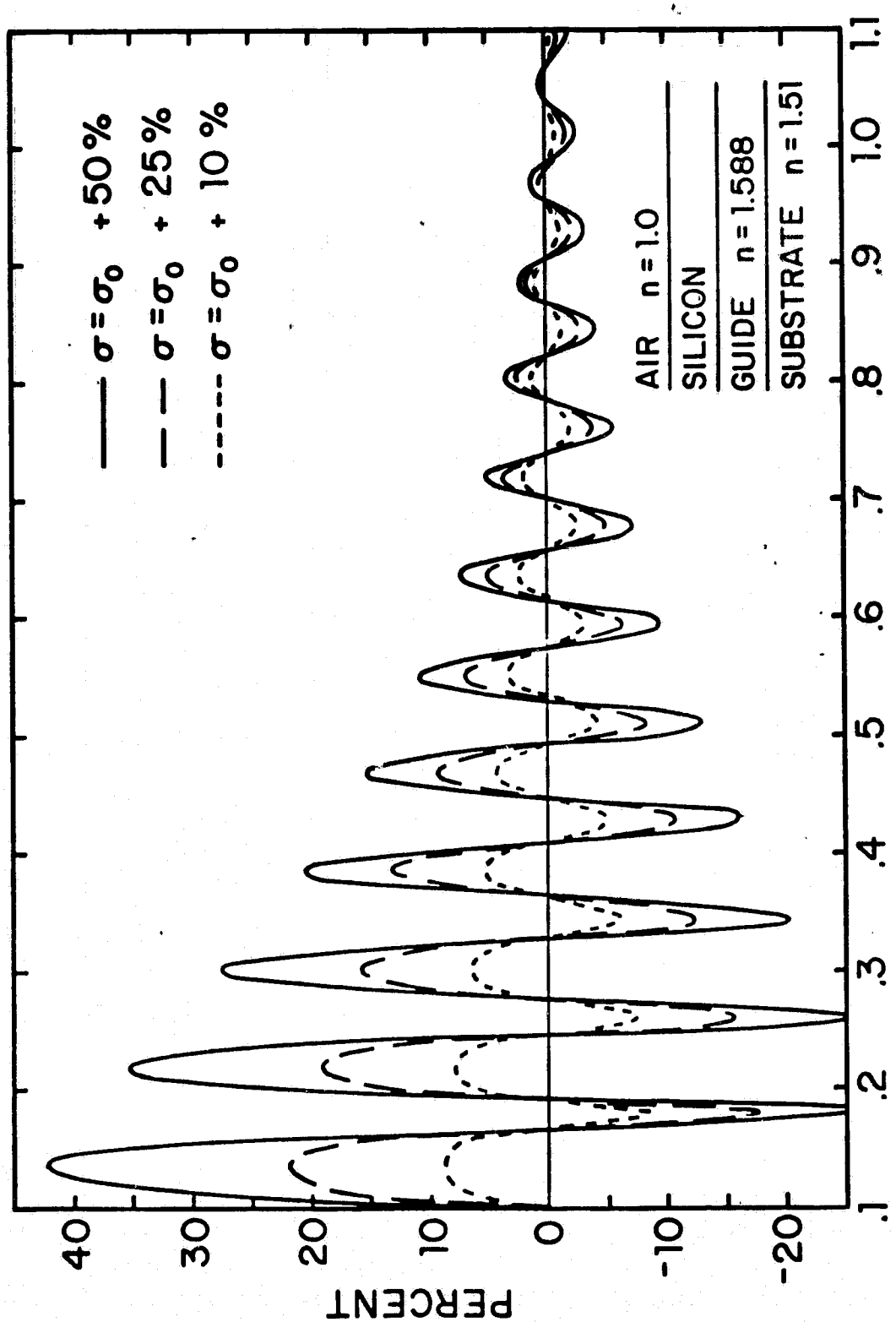

Figure 7. Change in attenuation with relative change in conductivity (σ_0).

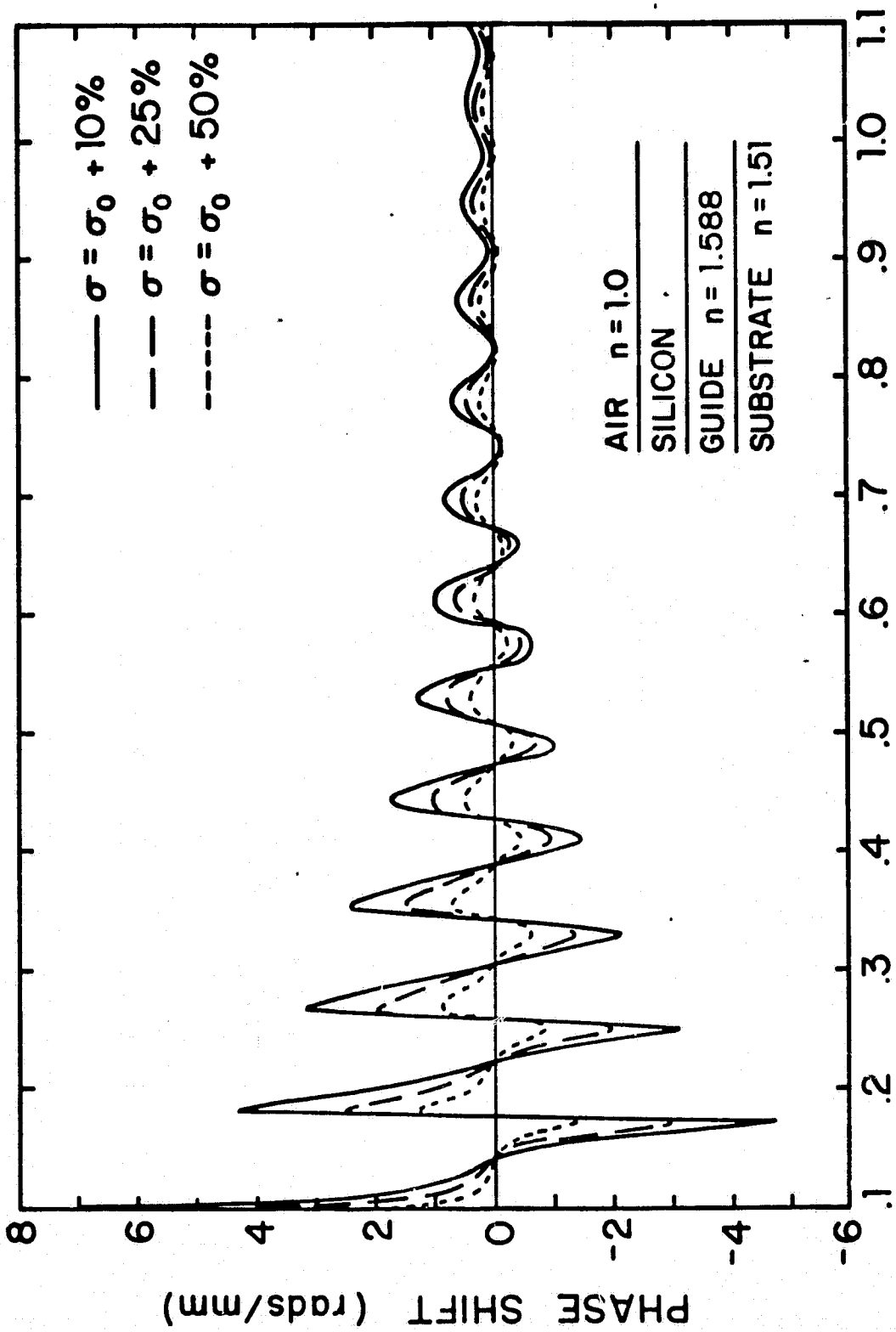

Figure 8. Change in mode index with relative change in conductivity (σ_0).

IV. Theoretical Predictions

The computer programs described in references 18 and 19 were used to calculate the characteristics of the clad waveguide at apropagation wavelength of 1150 nanometers since this was available for experimental measurements. This wavelength is also just below the band edge of silicon and thus any effects due to the band edge tail would be experimentally observable. The wavelength was also allowed to vary and it was noted that relatively sharp regions of absorption occurred which could be used for frequency filtering.

A. Calculations at 1150 Nanometers

Initial calculations for the attenuation and mode index of the four-layer semiconductor-clad guides were presented for a wavelength of 632.8 nm, and amplitude or phase modulation would be accomplished as a result of a change in the semiconductor conductivity via an incident light beam with photon energy above the bandgap of the silicon. It is evident, however, that the 632.8 nm guided wave will inadvertently excite the silicon cladding, since it is above the band gap. To circumvent this problem, the wavelength was changed to 1150 nm and the amplitude and phase characteristics of the guide were analyzed. This wavelength is such that the absorption coefficient of amorphous silicon is minimal [20, 21] and appreciable excitation of the silicon cladding by the 1150 nm guided wave is unlikely. Direct optical modulation, however, would still be realized by altering

the conductivity of the silicon with a light beam having photon energy above the band gap of silicon (in the visible region).

The attenuation and phase constant curves of Figures 9 and 10 were generated by varying the silicon cladding thickness from 0.01 to 1.0 μm (the phase constant, β, has been normalized by $k_0 = 2\pi/\lambda_0$ so that all curves show the mode index). Material parameters shown on Figures 9 and 10 are for a 1150 nm wavelength. The curves are again similar to exponentially damped sinusoids with extreme values of the mode index (β/k_0) corresponding to the median values (maximum slope) in the attenuation (α) curves. Extreme values of the α curve correspond to median values in the β/k_0 curves and the oscillations in both curves approach a median value at ten micrometers. Similar behavior was observed for a wavelength of 632.8 nm and results were described as a periodic coupling between the guided mode (TE_0) in the dielectric and the lossy TE' modes[1] of the semiconductor guide. Figures 9 and 10 show that such coupling still occurs and the amplitude of the oscillations has increased.

This coupling (or lack thereof) has a profound effect on the attenuation and phase characteristics of the original four-layer waveguide. Therefore, a partial structure consisting of a silicon guiding region surrounded by semi-infite layers of air and dielectric was analyzed.

The mode index and attenuation constants for the first few low order TE' modes in the silicon waveguide are shown in Figures

---

[1] TE'_i denotes guided modes in the semiconductor and TE_i denotes guided modes in the dielectric.

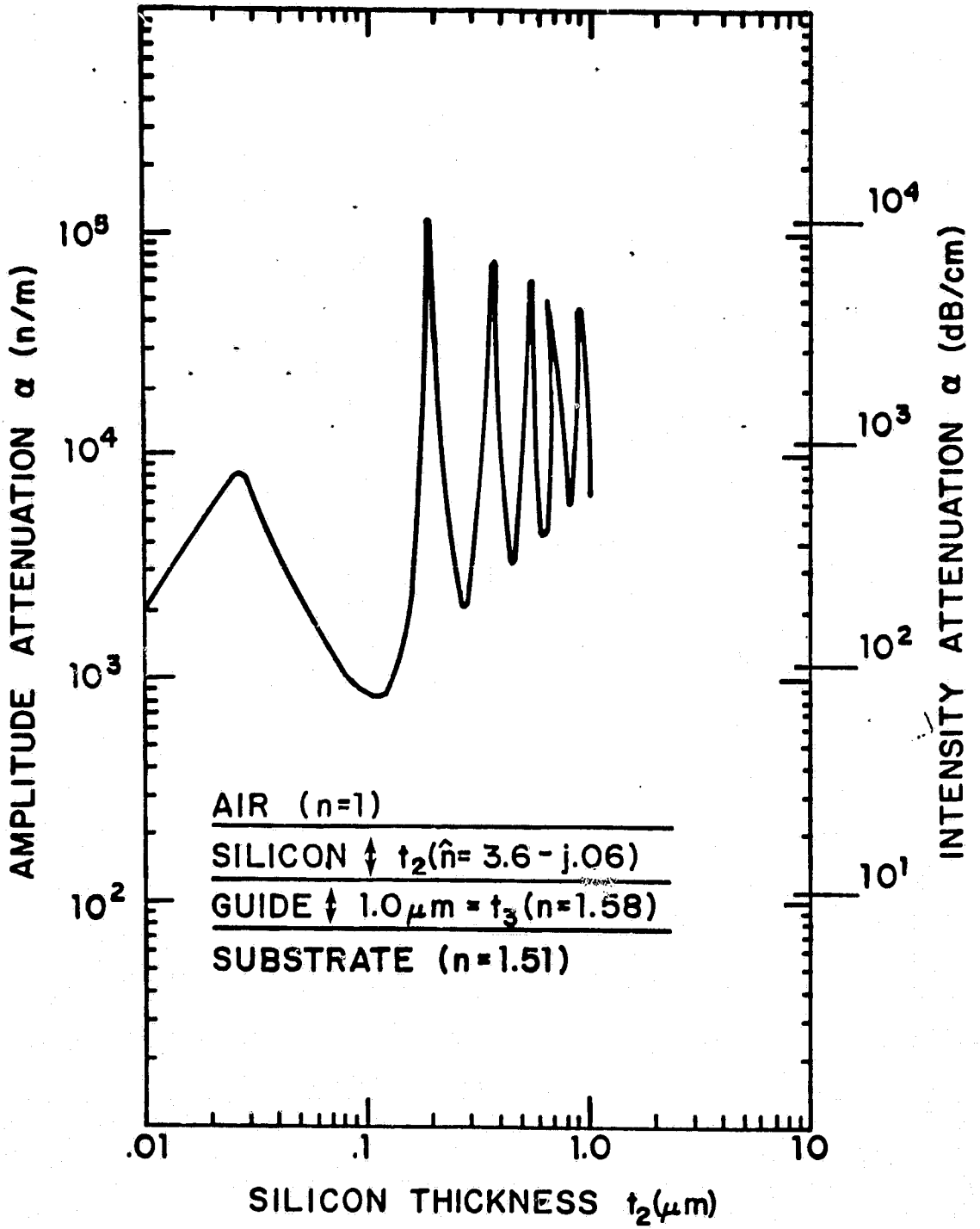

Figure 9. Attenuation characteristics of silicon-clad waveguide (TE_0 mode, wavelength = 1150 nanometers).

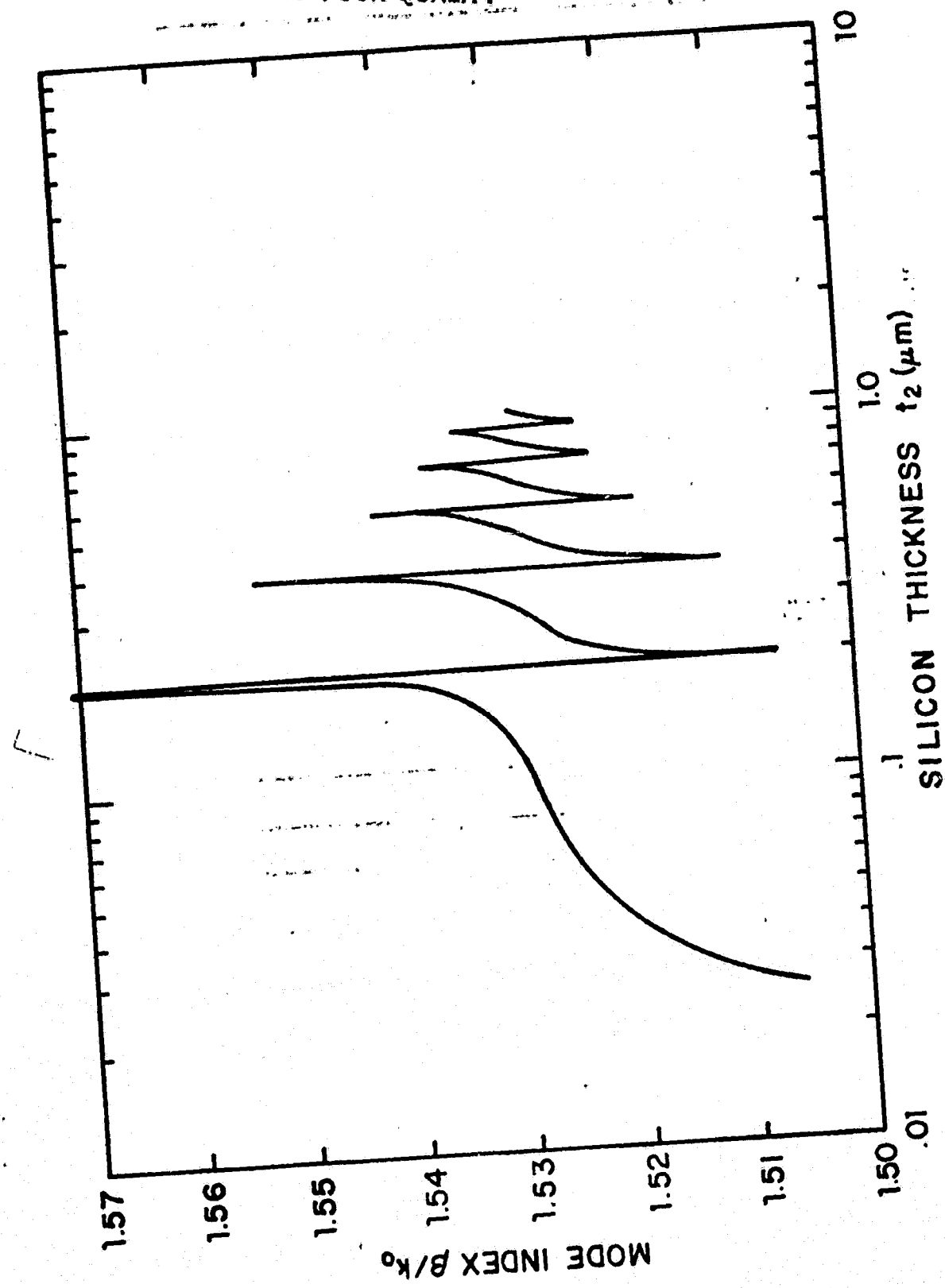

Figure 10. Mode index characteristics of silicon-clad waveguide (TE_0 mode, wavelength = 1150 nanometers).

11 and 12. All modes (except perhaps the lowest order TE'_0 mode) are very lossy and the attenuation increases for the higher order modes. In Figures 10 and 11 note that a phase match condition occurs between the TE_0 mode in the waveguide and the TE'_1 mode in the partial structure (air-silicon-dielectric) at $t_{Si} = 0.2$ μm. This phase match is present at each of the successively higher order TE' mode cutoff thicknesses and corresponds to the respective attenuation peaks on Figure 9 for the total structure. The sharp nulls in the attenuation curve, indicating very low coupling efficiency, occur at thicknesses midway between the cutoff value of two adjacent lossy TE' modes. Note, however, that the first peak on the four-layer attenuation curve (Figure 9) is considerably lower than the subsequent peaks. This behavior is unlike that of the attenuation curve presented at 632.8 nm (Figure 5). Observe that the TE'_0 mode of the three-layer guide (Figure 12) is reasonably low-loss, and that, although nearly complete transfer of energy between the guide and the silicon occurs for $t_{Si} = 0.025$ μm, coupling is into a low-loss mode. For the subsequent peaks on the attenuation curve (Figure 9), coupling is into high-loss modes of the partial structure and the attenuation of the four-layer guide is thus greater. For large silicon thickness, however, the four-layer attenuation curve (Figure 9) exponentially approaches that of the three-layer structures previously analyzed [22], where the semiconductor layer is considered semi-infinite. Similarly, the abrupt transitions on the mode index curve of the complete structure (Figure 10) occur when the phase match condition is

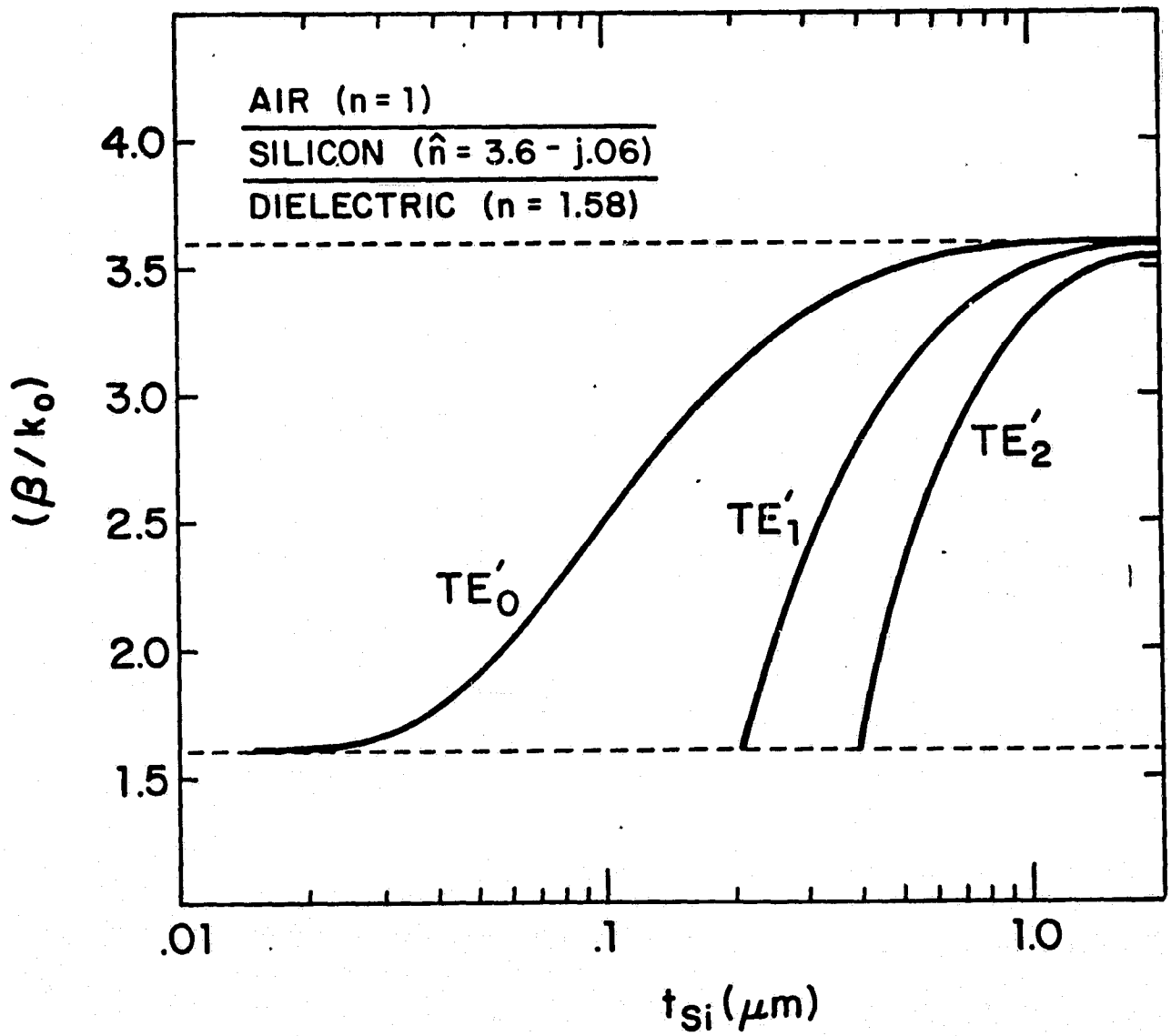

Figure 11. Mode index characteristics of silicon waveguide (wavelength = 1150 nanometers).

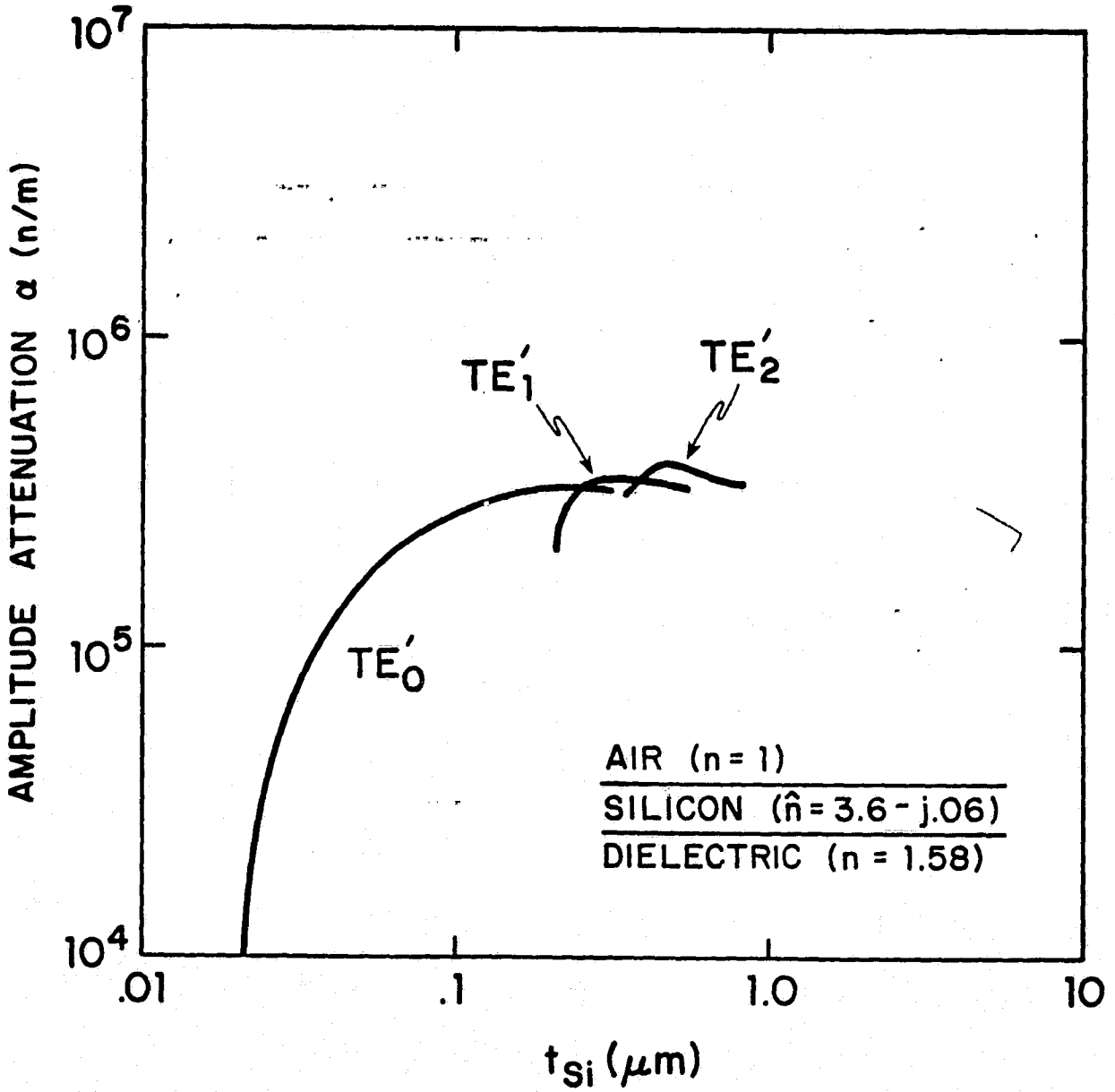

Figure 12. Attenuation characteristics of silicon waveguide (wavelength = 1150 nanometers).

satisfied and the guided waves couple into successively higher order modes of the partial structure. These results are similar to the power transfer calculations for linearly tapered directional couplers [23-25]. Finally, note that the period and amplitude of the attenuation characteristics of the silicon-clad guide are a function of the material permittivities for a given wavelenghth as Figure 5 (λ = 632.8 nm) and Figure 7 (λ = 1150 nm) indicate.

Calculations presented in this section demonstrate that the attenuation and mode index of the four-layer silicon clad planar dielectric waveguide behave as exponentially damped sinusoids for a wavelength of 1150 nm. The effect may be explained as a coupling between the basic TE_0 mode of the dielectric waveguide and the high loss TE' modes of the semiconductor guide. The oscillatory behavior of the attenuation and mode index curves, a necessary prerequisite for the direct modulation of the guided beam, is still apparent and detailed calculations of a direct optical modulation scheme at 632.8 nm are presented elsewhere [Appendix I]. These calculations at 1150 nm demonstrate that the required modulation technique is still feasible without inadvertent excitation of the silicon cladding by the guided light wave.

B. Frequency Filtering

The attenuation characteristics of silicon-clad waveguides are a function of the material permittivities for a particular wavelength as Figure 5 (λ_0 = 632.8 nm) and Figure 9 (λ_0 = 1150 nm) indicate. Based on the observed change in period and amplitude of the attenuation curve oscillations as the material parameters vary with wavelength, it is evident that selective frequency

filtering can be realized with a silicon-clad waveguide. In particular for a given silicon-cladding thickness, the attenuation will vary drastically as the material permittivities vary with wavelength, and through optimization of the semiconductor cladding thickness, a particular frequency filtering response may be obtained with the clad guide. For example, note that a silicon thickness t_{Si} = 0.10 μm lies in a range of high attenuation ($\alpha > 10^4$ n/m) on Figure 5 (λ = 632.8 nm), while it is in a region of low attenuation ($\alpha < 10^3$ n/m) on Figure 9 (λ = 1150 nm). It is this effect which will be used for frequency filtering. The permittivities of all four materials (air, silicon, guide, substrate) in the planar waveguide structure of interest vary with wavelength: however amorphous silicon is particularly sensitive to frequency variations as Table I indicates [21]. The predicted frequency filtering effect is due almost solely to a change in silicon permittivity. It should be again noted that the permittivity of amorphous silicon is highly dependent upon the method of preparation.

Attenuation versus silicon thickness curves similar to those of Figure 5 and Figure 9 were generated as the wavelength was allowed to change from 0.35 μm [17, 21] to 1.55 μm and the permittivities of the four layers consequently varied. All attenuation curves retained their characteristic oscillations; however, the amplitude and period of the oscillations were significantly altered. Similarly, the mode index versus silicon thickness curves retained their characteristic oscillatory behavior although the frequency and amplitude of the oscillations changed.

Table II

Amorphous Silicon Parameters as a Function of Wavelength

Wavelength (microns)	Refractive Index		Relative Permittivity	
	n	k	ε'_R	ε''_R
0.35	3.63	2.860	5.0	20.80
0.42	4.53	1.470	18.4	13.40
0.52	4.43	0.900	18.8	8.00
0.57	4.21	0.660	17.3	5.60
0.62	4.11	0.388	16.8	3.20
0.65	4.04	0.289	16.3	2.35
0.69	3.97	0.188	15.8	1.50
0.74	3.88	0.155	15.0	1.20
0.89	3.67	0.068	13.5	0.50
1.00	3.65	0.062	12.3	0.45
1.15	3.59	0.056	12.9	0.40
1.24	3.55	0.039	12.6	0.28
1.55	3.52	0.028	12.4	0.20

Figures 13-15 were obtained by assuming a given silicon thickness in the four-layer planar structure and allowing the wavelength to vary (and consequently the material permittivities). The resulting attenuation (dB) for a 1 mm wide silicon bar is plotted vertically in Figures 13-15.

A high pass frequency filter is realized in Figure 13. Insertion loss is approximately 10 dB for wavelengths greater than 1.0 μm for the three silicon thicknesses considered (t_{Si} 0.06, 0.08, 0.13 μm). The particular filter characteristics may be adjusted by varying the silicon thickness.

Filters with passband wavelengths of 0.6 μm to 0.9 μm are shown in Figure 14. Note that both the exact location of the pass band and the insertion loss may be varied for the three silicon thicknesses of interest (t_{Si} = 0.03, 0.04, 0.05 μm) and that high attenuation occurs immediately outside of this pass band region.

Additional filter characteristics are presented in Figure 5 and Appendix II. The effect of a silicon dioxide buffer layer to reduce overall attenuation is considered in Appendix II.

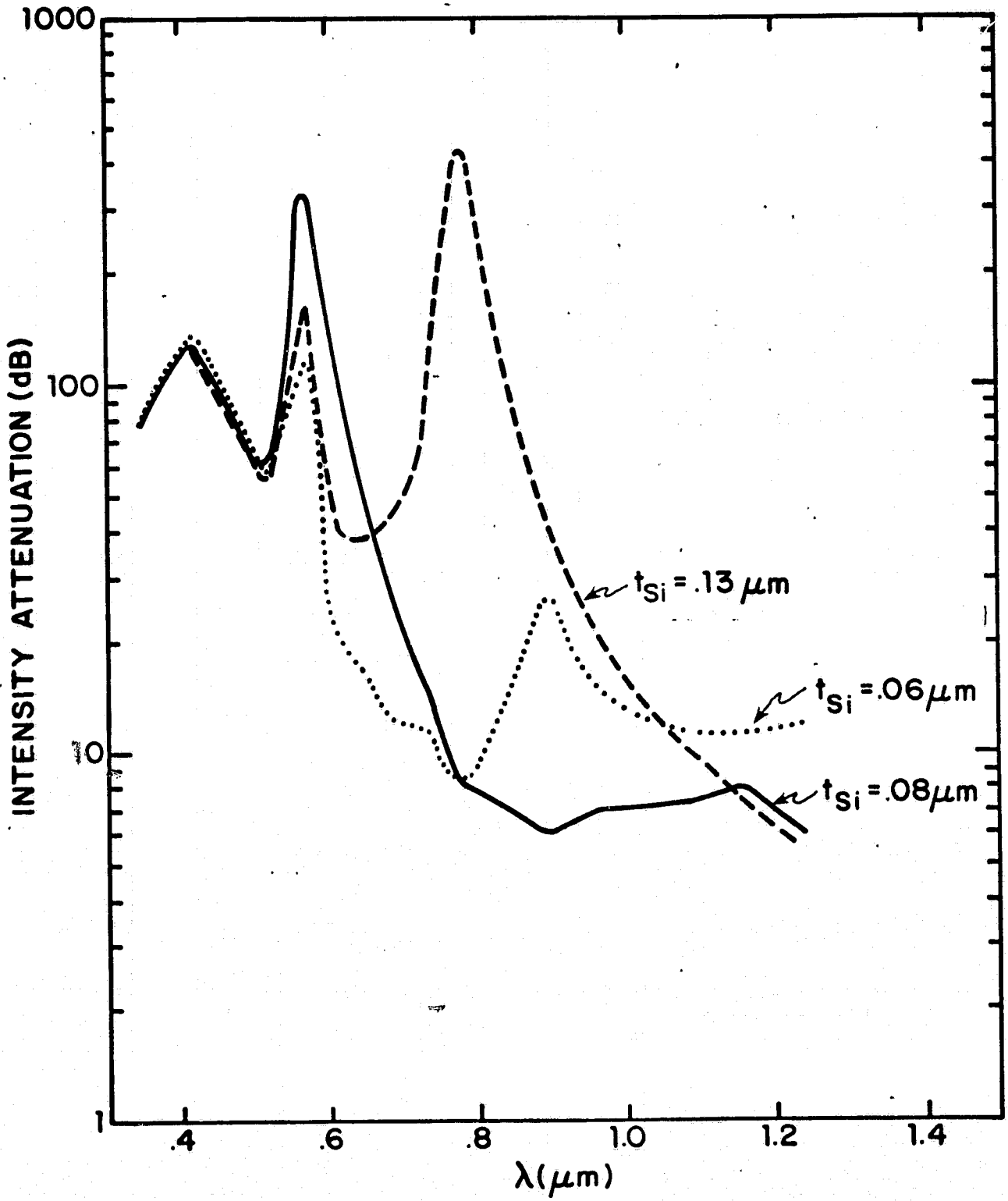

Figure 13. Frequency response of silicon-clad waveguide. (t_{Si} = 0.06, 0.08, 0.13 μm)

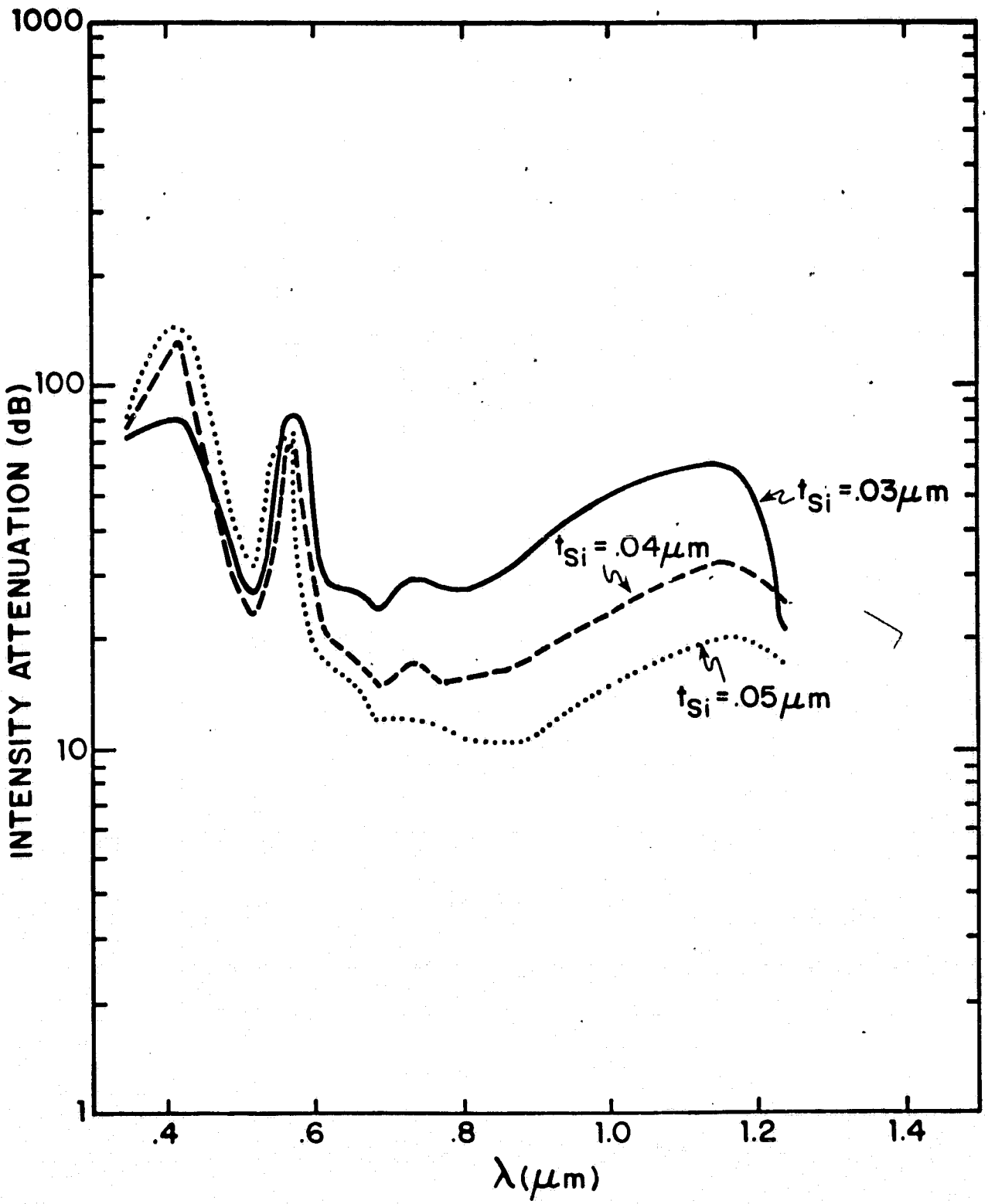

Figure 14. Frequency response of silicon-clad waveguide. (t_{Si} = 0.03, 0.04, 0.05 μm)

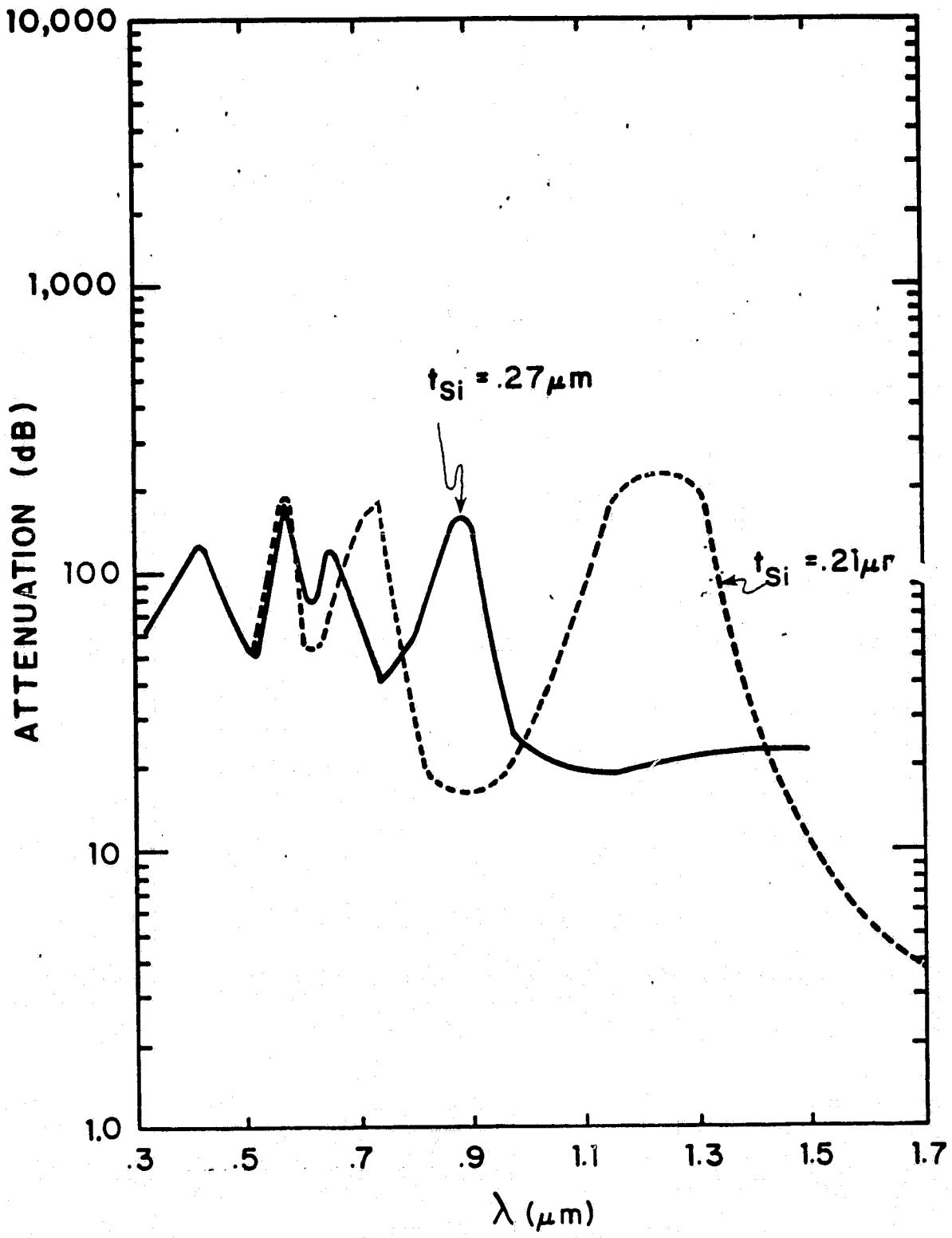

Figure 15. Frequency response of silicon-clad waveguide. (t_{Si} = 0.21, 0.27 μm)

V. Experimental Studies

This section describes experiments which were performed to verify the effects of buffer layers, light modulation and filtering as described in the previous sections.

A. Buffer Layer Fabrication

Since even relatively short sections of semiconductor-clad waveguides are lossy (1 mm length of Si at t_2 = 0.05 μm, α > 10 dB), the attenuation must be reduced significantly for a practical device. Thin dielectric buffer layers are commonly used to lower the attenuation losses of metal-clad dielectric waveguides [26]. These layers are placed between the dielectric core and the metal, and act as buffers to remove a large proportion of the field from the metal cladding. The effect of a silicon dioxide (SiO_2) buffer layer on the attenuation versus silicon thickness characteristics is considered in Appendix I, and results indicate that the absolute attenuation may be reduced significantly while still preserving the damped sinusoidal behavior apparent in the curves of Figures 5 and 6.

Fabrication of these low refractive index buffer layers was then attempted; low loss guides were prepared using an ion-exchange technique [27-30] and silicon dioxide was deposited using a radio frequency sputtering system. For each run, the system was pre-pumped to a base pressure less than 5×10^{-6} Torr and all sputtering was performed in an argon atmosphere at 10^{-2} Torr. Initial SiO_2 films appeared to have a refractive index greater than that of the ion-exchange guide (n = 1.58) as the guided

wave was severely attenuated upon encountering the SiO_2 film. Experiments indicate, however, that the density of the film (and thus its refractive index) may be controlled by adjusting the powers coupled into the upper and lower plates of the sputtering system it thus appears that further optimization of certain sputtering system parameters may be required before a buffer layer film of appropriate refractive index and quality is realized.

B. Modulation Effects

Experimental devices were constructed to verify the predicted modulation capabilities of the semiconductor-clad waveguides. The amplitude and phase modulators described utilize light-induced changes in the imaginary portion of the permittivity of the semiconductor cladding to vary the propagation characteristics of the guided wave; thus, photoconductive silicon is necessary; however, amorphous silicon (sputtered) is permeated with dangling bonds which render the sputtered silicon photoelectrically and photoconductively dead. One solution is to sputter in an argon/hydrogen gas mixture which effectively passivates the dangling bonds [20]. It appears, however, that the resultant photoconductive properties of the argon-hydrogen sputtered silicon is a complicated function of several sputtering system parameters (gas pressure, gas composition, target-to-substrate spacing, sputtering power, etc.). Initial attempts at sputtering in a 99% Ar-1% H_2 mixture did not yield silicon with a measureable photoconductive response and thus modulation experiments have proven unsuccessful.

The experimental setup was as follows: A 5 mW He-Ne (632.8 nm) laser was coupled into the silicon-clad guide using a prism coupler. An HP5082-4205 photodiode was positioned approximately 2 mm from the output side of the silicon bar to make scattered light measurements, while a 2W Ar laser illuminated the silicon bar (a No. 24 Wratten filter was placed over the detector head to filter out the Ar laser). No change in scattered light at the output side of the silicon-clad waveguide was observed.

Possible explanations include the previously mentioned difficulties with the fabrication of photoconductive silicon and also, lack of significant absorption of the illuminating laser source by the silicon cladding. Calculations indicate that only 5% of the incident photon flux will be absorbed by the silicon ($\alpha \approx 10^4$ cm^{-1} at $\lambda = 0.5$ μm) for a silicon thickness of 0.05 μm. Inadvertent excitation of the silicon cladding by the 632.8 nm guided wave was also addressed in Section 3A.

C. Filter Characteristics

Experimental verification of the predicted filter response curves of the silicon-clad waveguides was attempted and preliminary confirmation of the attenuation versus guide wavelength characteristics is presented in this section. Low-loss, single-mode optical waveguides were diffused into soda-lime glass using an ion-exchange fabrication technique [28-31]. Uniform silicon films 1 mm wide and extending across the waveguide were deposited using a radio frequency sputtering system. For each run, the system was pre-pumped to a base pressure less than 5 x 10^{-6} Torr

and all sputtering was performed in an argon atmosphere at a pressure of 10^{-2} Torr. A number of uniform silicon films with thicknesses in the range of 0.02 μm to 0.4 μm were fabricated.

Determination of the filter characteristics necessitates waveguide attenuation measurements as a function of guide wavelength. Unfortunately, both the fluid-coupling and sliding output prism schemes require the coupling out of the guided wave and are plagued with experimental inaccuracies for the measurement of the high predicted attenuations [32], it was thus decided to measure the light scattered from the guided beam using an apertured silicon photo diode.

The detector used was a current active HP5082-4205 photo diode connected to a Photodyne Model 22XLA Fiber Optic Multimeter. A Coherent M 599.01 Dye Laser pumped by an Innova 90-2 Argon Laser was coupled into the silicon-clad guide using a prism coupler. The detector head was positioned approximately 2 mm from the input side of the silicon bar and scattered light measurements were recorded as the dye laser was tuned; the photodetector was then positioned approximately 2 mm from the output side of the silicon bar and measurements were again taken as a function of laser wavelength. Laser output power was continuously monitored. The difference between the two measurements yields the attenuation for a given wavelength, and results for a silicon cladding thickness of 0.04 μm are shown in Figure 16. Despite the limited wavelength range available with the Rhodamine 590 Dye (570-635 nm), the tendency for the attenuation to increase considerably in the lower wavelength region is clearly apparent,

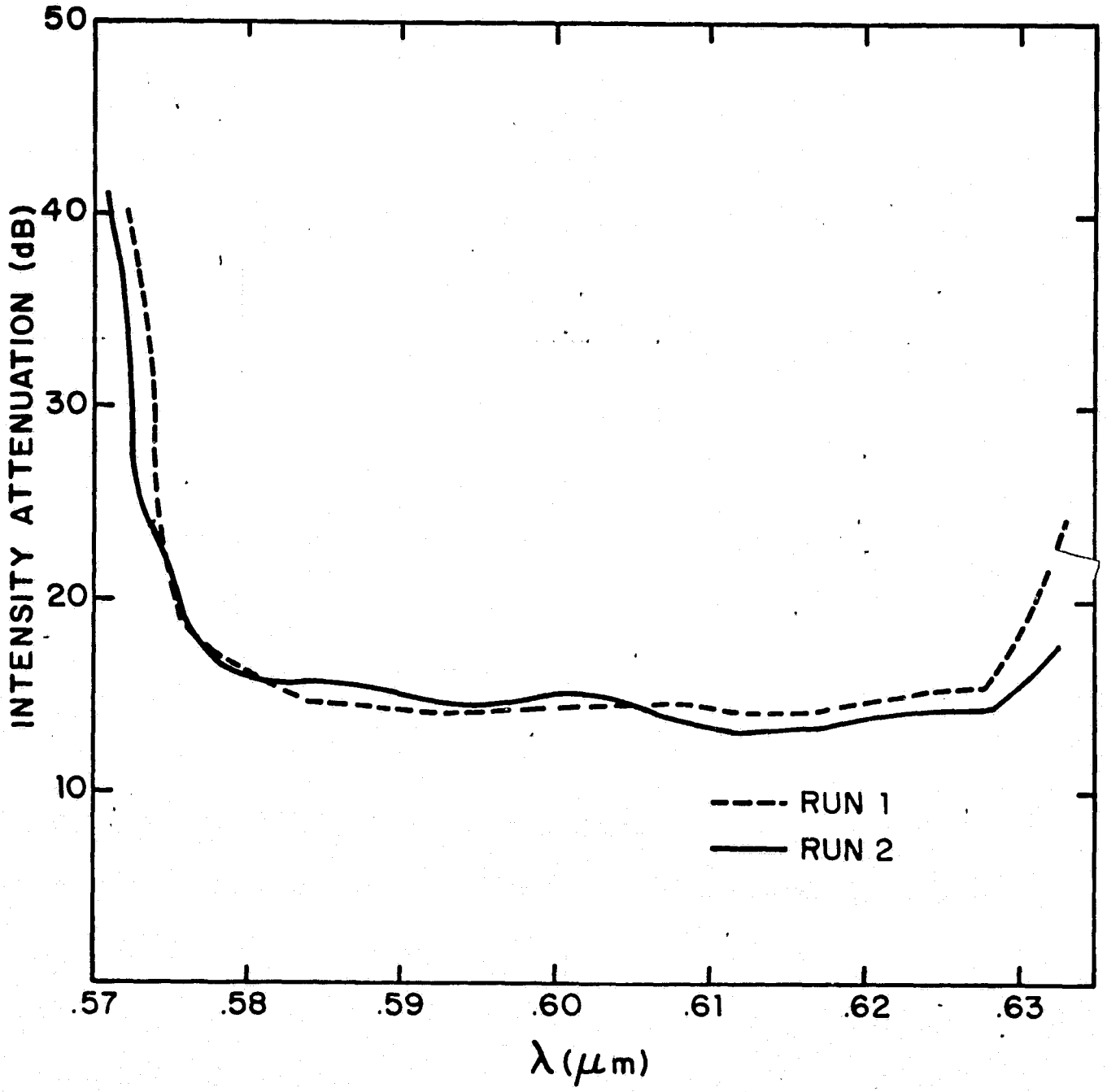

Figure 16. Experimental filter response. (t_{Si} = 0.04 μm)

as computer calculations predict (Figure 17). Subsequent attenuation measurements were attempted from 488-520 nm using the argon laser but the waveguides strongly fluoresced. It should be noted that fluorescence was not observed over the wavelength range in Figures 18-19, and is thus not a significant loss mechanism for this region. This fluorescence has been previously discussed and incorrectly attributed to the silver ions present in the ion-exchange waveguides [18]. We observed broad band red-orange fluorescence in the Fischer brand microscope slides which are being used as substrates for the waveguide structure. The fluorescence is thus most likely due to trace impurities (Fe, Eu) present in the microscope glass [33].

It became apparent, then, that an alternate waveguide structure had to be used. The formation of ion-exchange waveguides from silver nitrate melts has traditionally been attributed to the diffusion of silver ions into soda-lime glass and the subsequent replacement of sodium ions which diffuse out of the glass (an exchange process); however, we have successfully fabricated single mode waveguides by diffusing silver ions into silicon dioxide (quartz). These results indicate that a diffusion rather than an exchange process may be the controlling factor in the formation of the "ion-exchange" waveguides; furthermore, it was noted that the diffused waveguides do not fluoresce.

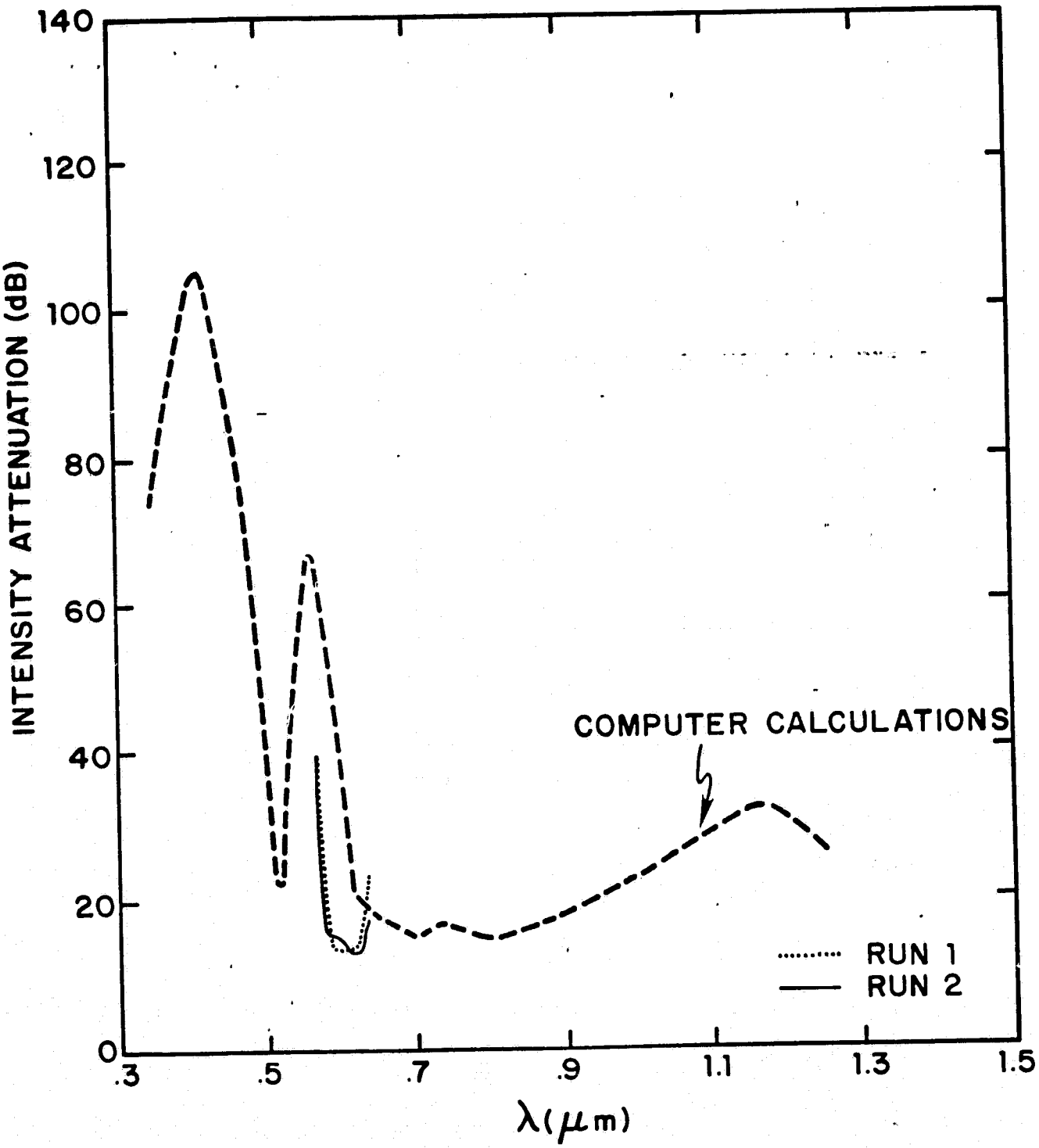

Figure 17. Filter response. (t_{Si} = 0.04 μm)

VI. Conclusions

A number of important conclusions can be drawn from this work. The investigation of the complex permittivity near the band gap edge indicates that the absorption coefficient may be shifted by application of an electric field or through generation of electron-hole pairs; thus direct optical modulation of a guided wave by photon-induced conductivity changes in a semiconductor-cladding still appears feasible. Experiments thus far with silicon-clad guides have yielded negative results; further experiments with GaAs-clad guides may be more fruitful since calculations indicate that the shift in the absorption coefficient is only appreciable in direct band gap materials. Buffer-layer fabrication problems may be overcome through optimization of certain deposition system parameters. Frequency filtering has also been suggested for these clad guides and preliminary experimental results have confirmed the predicted characteristics. These and other areas are currently being examined.

References

1. J. Kavanagh and T.E. Batchman, "Investigation of Active Devices for Integrated Optics," Report No. 1 to Telecom Australia (C.O. 46764), Univ. of Queensland, Electrical Engineering Dept., Brisbane, Australia, 1978.

2. M. Ali Omar, Elementary Solid State Physics, Addison Wesley Publishing Co., Reading, Mass., 1975, Ch. 6, pp. 292-300.

3. F.K. Reinhart, "Electroabsorption in $Al_yGa_{1-y}As$-$Al_xGa_{1-x}As$ double heterostructures," Appl. Phys. Lett., Vol. 22, No. 8, pp. 372-4, April 15, 1973.

4. C.H. Lee, P.S. Mak, and A.P. DeFonzo, "Optical control of millimeter wave propagation in dielectric waveguides," IEEE J. of Quantum Electron., Vol. QE-16, No. 3, pp. 277-288, March 1980.

5. R.A. Smith, Semiconductors, Cambridge University Press, 1978.

6. J. Tauc, editor, Amorphous and Liquid Semiconductors, Plenum Press, 1974.

7. R.H. Bube, Photoconductivity of Solids, Wiley and Sons, 1960.

8. T.S. Moss, Photoconductivity in the Elements, Academic Press, 1952.

9. J.D. Dow and D. Redfield, "Electroabsorption in semiconductors: the excitonic absorption edge, Phys. Rev. B, Vol. 1, No. 8, pp. 3358-3370, April 15, 1970.

10. T. Tamir, ed., Topics in Applied Physics (Volume 7): Integrated Optics, New York: Springer-Verlag, 1979, pp. 243-302.

11. A.F. Gibson, "Infra-red and microwave modulation using free carriers in Semiconductors," J. Scientific Instruments, Vol. 35, No. 8, pp. 273-278, Aug. 1958.

12. J.S. Blakemore, "Semiconducting and other major properties of gallium arsenide," J. Appl. Phys, Vol. 53, No. 10, pp. R123-170, October 1982.

13. J.G. Mendoza-Alvarez, F.D. Nunes, and N.B. Patel, "Refractive index dependence on free carriers for GaAs," J. Appl. Phys, Vol. 51, No. 8, pp. 4365-4367, August 1980.

14. C.J. Hwang, "Optical properties of n-type GaAs," J. Appl. Phys., Vol. 40, No. 9, pp. 3731-3739, August 1969.

15. T.E. Batchman and S.C. Rashleigh, "Mode-selective properties of a metal-clad dielectric-slab waveguide for integrated optics," IEEE J. Quantum Electron., (corresp.), Vol. QE-8, pp. 848-850, November 1972.

16. R.B. Smith and G.L. Mitchell, "Calculation of complex propagating modes in arbitrary plan-layered complex dielectric structures," E.E. Tech. Report No. 206, University of Washington, National Science Foundation Grant: ENG 76-09937, December 1977.

17. D.E. Gray, Ed., American Institute of Physics Handbook, 2nd Edition, New York: McGraw-Hill, 1963, Ch. 6, pp. 102-122.

18. T.E. Batchman, "Investigation of Direct Integrated Optics Modulators," Semi-Annual Status Report, NASA Grant NSG 1567, UVA Report No. 52 8171/EE79/01, July 1979.

19. T.E. Batchman, "Investigation of Direct Integrated Optics Modulators," Semi-Annual Status Report, NASA Grant NSG 1567, UVA Report No. 52 8171/EE80/104, October 1980.

20. M.H. Brodsky, ed., "Amorphous semiconductors," Topics in Applied Physics, Vol. 36 (New York) Springer-Verlag, 1979, pp. 1-7.

21. D.T. Pierce and W.E. Spicer, "Electronic structure of amorphous Si from photoemission and optical studies," Phys. Review B, Vol. 5, No. 8, pp. 3017-3029, April 15, 1972.

22. T.E. Batchman and K.A. McMillan, "Measurement on positive permittivity metal-clad waveguides," IEEE J. Quantum Electron., Vol. QE-13, No. 4 pp. 187-192, April 1977.

23. A.L. Jones, "Coupling of optical fibers and scattering in fibers," J. Opt. Soc. Am., Vol. 55, No. 3, pp. 261-271, March 1965.

24. T.K. Lim, B.K. Garside, and J.P. Marton, "An analysis of optical waveguide tapers," Appl. Phys., Vol. 18, pp. 53-62, January 1979.

25. R.B. Smith, "Analytic solutions for linearly tapered directional couplers," J. Opt. Soc. Am., Vol. 66, No. 9, pp. 882-892, September 1976.

26. I.P. Kaminow, W.L. Mammel and H.P. Weber, "Metal-clad optical waveguide: analytical and experimental study," Appl. Opt., Vol. 13, pp. 396-405, Feb. 1974.

27. Y. Yamamoto, T. Kamiya and H. Yanai, "Characteristics of optical guided modes in multi-layer metal-clad planar optical guide with los-index dielectric buffer layer," IEEE J. Quantum Electron., Vol. QE-11, pp. 729-736, September 1975.

28. G. Stewart, C.A. Miller, P.J.R. Laybourn, C.D.W. Wilkinson and R.M. DeLaRue, "Planar optical waveguides formed by silver-ion migration in glass," IEEE J. Quantum Electron., Vol. QE-13, pp. 192-200, April 1977.

29. G. Stewart and P.J.R. Laybourn, "Fabrication of ion-exchanged optical waveguides for dilute silver nitrate melts," IEEE J. Quantum Electron., Vol. QE-14, pp. 930-934, December 1978.

30. T.G. Giallorenzi, E.J. West, R. Kirk, R. Ginther and R.A. Andrews, "Optical waveguides formed by thermal migration of ions in glass," Appl. Opt., Vol. 12, No. 6, pp. 1240-1245, June 1973.

31. A. Gedeon, "Formation and characteristics of graded-index optical waveguides buried in glass," Appl. Phys., Vol. 6, pp. 223-228, March 1975.

32. I.P. Kaminow, W.L. Mammel, and H.P. Weber, "Metal-clad optical waveguides: analytic and experimental study," Appl. Opt., Vol. 13, pp. 396-405, February 1974.

33. J. Wong and C.A. Angell, Glass Structure and Spectroscopy, New York: Marcel Dekker, Inc., 1976, Chapter 6.

34. D.E. Carlson and C.R. Wronski, "Amorphous Silicon Solar Cell," Appl. Phys. Lett., Vol. 28, No. 11, pp. 671-673, June 2, 1976.

Appendix

Publications

The following papers were published during the time of this contract.

1. G.M. McWright and T.E. Batchman, "Four-and Five-Layer Silicon-Clad Dielectric Waveguides," NASA Conference Publication 2207: Optical Information Processing for Aerospace Applications (Hampton, VA, August 18-19, 1981), pp. 217-230.

2. T.E. Batchman and G.M. McWright, "Mode Coupling Between Dielectric and Semiconductor Planar Waveguides," IEEE Journal of Quantum Electronics, Vol. QE-18, No. 4, pp. 782-788, April 1982. (A Joint Special Issue on Optical Guided Wave Technology, also published in IEEE Transactions on Microwave Theory and Techniques, Vol. MTT-30, No. 4, pp. 628-634, April, 1982).

3. G.M. McWright, T.E. Batchman, and M.S. Stanziano, "Measurement and Analysis of Periodic Coupling in Silicon-Clad Planar Waveguides," IEEE Journal of Quantum Electronics, Vol. QE-18, No. 10, Oct. 1982. (A Second Joint Special Issue on Optical Guided Wave Technology, also published in IEEE Transactions on Microwave Theory and Techniques, Vol. MTT-30, No. 10, Oct. 1982).

FOUR- AND FIVE-LAYER SILICON-CLAD DIELECTRIC WAVEGUIDES*

Glen McWright and T. E. Batchman
University of Virginia
Charlottesville, Virginia

ABSTRACT

Computer modeling studies on four-layer silicon-clad planar dielectric waveguides indicate that the attenuation (α) and mode index (β/K) behave as exponentially damped sinusoids as the silicon thickness is increased. The observed effect can be explained as a periodic coupling between the guided modes of the lossless structure and the lossy modes supported by the high-refractive index silicon. Furthermore, the attenuation and mode index are significantly altered by conductivity changes in the silicon. An amplitude modulator and phase modulator have been proposed using these results. Predicted high attenuations in the device may be reduced significantly with a silicon dioxide buffer layer.

INTRODUCTION

A need has arisen for direct optical modulation technology. This need has arisen from the search for faster digital switches, higher capacity data channels, and light, compact data preprocessing equipment for satellites. One promising technology that has been examined is the modulation of a guided light wave via photoconductivity changes in a semiconductor cladding.

Computer modeling studies on four- and five-layer, silicon-clad, planar dielectric waveguides indicate that the propagation characteristics can be altered by changes in the complex permittivity of the silicon and in the thickness of the silicon. Using these predictions, an intensity modulator and a phase modulator based on photon-induced conductivity changes in the semiconductor cladding have been studied.

SEMICONDUCTOR-CLAD WAVEGUIDES

The four-layer planar waveguide structure under consideration is shown in Figure 1, where it is assumed that light is propagating in the dielectric (N_3) and all materials are lossless except for the semiconductor (N_2). We desire to solve for the complex mode propagation constant ($\alpha + j\beta$).

*Research sponsored by NASA-Langley Research Center under Grant NSG-1567.

One technique (1) extends Maxwell's equations and boundary conditions to numerically solve a transcendental equation relating the attenuation constant (α) and phase constant (β) to the material types and thicknesses of the waveguide structure (hereafter refered to as PROGRAM WAVES).

A more efficient method (2) utilizes a matrix representation of Maxwell's equations, field solutions and boundary conditions in each waveguide layer (hereafter refered to as PROGRAM MODEIG). The matrices are multiplied and a characteristic matrix for the entire structure is obtained which yields the attenuation constant and phase constant.

The waveguide consists of a semi-infinite glass substrate, a polystyrene core of thickness 1 micrometer, a silicon cladding of .01 micrometer to 10 micrometers in thickness, and a semi-infinite layer of air. Each material is characterized by a complex relative permittivity, $\hat{\epsilon}$; a free space wavelength of 632.8 nanometers is assumed and material parameters are shown for this wavelength (Fig. 1) Layers N_1, N_3, and N_4 are lossless dielectrics, so ϵ_r is real; however, at optical frequencies the permittivity of the silicon (N_2) is complex ($\epsilon_r = \epsilon'_r + j\epsilon''_r$), and the complex part is a linear function of the conductivity ($\epsilon''_r = \sigma/\omega\epsilon_o$).

PREDICTED CHARACTERISTICS

The curves presented in Figures 2 and 3 were generated by repeated use of our own PROGRAM WAVES and later confirmed with PROGRAM MODEIG. The silicon cladding was varied from .01 micrometer to 10 micrometers and the complex mode propagation constant was calculated. The expected result was that as the cladding thickness was reduced to zero, the attenuation decreases to zero in a well-behaved manner; however, the results were not well-behaved when the silicon thickness falls below 1 micrometer. The curves are similar to exponentially damped sinusoids. Extreme β/K variations correspond to median values in the α-curve, and extreme α variations correspond to median β/K values. By increasing the conductivity of the silicon cladding, the amplitude of the curve oscillations decreases slightly, and the α-curve shifts vertically to a higher attenuation. The percent change in attenuation compared to dark conditions ($\sigma = \sigma_o$) for different conductivities ($\sigma = 1.1\ \sigma_o$, $\sigma = 1.25\ \sigma_o$, $\sigma = 1.5\ \sigma_o$) is shown in Figure 4. The β/K curves shift for a conductivity change, as well, although not in such a well-defined manner. The percent phase shift compared to dark conditions ($\sigma = \sigma_o$) for different conductivity changes is shown in Figure 5. These effects will be used for intensity and phase modulation in a device where a signal source induces photoconductivity changes in a thin silicon cladding on a waveguide, thus modulating a coherent beam in the guide.

FIELD CALCULATIONS

We now consider the problem of correlating the local maximum/minimum points on the attenuation and mode index curves with the electric and magnetic field distributions in the waveguide layers. Results indicate that the presence of a thin silicon film (<98Å) has little effect on the wave function profiles; the profiles are similar to those of the three-layer lossless structure (air-dielectric-substrate). For the thick silicon film structure, however, the lowest order mode of the lossless three-layer structure couples to the modes associated with the

semiconductor film (the high-refractive index silicon behaves as a waveguide). Furthermore, the coupling between the modes supported by the three-layer lossless structure and the high loss TE' modes* of the silicon waveguide determines the attenuation and phase of the complete four-layer structure.

Our results can be described as periodic coupling between the guided mode and other leaky modes of the same guide. First, we examine the partial structure consisting of a silicon guiding region surrounded by semi-infinite layers of air and polystyrene. The attenuation and mode index are shown in Figures 6 and 7. We note a phase match condition between the modes of the partial structure (air, silicon guide, polystyrene) and the TE_0 mode of the complete waveguide at cutoff thicknesses** for successively higher order modes of the partial structure. The sharp peaks on the attenuation curve, for the four-layer structure, occur whenever the guided wave is strongly coupled into the high-loss modes of the silicon partial structure; conversely, the sharp nulls of apparently zero coupling efficiency occur at thicknesses midway between the values for two adjacent leaky modes of the partial structure. This is similar to the results of power transfer calculations for linearly tapered directional couplers (3, 4). The abrupt transitions on the mode index curve of the complete structure occurs when the phase match condition is satisfied and the guided wave couples into successively higher order modes of the partial structure.

We now consider our results in terms of the electric and magnetic field distributions at the local maximum/minimum points on the attenuation vs. silicon thickness curve. The real part of the TE_0 mode electric field profile in the transverse direction is shown for a cladding thickness, t_2 = .007 micrometers (Figure 8(a)). We recall that this thickness is below the cutoff value for the silicon waveguide structure; note that the wave function profile is not appreciably distorted.

For the first local minimum (t_2 = .05μm), we observe that the field strength at the silicon-dielectric interface approaches zero. We also note the exponentially decaying solutions in the outer, semi-infinite layers as expected. For the first local maximum (t_2 = .09μm), we observe a sharp peak in the wave function profile at the silicon-dielectric interface as coupling to the TE'_1 mode of the silicon guide occurs (Figures 8(b) and 8(c)).

Similar behavior is noted for the next local minimum/maximum pair, Figures 9(a) and 9(b), (t_2 = .13μm and t_2 = .18μm). The field strength is effectively zero at the silicon-dielectric interface for the local minimum, and a sharp peak in the wave function is evident for the local maximum as coupling to the TE'_2 mode of the silicon guide occurs. We also note that the field begins to oscillate in the semiconductor cladding as we couple into the higher order modes of the silicon waveguide structure.

Again, for the next local minimum/maximum pair (t_2 = .22μm and t_2 = .26μm) the number of field oscillations in the silicon increases. (See figures 9(c) and 9(d).) The increase or reduction in field strength at the silicon-dielectric interface is also apparent. At this local maximum (t_2 = .26μm), there is the sharp field peak at the interface, but the field decays rapidly through the dielectric indicating almost complete energy transfer. For the other maxima cases considered, the sharp

---

* TE'_1 denotes guided modes in the semiconductor and TE_i denotes guided modes in the dielectric.

** Cutoff for the silicon guide occurs when $(\beta/K)_{Si} < n_{polystyrene}$.

peak was evident at the interface, however, a sizable field was still present in the polystyrene dielectric. This indicates that the local maximum (and likely, minimum) values used for the calculations are not the precise values as in the former case (Figures 9(a) and 9(b)).

The field plots indicate, then, that the attenuation and mode index of the four-layer structure may be explained quite simply as a coupling between the basic three-layer lossless waveguide (air-dielectric-substrate) modes and the high loss TE' modes of the silicon guide. For a local minimum on the attenuation-thickness curve, the field at the semiconductor interface is zero, and for a local maximum, a sizable field is set up at the interface which decays rapidly through the guide and substrate. Finally, the number of field oscillations in the silicon increases as we couple into the higher order modes of the partial structure.

REDUCTION IN ATTENUATION THROUGH USE OF FIVE-LAYER STRUCTURE

Thin dielectric buffer layers have been used to lower the attenuation losses of metal-clad dielectric waveguides (5). These layers are placed between the dielectric core and the metal, and act as buffers to remove a large portion of the field from the metal claddings. We now consider the effect of an SiO_2 buffer layer on the attenuation vs. silicon thickness characteristics.

The result for an SiO_2 buffer layer ($\varepsilon_r = 2.12$) of several different thicknesses is shown in Figure 10. We note the familiar damped sinusoidal behavior and the corresponding reduction in attenuation.

The result for an SiO_2 buffer layer ($t_{SiO_2} = 2000\text{Å}$) of several different permittivities is shown in Figure 11. Again we note the damped sinusoidal behavior and the corresponding reduction in attenuation.

Our studies indicate, then, that the attenuation may be reduced significantly with an SiO_2 buffer layer while still preserving the oscillatory behavior of the attenuation curve; more effective reduction is accomplished with a lower permittivity buffer layer. Also, a buffer layer increases the β/K values slightly but decreases the amplitude of the oscillations on the β/K-thickness curve.

CONCLUSIONS

Computer modeling studies on four-layer silicon-clad dielectric waveguides indicate that the attenuation (α) and mode index (β/K) behave as exponentially damped sinusoids as the silicon thickness is increased. The observed effect can be explained quite simply as a periodic coupling between the guided modes of the lossless structure and the lossy modes supported by the high-refractive index silicon. Furthermore, the attenuation and mode index are significantly altered by conductivity changes in the silicon; an amplitude modulator and an intensity modulator have been proposed using these results. Predicted high attenuations in the device may be reduced significantly with a silicon dioxide buffer layer between the semiconductor and the polystyrene guide.

Experimental confirmation of the predicted characteristics is still necessary. A number of thin-silicon film waveguides have been RF sputtered but attenuation measurements to verify the damped oscillatory behavior are forthcoming. Conductivity variations of the silicon should demonstrate the modulation capabilities.

REFERENCES

1. Batchman, T.E.: Investigation of Direct Integrated Optics Modulators - Applicable to Data Preprocessors. UVA/528171/EE80/102 (NASA Grant NSG-1567), Univ. of Virginia, Mar. 1980. (Available as NASA CR-162894)

2. Smith, Robert G., and Mitchell, Gordon C., "Calculation of Complex Propagating Modes in Arbitrary, Plane-Layered Complex Dielectric Structures", E.E. Tech. Report No. 206, University of Washington, National Science Foundation Grant; Eng. 76-09937.

3. Jones, Alan L., "Coupling of Optical Fibers and Scattering in Fibers", J. Opt. Soc. Amer., Vol. 55, No. 3, March 1965, pp. 261-71.

4. Smith, Robert B., "Analytic Solutions for Linearly Tapered Directional Couplers", J. Opt. Soc. Amer., Vol. 66, No. 9, September, 1976, pp. 882-92.

5. Rashleigh, S. C., Planar Metal-Clad Dielectric Optical Waveguides, Ph.D. Thesis, University of Queensland, Brisbane, Australia, May, 1975, pp. 190-220.

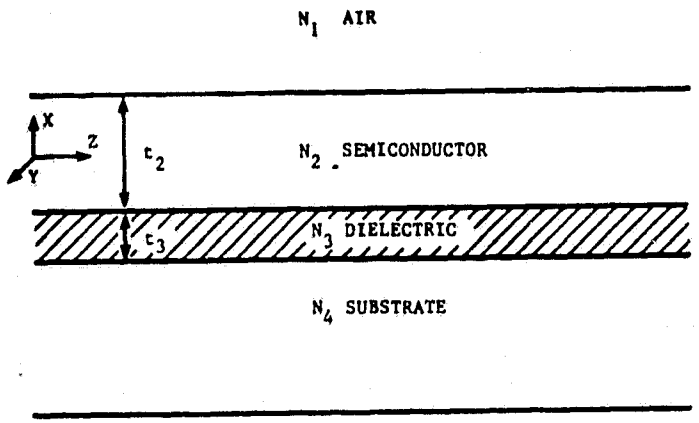

Figure 1.- Four-layer planar waveguide structure.

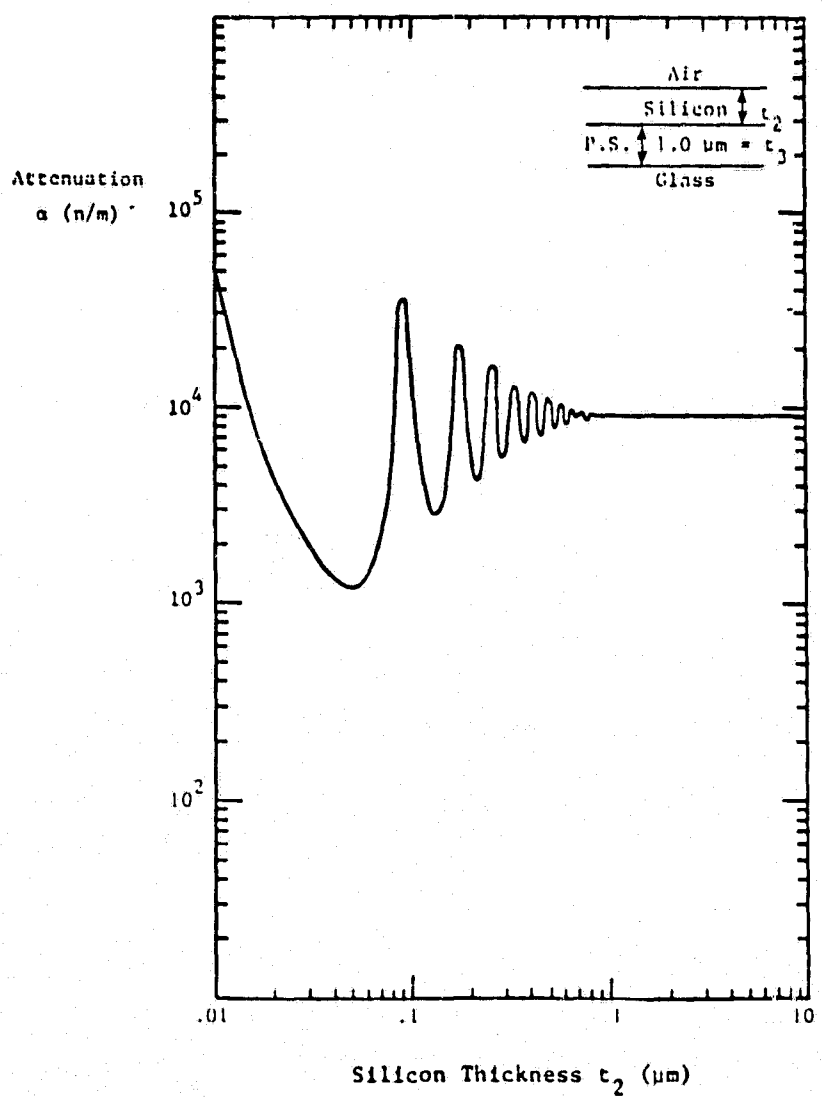

Figure 2.- Attenuation characteristics of silicon-clad waveguide (TE_0 mode, normal conductivity).

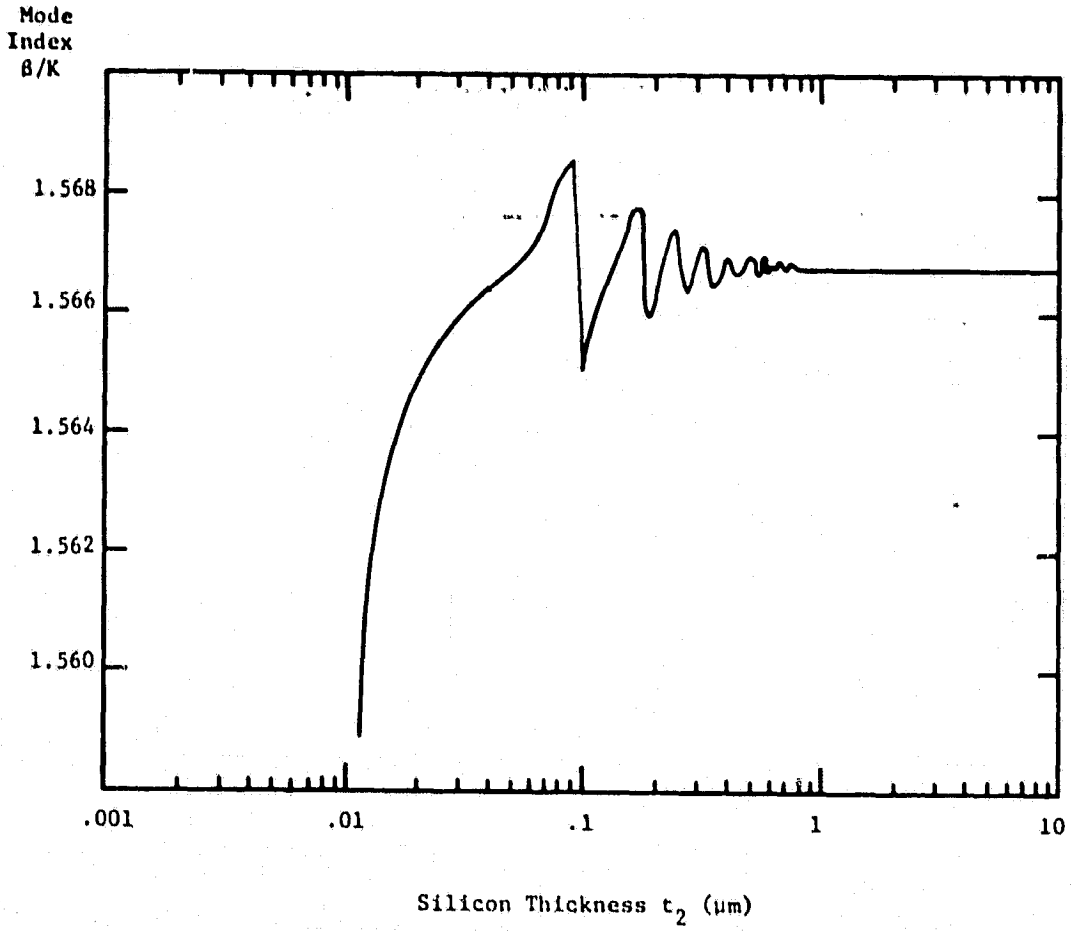

Figure 3.- Mode index characteristics of silicon-clad waveguide (TE_0 mode, normal conductivity).

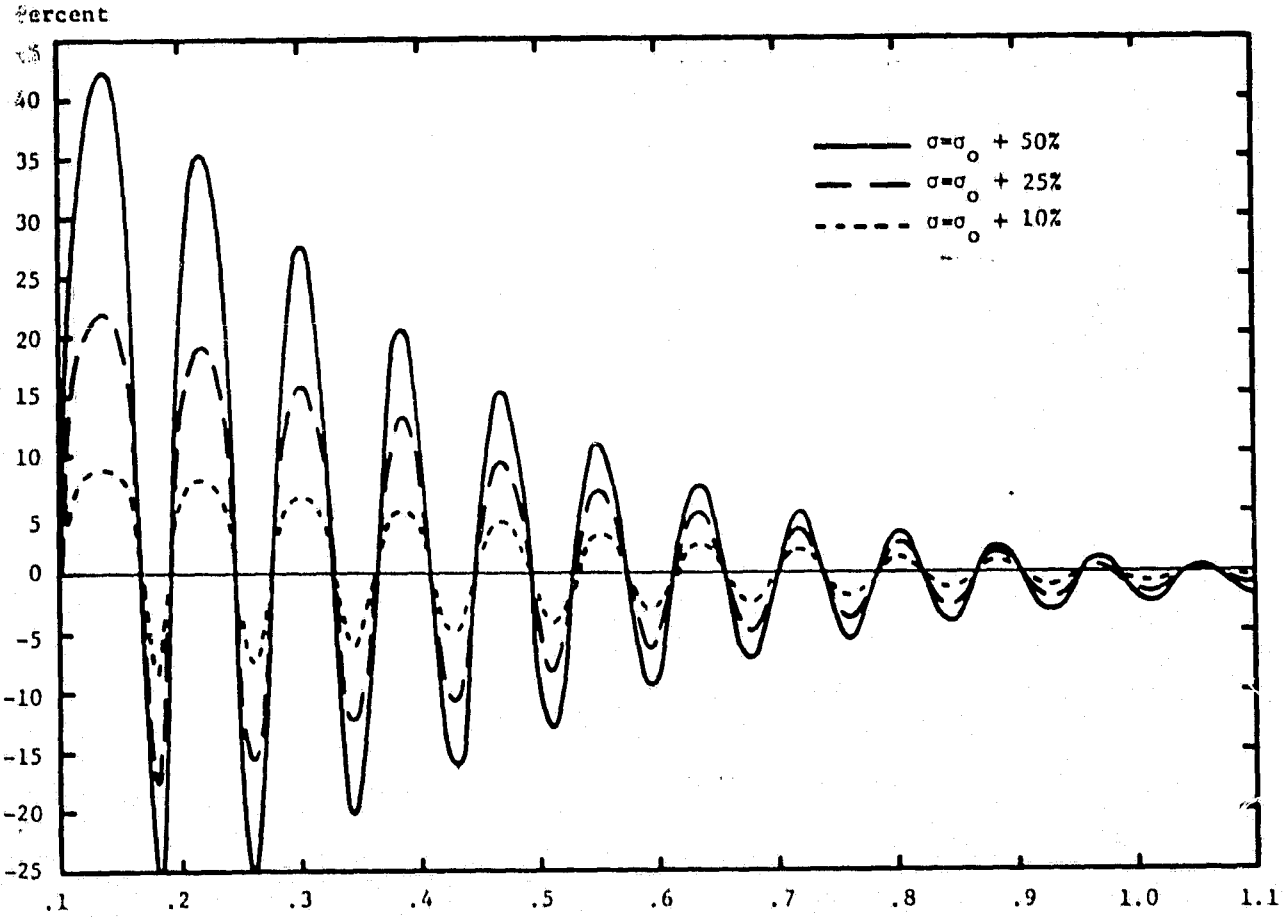

Figure 4.- Change in attenuation with relative change in conductivity (σ_o).

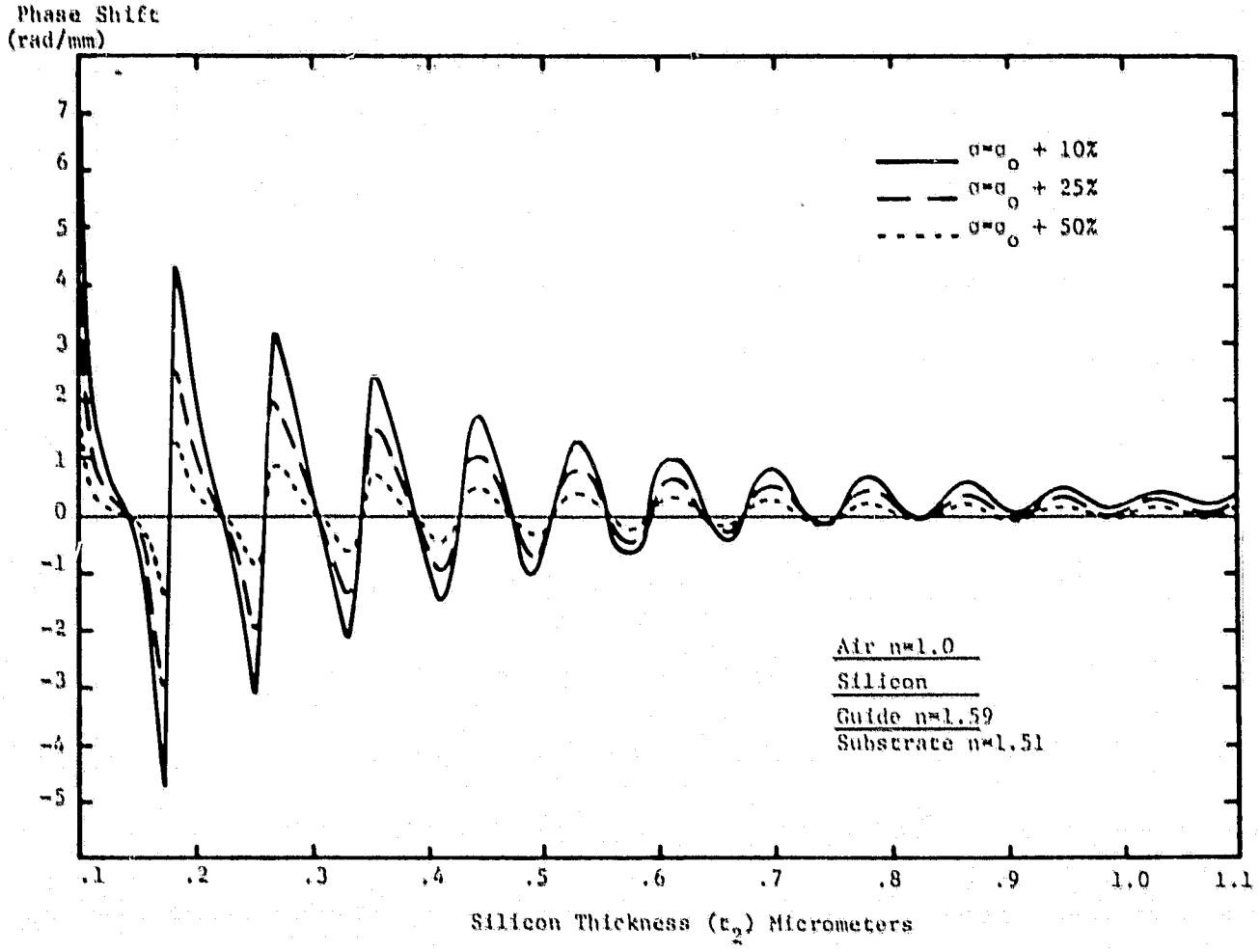

Figure 5.- Change in mode index with relative change in conductivity (σ_o).

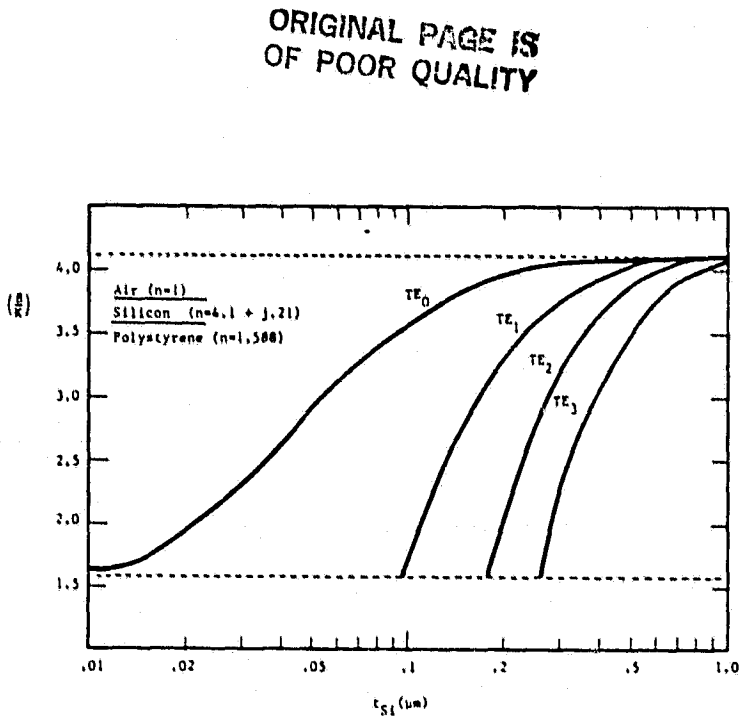

Figure 6.- Attenuation characteristics of silicon waveguide.

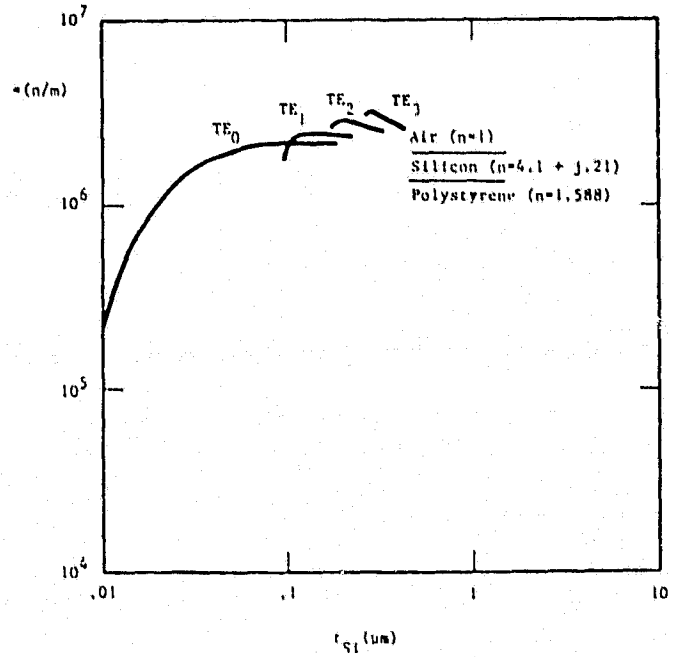

Figure 7.- Mode index characteristics of silicon waveguide.

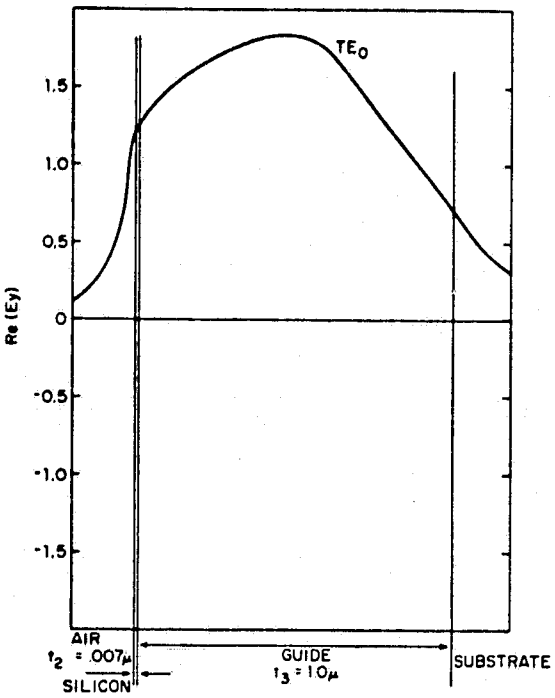

(a) t_{Si} = 0.007μm (below cutoff).

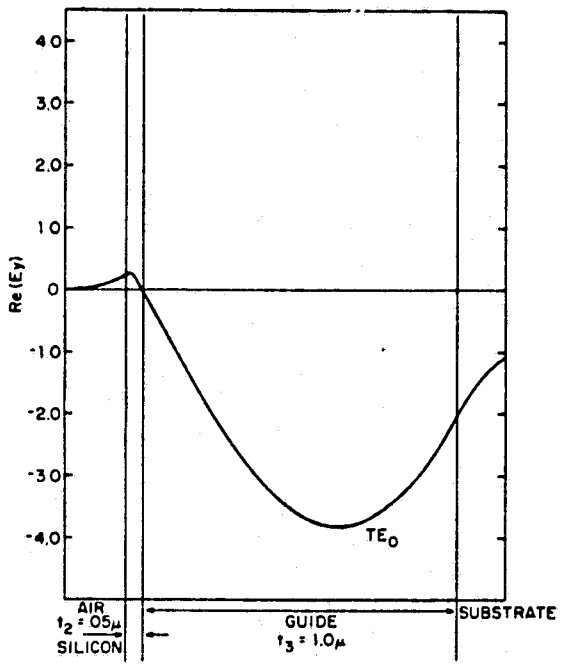

(b) t_{Si} = 0.05μm (local minimum).

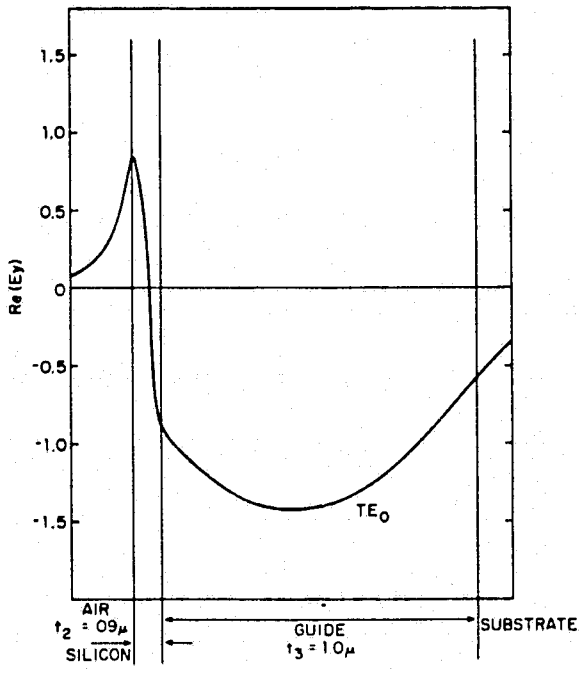

(c) t_{Si} = 0.09μm (local maximum).

Figure 8.- Wave function profile.

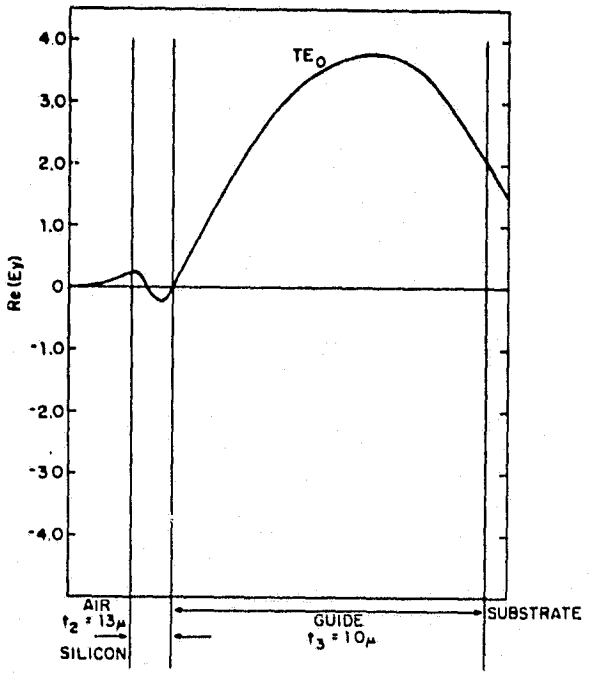

(a) t_{Si} = 0.13μm (local minimum).

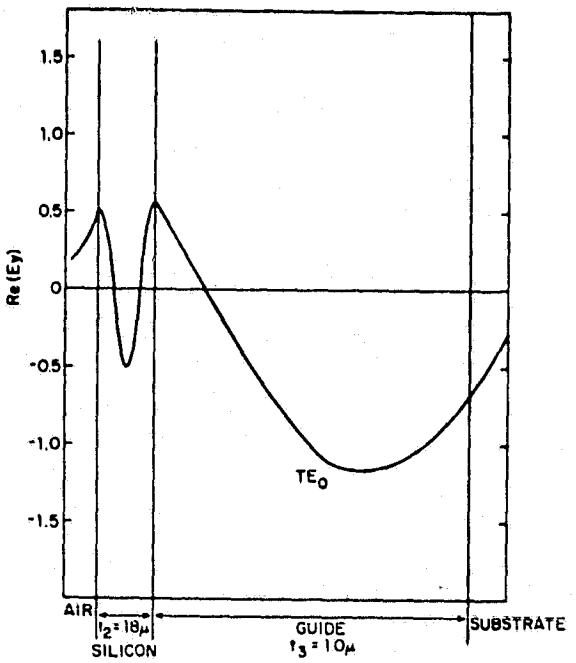

(b) t_{Si} = 0.18μm (local maximum).

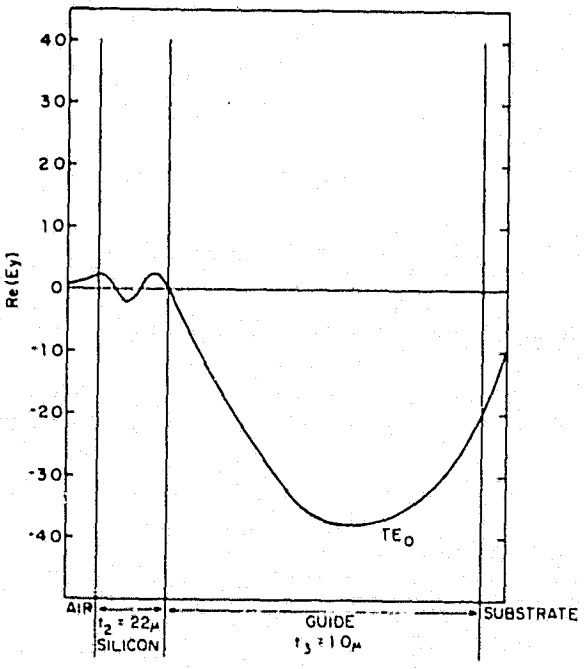

(c) t_{Si} = 0.22μm (local minimum).

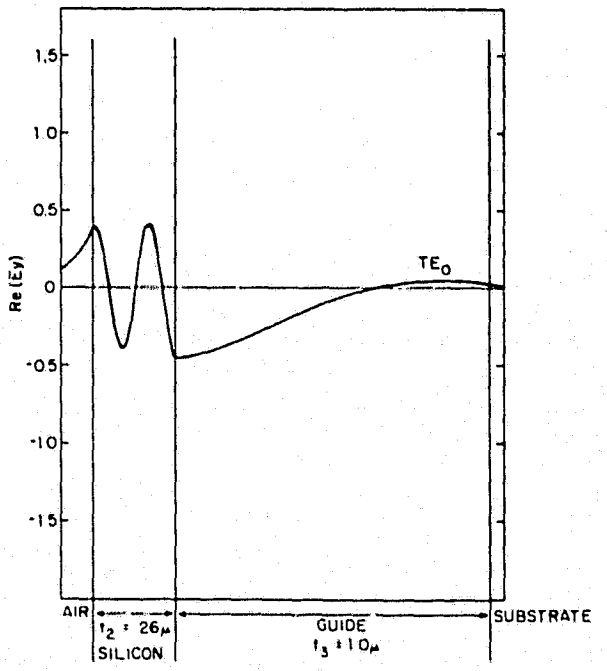

(d) t_{Si} = 0.26μm (local maximum).

Figure 9.- Wave function profile.

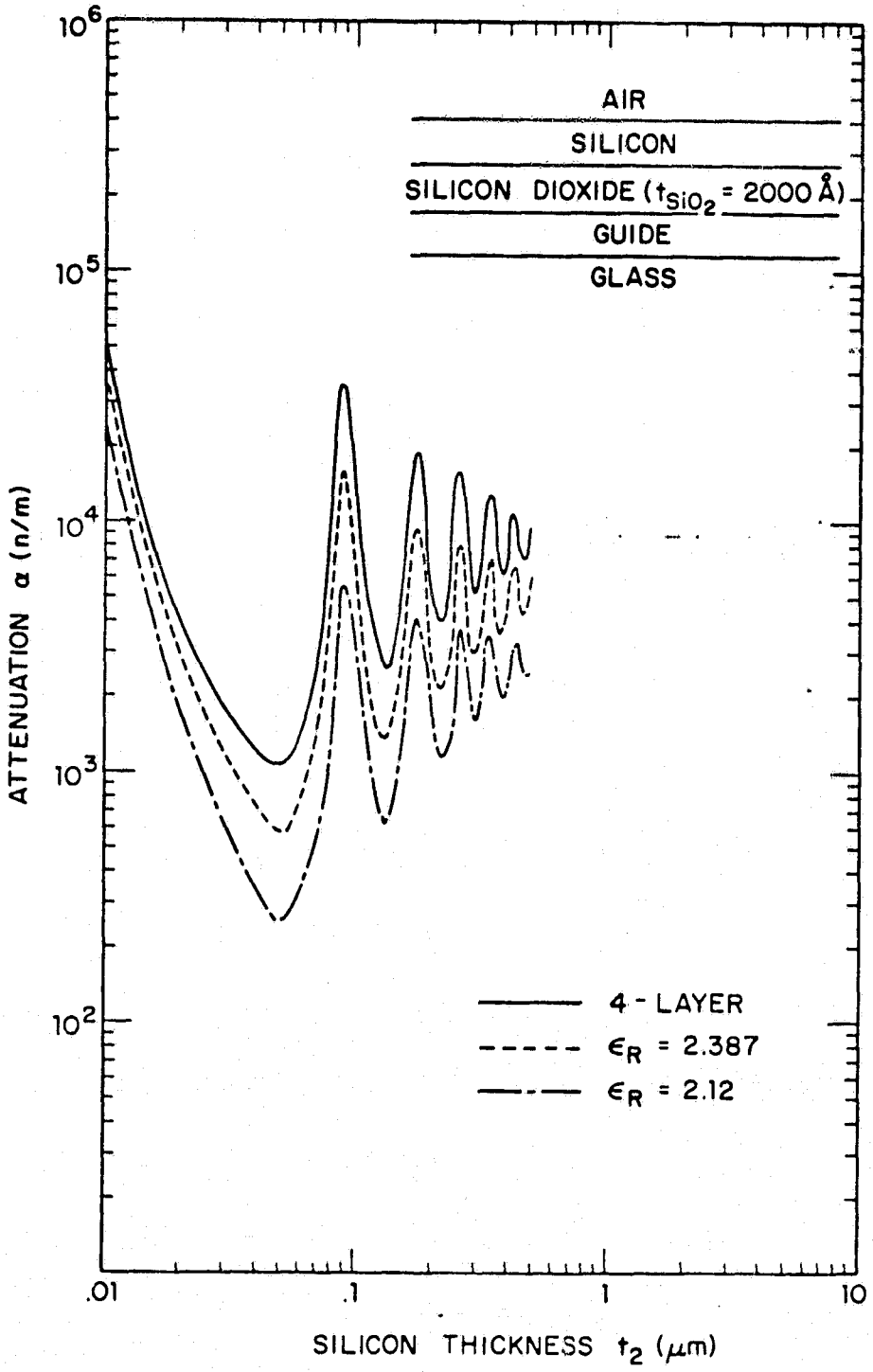

Figure 10.- SiO_2 buffer layer (ε_r = 2.12) of different thicknesses.

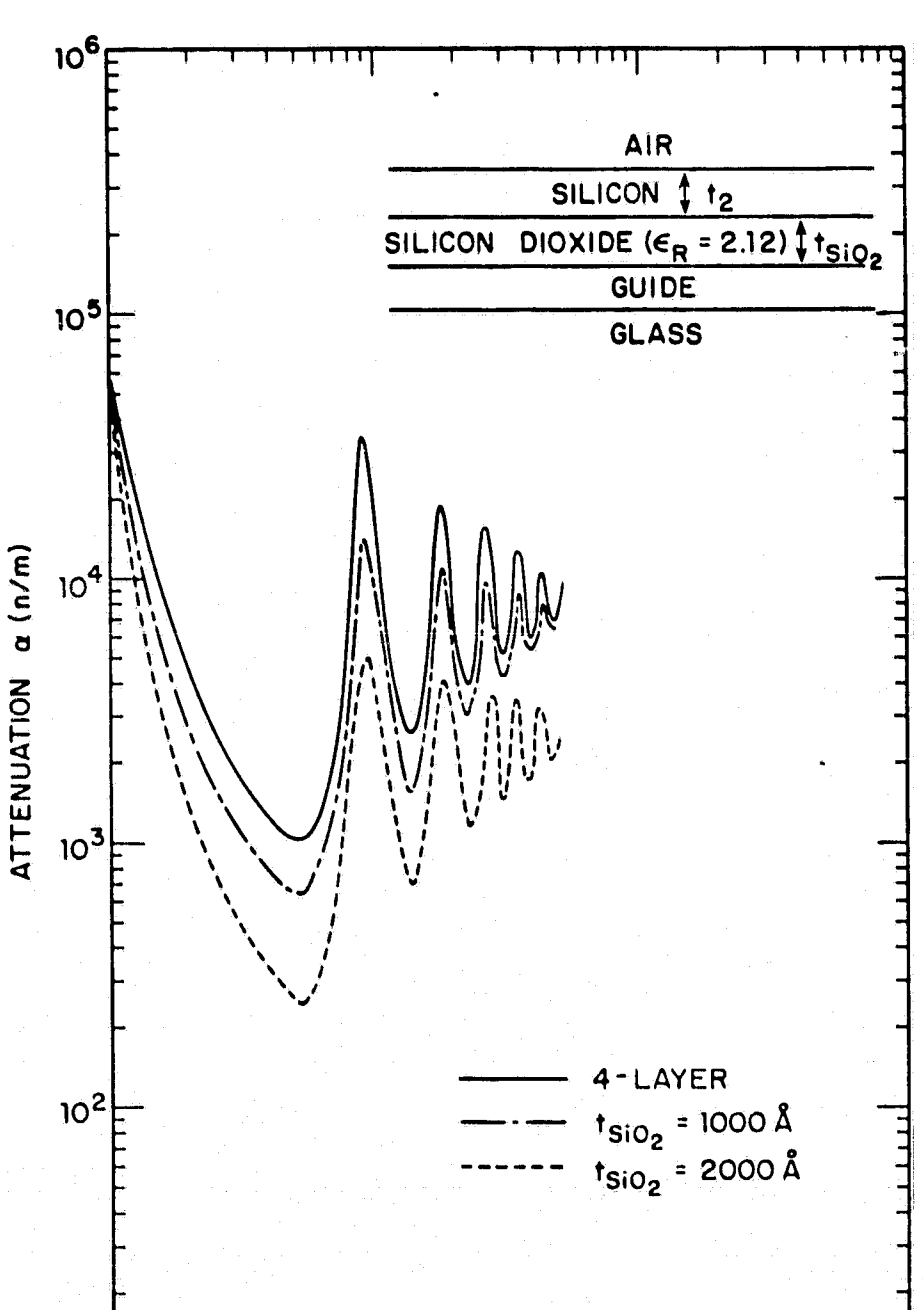

Figure 11.- SiO_2 buffer layer (t_{SiO_2} = 2000Å) of different permittivities.

Mode Coupling Between Dielectric and Semiconductor Planar Waveguides

T. E. BATCHMAN, MEMBER, IEEE, AND GLEN M. MC WRIGHT, STUDENT MEMBER, IEEE

Abstract—Computer modeling studies on four-layer silicon-clad planar dielectric waveguides indicate that the attenuation and mode index behave as exponentially damped sinusoids when the silicon thickness is increased. This effect can be explained as a periodic coupling between the guided modes of the lossless structure and the lossy modes supported by the high refractive index silicon. Furthermore, the attenuation and mode index are significantly altered by conductivity changes in the silicon. An amplitude modulator and phase modulator have been proposed using these results. Predicted high attenuations in the device may be reduced significantly with a silicon dioxide buffer layer.

I. Introduction

THERE has been considerable interest in metal-clad optical waveguides since they are used for electrooptic and magnetooptic devices [1]-[10]. It has also been suggested that metal-clad optical guides be used as polarizers for integrated optics [11]. Semiconductor-clad or positive-permittivity metal-clad waveguides have been analyzed more recently, and measurements have confirmed the predicted characteristics of such guides [12], [13]. Both the metal- and semiconductor-clad guides are extremely lossy in the visible region, especially when the waveguide thickness is thin enough to preclude all but the lowest order TE or TM modes from propagation. Partly because of these high losses, semiconductor-clad waveguides have found few applications in integrated optical devices, although it has been suggested by Lee *et al.* [14] that such waveguides be used for optical control of millimeter-wave propagation in dielectric waveguides. The calculations presented here will suggest two applications for these clad waveguides in the optical propagation region.

The permittivity of a lossy material is given by

$$\hat{\epsilon}_r = \epsilon' - j\epsilon'' = \epsilon' - j\frac{\sigma}{\omega\epsilon_o} \tag{1}$$

where σ is the conductivity of the metal at frequency ω. The permittivity can also be expressed in terms of the refractive index as

$$\hat{n} = \hat{\epsilon}^{1/2} = n - jk \tag{2}$$

where n and k are the real and imaginary parts of the refractive index, respectively. Although values for these parameters are sometimes hard to find, they are usually available for bulk semiconductors [15]. Values for amorphous and polycrystalline films formed by vacuum deposition are not as readily available [16], [17] since they often depend on the deposition technique used. The complex nature of the material permittivity makes the analysis of even planar waveguide structures difficult, and thus, elaborate computer solution techniques must be employed. Although Lee *et al.* [14] have shown that both the real and imaginary parts of the permittivity vary with incident light intensity, the variation in the real part can be shown to be relatively small compared to the imaginary part. It has thus been assumed that if light is incident on the semiconductor cladding, then the major change will be in the conductivity, which is given by

$$\sigma = \sigma_o + e\,\Delta n(\mu_e + \mu_h) \tag{3}$$

where μ_e and μ_h are the electron and hole mobilites, respectively. The dark conductivity σ_o is then changed by the creation of a number of hole-electron pairs $\Delta n = \Delta p$. The total conductivity, and consequently, complex permittivity of any semiconductor can thus be changed by the creation of hole-electron pairs.

During an investigation of planar waveguide structures which utilize this externally induced permittivity change, it was discovered that these structures exhibit periodic coupling between modes in the dielectric waveguide and a semiconductor cladding. It was further noted that changes in the conductivity of this lossy semiconductor cladding produced relatively large changes in the attenuation and phase constants of the propagating mode in the dielectric waveguide. The periodic coupling and the resulting modulation effects are discussed in detail in the following paragraphs.

II. Theory and Notation

The four-layer planar waveguide structure under consideration is shown in Fig. 1 where the guided light is propagating in the z-direction in the dielectric (N_3), and it is assumed there is no variation in the y-direction. All materials are lossless except for the semiconductor (N_2). The dispersion relations for this structure are well known, and two methods of solution for the complex mode propagation constant ($\alpha + j\beta$) have been described previously [8], [18].

In the first technique, the operator selects initial guesses for α and β and convergence factors for error estimation. The computer then uses a random walk technique to calculate values for α and β satisfying the dispersion relation for the structure of interest [8]. In the second method, matrices are created for each layer based on given constraints and a characteristic matrix for the entire structure is obtained. Solving

Manuscript received September 2, 1981; revised October 2, 1981. This work was supported by the NASA Langley Research Center.

The authors are with the Department of Electrical Engineering, University of Virginia, Charlottesville, VA 22901.

0018-9197/82/0400-0782$00.75

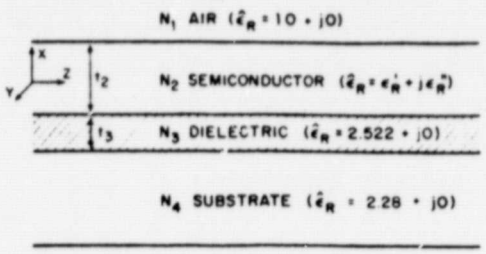

Fig. 1. Four-layer planar waveguide structure.

for the eigenvalues yields the complex mode propagation constant. Calculations presented here were originally obtained using the dispersion relation approach and later confirmed with the eigenvalue method [18].

The waveguide consists of a semi-infinite glass substrate, a dielectric core of thickness 1 μm, a semiconductor cladding varying from 0.01 to 10 μm in thickness, and a semi-infinite layer of air. A free-space wavelength of 632.8 nm was assumed, and all material parameters shown in Fig. 1 are for this wavelength. The three most common semiconductors, silicon, gallium arsenide, and germanium, were used as the cladding layer, and relative permittivity values are summarized in Table I. Bulk values have been used where data were not available for thin films. As previously noted, the refractive index of thin amorphous semiconductor films depends on the method of deposition and any impurities deliberately or accidently added to the semiconductor [19], [20]. Measurements of deposited films will thus be required before experimental results can be compared to the predictions presented here.

III. Comparison of Cladding Materials

Silicon was selected as the first semiconductor cladding material to be investigated, and the attenuation and phase constant curves of Figs. 2 and 3 were generated by varying the cladding thickness from 0.01 to 10 μm. (The phase constant β has been normalized by $k_o = 2\pi/\lambda_o$ so that all curves show the mode index.) All other parameters were held constant in these calculations and results were confirmed by using both computer solution techniques [8], [18]. It was initially expected that decreasing the lossy cladding thickness to 0.01 μm would reduce the attenuation to zero in a well-behaved manner; however; the results were not as expected below a silicon thickness of 1.0 μm. The curves are similar to exponentially damped sinusoids, with extreme values of the mode index (β/k_o) curves corresponding to the median values (maximum slope) in the attenuation (α) curves. Extreme values of the α curve correspond to median values in the β/k_o curves and the oscillations in both curves approach the median value at 1.0 μm.

Since the period of these oscillations (0.08–0.09 μm) is not a fraction of the wavelength of light in the dielectric (λ_d = 0.3985 μm), it must be related to either the waveguide structure or the properties of the semiconductor cladding. Gallium arsenide, which has a complex permittivity that is nearly the same as silicon, was used for the next series of calculations. The attenuation and phase characteristics were almost identical to those of silicon, and varying the dielectric waveguide thickness t_3 to 0.8 μm had little effect on the characteristics.

TABLE I
Semiconductor Parameters at λ = 632.8 nm

Material	Relative Permittivity ε_r'	Relative Permittivity ε_r''	Refractive Index n	Refractive Index k
Silicon*	16.76	1.75	4.1	0.213
Gallium Arsenide	14.3	1.21	3.79	0.16
Germanium*	14.43	19.54	4.4	2.22

* values for amorphous thin films

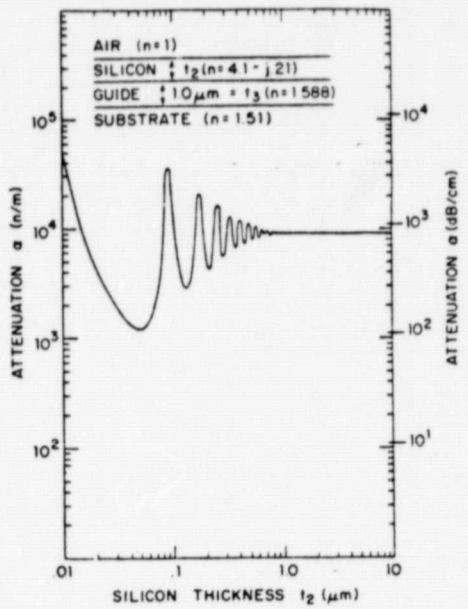

Fig. 2. Attenuation characteristics of silicon-clad waveguide (TE_0 mode, normal conductivity).

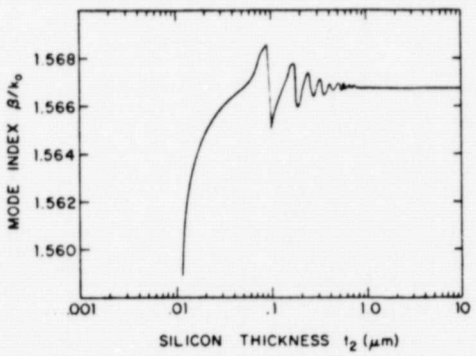

Fig. 3. Mode index characteristics of silicon-clad waveguide (TE_0 mode, normal conductivity).

The dielectric and glass layers were interchanged (i.e., glass substrate, GaAs, dielectric, air) and the rate of exponential decay increased, but the period remained constant.

As Table I indicates, the permittivity of germanium has a significantly larger imaginary part and would thus be expected to have the largest effect on the observed characteristics. Figs. 4 and 5 show that the larger conductivity of germanium nearly eliminates the damped oscillatory behavior in the thickness region of interest. The damping is so rapid that it is difficult to determine an oscillation period.

A similar effect had been noted by Heavens [21] and Strat-

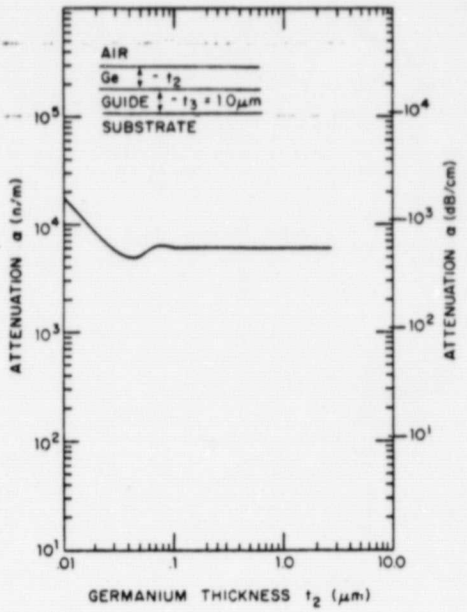

Fig. 4. Attenuation characteristics of germanium-clad waveguide.

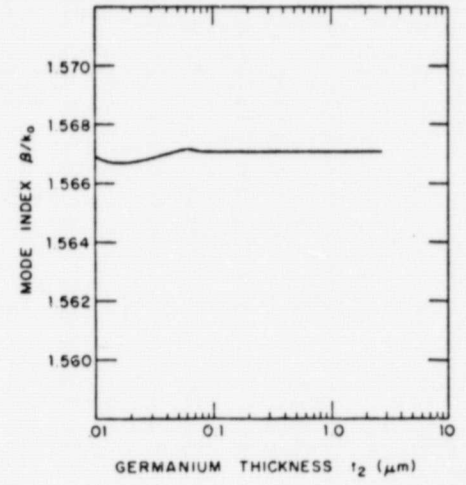

Fig. 5. Mode index characteristics of germanium-clad waveguide.

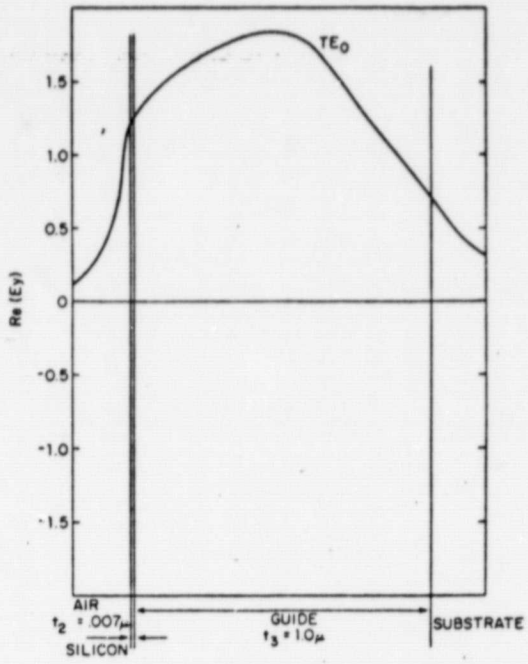

Fig. 6. Wave function profile, t_{Si} = 0.007 μm.

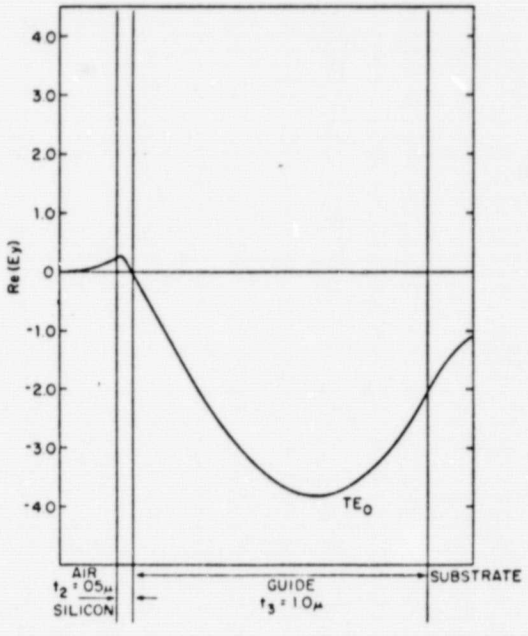

Fig. 7. Wave function profile, t_{Si} = 0.05 μm (local minimum).

ton [22] for semiconductor and metal films, respectively. Heavens considers thin films of a material with $n = 2$ and k varying, and calculates the expected phase change on reflection of a normally incident wave on an air-film surface. For very small k, the phase change oscillates, while for large k, the phase changes very little until the film thickness approaches zero. Neither author makes use of this property or considers such materials as waveguide claddings. To better understand the oscillatory behavior, the electric and magnetic field distributions in the four-layer waveguide were examined at the local maxima and minima points on the attenuation versus silicon thickness curve. The real part of the TE_0 mode electric field profile in the transverse direction is shown for a cladding thickness $t_2 = 0.007$ μm (Fig. 6). Note that the profile is everywhere positive and not appreciably distorted from that for the TE_0 mode of a three-layer lossless dielectric waveguide.

For the first local minimum at $t_2 = 0.05$ μm, the field begins to oscillate and crosses the zero axis at the silicon-dielectric interface (Fig. 7). For the local maximum at $t_2 = 0.09$ μm, the wave function profile has a sharp peak at the interface and oscillations continue (Fig. 8). Similar behavior is observed for the next local minimum and maximum pair ($t_2 = 0.13$ μm and $t_2 = 0.18$ μm, respectively). The field strength is effectively zero at the silicon-dielectric interface for the minimum and reaches a sharp peak at the interface for the maximum point on the attenuation curve.

As Figs. 9 and 10 indicate, this behavior continues for the next minimum and maximum pair ($t_2 = 0.22$ and 0.26 μm, respectively). It is now evident that the field in the silicon adds another $\frac{1}{4}$ cycle of oscillation between each maxima and

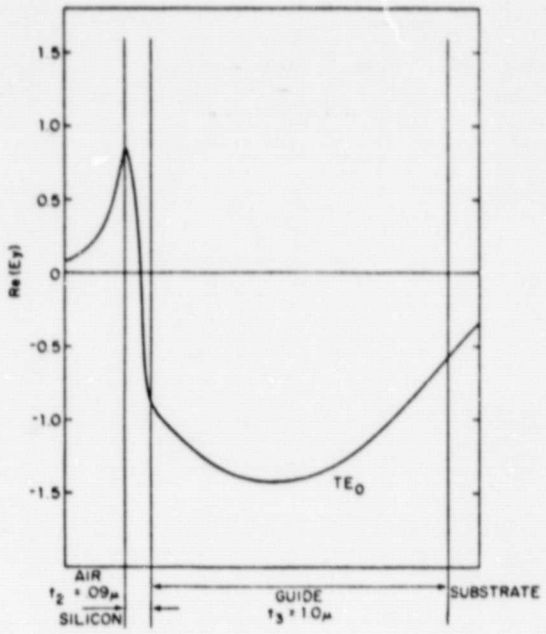

Fig. 8. Wave function profile, $t_{Si} = 0.09$ μm (local maximum).

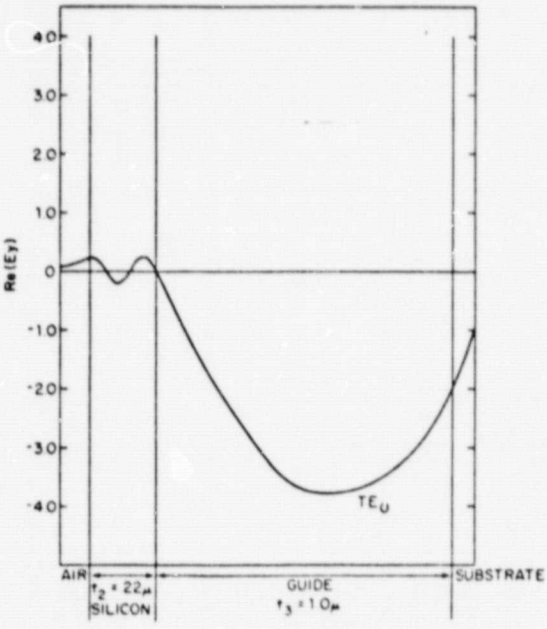

Fig. 9. Wave function profile, $t_{Si} = 0.22$ μm (local minimum).

minima, which suggests that as the silicon thickness increases, the energy from the dielectric waveguide couples into higher order modes in the silicon which now behaves as a lossy waveguide. Fig. 10 also exhibits the characteristic sharp peak at the interface but the field in the dielectric decays very rapidly, indicating almost complete energy transfer to the silicon. For the other maxima shown, there was still a sizable field in the dielectric waveguide, which suggests the local maxima and, likely, the minima values used for the field calculations were not the precise values. Additional calculations confirmed that a significant field again existed in the dielectric when t_2 was changed from 0.26 μm to 0.26 ± 0.005 μm.

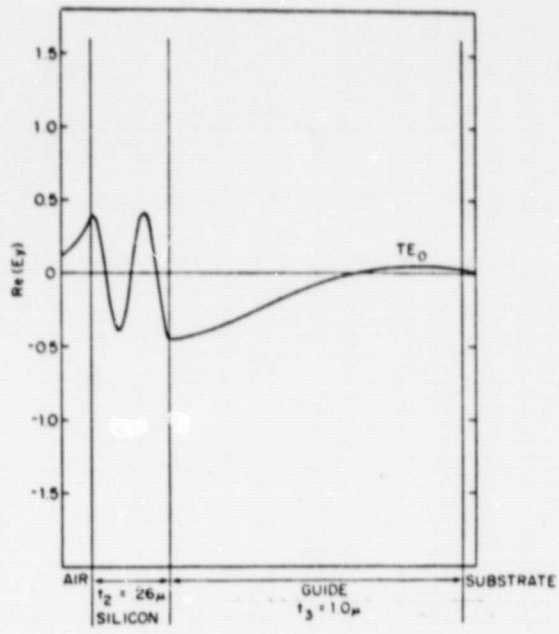

Fig. 10. Wave function profile, $t_{Si} = 0.26$ μm (local maximum).

It is evident from the field distributions that the presence of extremely thin films of silicon (<100 Å) has little effect on the dielectric waveguide; it behaves as a three-layer lossless structure (air-dielectric-substrate). For thicker silicon films, however, the TE_0 mode of the dielectric waveguide couples into the modes associated with the semiconductor film. As might be expected, the high refractive index silicon behaves as a lossy waveguide.

IV. Analysis of Coupling Characteristics

The results discussed above can be described as a periodic coupling between the guided mode (TE_0) in the dielectric and the lossy TE′ modes[1] of the semiconductor waveguide. This coupling has a profound effect on the attenuation and phase characteristics of the original four-layer waveguide. Since the field plots indicate successive coupling to higher order modes in the silicon layer, a partial structure consisting of a silicon guiding region surrounded by semi-infinite layers of air and dielectric was analyzed.

Figs. 11 and 12 show the mode index and attenuation constants for the first few low-order TE′ modes in the silicon waveguide. All modes are very lossy, and the attenuation increases for the higher order modes. In Fig. 11, note that a phase match condition between the TE′ modes of the partial structure (air-silicon-dielectric) and the TE_0 mode of the complete waveguide (Fig. 3) occurs at the cutoff thickness for successively higher order modes of the partial structure. The sharp peaks on the attenuation curve for the four-layer structure (Fig. 2) occur whenever the guided wave mode index matches that of one of the high loss TE_i' modes of the partial structure. The sharp nulls in the attenuation curve, indicating very low coupling efficiency, occur at thicknesses midway

[1] TE_i' denotes guided modes in the semiconductor and TE_i denotes guided modes in the dielectric.

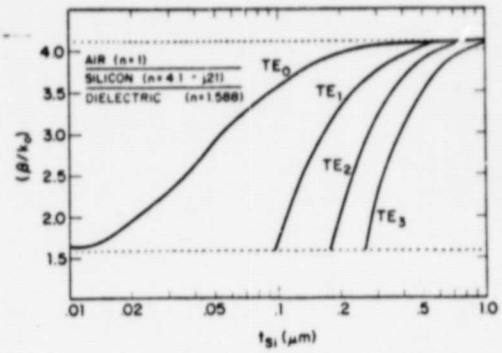

Fig. 11. Mode index characteristics of silicon waveguide.

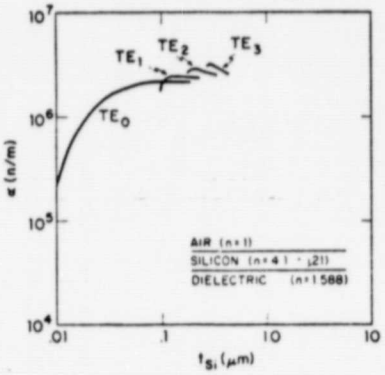

Fig. 12. Attenuation characteristics of silicon waveguide.

between the cutoff value of two adjacent lossy TE′ modes. Fig. 11 also indicates that the TE_0' mode in silicon does not cut off sharply as the higher order modes do. Lack of a well-defined cutoff is a characteristic usually associated with the TM_0 and surface wave modes [12]. The abrupt transitions on the mode index curve of the complete structure (Fig. 3) occur when the phase match condition is satisfied and the guided waves couple into successively higher order modes of the partial structure. These results are similar to the power transfer calculations for linearly tapered directional couplers [23]-[25] where the semiconductor is assumed to be lossless at the wavelength of interest.

Close examination of Fig. 2 indicates that the attenuation in the region of an oscillation minima is governed by an equation of the form

$$\alpha = K(1 - e^{-\alpha_i t_{2_i}} \cos \omega t_{2_i}) \tag{3}$$

where

K = semi-infinite attenuation of the four-layer waveguide (i.e., when $t_2 \to \infty$),
α_i = attenuation (n/m) of the three-layer silicon waveguide at thickness t_{2_i},
t_{2_i} = thickness of the silicon at any point near a local minima (i) in the range $0.1 < t_2 < 1.0\ \mu$m,
ω = period of the oscillation determined by the cutoff thickness of each TE′ mode.

For the silicon waveguide of Fig. 2, this equation becomes

$$\alpha = 9.1 \times 10^3 \left[1 - e^{-\alpha_i t_{2_i}} \cos\left(\frac{2\pi \times 10^6}{0.085} t_{2_i}\right)\right] \text{n/m}. \tag{4}$$

The field plots and the analysis of the partial structure indicate, then, that the attenuation and mode index of the four-layer structure may be explained as a coupling between the basic TE_0 mode of the dielectric waveguide and the high-loss TE′ modes of the semiconductor guide. As more TE′ modes are excited, the effect on the TE_0 mode becomes negligible and the waveguide characteristics exponentially approach those of the three-layer structures previously analyzed [12], where the semiconductor layer is considered semi-infinite.

V. Applications

The imaginary portion of the relative permittivity of a semiconductor is a linear function of the conductivity and can thus be externally varied. Based on the observed attenuation and phase characteristics of germanium-clad waveguides (ϵ_r'' large), the conductivity of silicon was increased by 10, 25, and 50 percent to confirm that the amplitude of the oscillations decrease with increasing conductivity. The attenuation and phase oscillations both decrease in proportion to the increase in conductivity of the silicon layer. The calculated percentage change in attenuation and relative phase shift with conductivity as a parameter are shown in Figs. 13 and 14, respectively. Fig. 13 shows the percentage change in attenuation compared to the normal attenuation calculated with $\sigma = \sigma_o$ (dark conductivity). The curve crosses the horizontal axis when the attenuation is equal to that of the 10 μm silicon thickness structure. Fig. 14 shows the relative change in phase shift compared to the $\sigma = \sigma_o$ value, where the phase shift is given per millimeter of length of silicon in the z-direction. Both the attenuation and phase shift changes increase with increasing conductivity, and the percentage change increases as the silicon thickness approaches 0.1 μm. Both changes are large enough to be readily measurable and useful for device application.

One device utilizing these effects would be a waveguide amplitude or phase modulator. To amplitude modulate, a film of either silicon or gallium arsenide would be deposited on a dielectric waveguide transverse (y) to the direction of propagation (z). The thickness of the film would be determined by the type of modulator desired. For example, an amplitude modulator might be constructed with a silicon thickness of 0.05 or 0.13 μm (in the x-direction). The length of the modulator in the z-direction would likely be less than 1 mm. To modulate the light wave in the dielectric guide, the semiconductor conductivity could be varied by a variety of methods including heat, electric fields, or an incident incoherent light beam with photon energy above the bandgap of the silicon. In a similar manner, a phase modulator could be constructed by selecting the semiconductor thickness to produce maximum phase shift with conductivity change.

Since even relatively short sections of semiconductor-clad waveguides are lossy (1 mm length of Si at $t_2 = 0.05\ \mu$m, $\alpha > 10$ dB), the attenuation must be reduced significantly for a practical device. Thin dielectric buffer layers are commonly used to lower the attenuation losses of metal-clad dielectric waveguides [26], [27]. These layers are placed between the dielectric core and the metal, and act as buffers to remove a large proportion of the field from the metal cladding. The effect of a silicon dioxide (SiO_2) buffer layer on the attenuation versus silicon thickness characteristics are investigated.

The results for silicon dioxide buffer layers of several different thicknesses and two different permittivities are shown

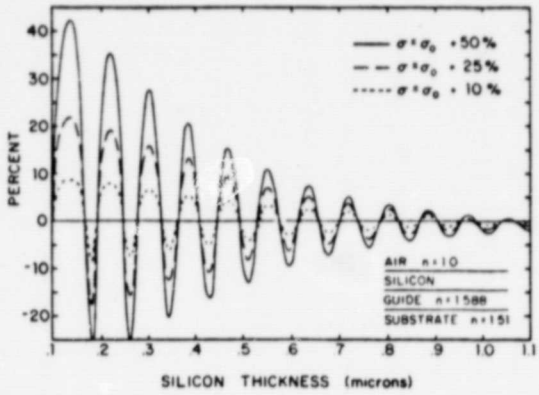

Fig. 13. Change in attenuation with relative change in conductivity (σ_0).

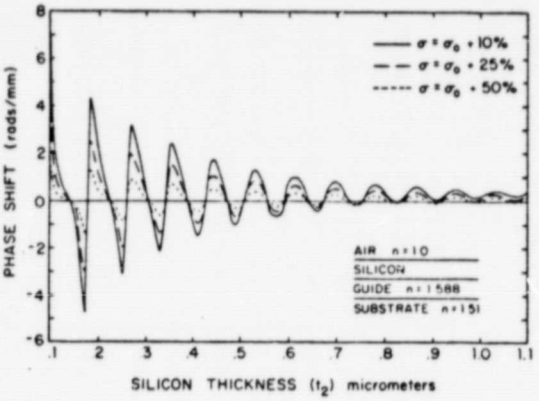

Fig. 14. Change in mode index with relative change in conductivity (σ_0).

in Figs. 15 and 16. Note that the familiar damped sinusoidal behavior is present and that the attenuation is reduced significantly. It was also found that the buffer layer increases the mode index slightly and decreases the amplitude of the oscillations, but the phase shift is still large enough to be useful for modulation.

In addition to the previously suggested tapered coupler [24], it may be possible to use the effect in a coupling or switching layer between two dielectric waveguides. If the semiconductor layer were sandwiched between two dielectric waveguides, the field coupling between the two dielectrics could be controlled by changing the conductivity of the semiconductor. The semiconductor film thickness would be selected to provide maximum field strength to the semiconductor and thus, the second waveguide. Increasing the semiconductor conductivity would then decrease the coupling between waveguides. A semiconductor film would also be applicable to fiber-to-waveguide couplers [28], [29] where the coupling could be varied through changes in the semiconductor conductivity.

VI. Conclusions

It has been shown that dielectric waveguides clad with lossy semiconductor films exhibit a damped periodic oscillation in their attenuation and phase characteristics. This is due to the periodic coupling between the lossy guided modes in the silicon film and the TE_0 mode in the dielectric waveguide. Suggested applications for this effect as modulators and waveguide switches have yet to be experimentally verified, and the practical application of such devices will depend upon how efficiently the semiconductor conductivity can be varied by an external source. Experimental devices are currently being constructed to verify the predicted effects.

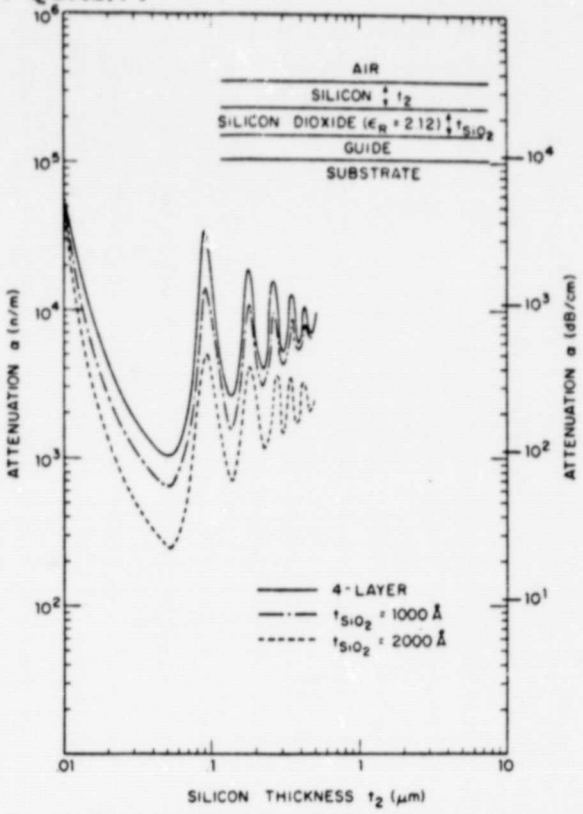

Fig. 15. SiO_2 buffer layer ($\epsilon_R = 2.12$) of different thicknesses.

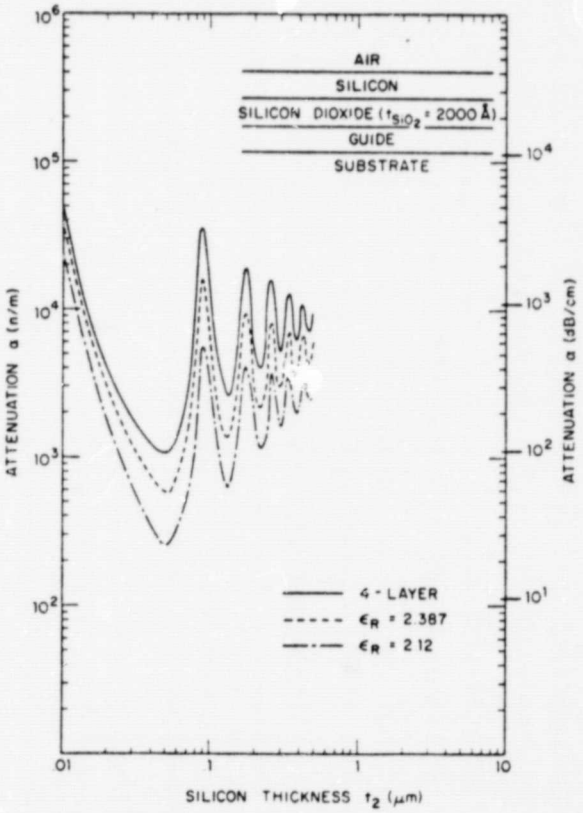

Fig. 16. SiO_2 buffer layer ($t_{SiO_2} = 2000$ Å) of different permittivities.

REFERENCES

[1] H. J. Fink, "Propagation of waves in optical waveguides with various dielectric and metal claddings," *IEEE J. Quantum Electron.*, vol. QE-12, pp. 365-367, June 1976.

[2] Y. Yamamoto, T. Kamiya, and H. Yanai, "Characteristics of optical guided modes in multilayer metal-clad planar optical guide with low-index dielectric buffer layer," *IEEE J. Quantum Electron.*, vol. QE-11, pp. 729-736, Sept. 1975.

[3] J. N. Polky and G. L. Mitchell, "Metal-clad planar dielectric waveguide for integrated optics," *J. Opt. Soc. Amer.*, vol. 64, pp. 274-279, Mar. 1974.

[4] S. C. Rashleigh, "Four-layer metal-clad thin film optical waveguides," *Opt. and Quantum Electron.*, vol. 8, pp. 49-60, Jan. 1976.

[5] I. P. Kaminow, W. L. Mammel, and H. P. Weber, "Metal-clad optical waveguides: Analytical and experimental study," *Appl. Opt.*, vol. 13, pp. 396-405, Feb. 1974.

[6] Y. Takano and J. Hamasaki, "Propagating modes of a metal-clad dielectric-slab waveguide for integrated optics," *IEEE J. Quantum Electron.*, vol. QE-8, pp. 206-212, Feb. 1972.

[7] Y. Suematsu *et al.*, "Fundamental transverse electric field (TE_0) mode selection in thin-film asymmetric light guide," *Appl. Phys. Lett.*, vol. 21, pp. 291-293, Sept. 1972.

[8] T. E. Batchman and S. C. Rashleigh, "Mode-selective properties of a metal-clad dielectric-slab waveguide for integrated optics," *IEEE J. Quantum Electron.*, vol. QE-8, pp. 848-850, Nov. 1972.

[9] E. M. Garmire and H. Stoll, "Propagation losses in metal-film-substrate optical waveguides," *IEEE J. Quantum Electron.*, vol. QE-8, pp. 763-766, Oct. 1972.

[10] Y. Yamamoto, T. Kamiya, and H. Yanai, "Propagation characteristics of a partially metal-clad optical guide: Metal clad optical stripline," *Appl. Opt.*, vol. 14, p. 322, Feb. 1975.

[11] K. H. Rollke and W. Sohler, "Metal clad waveguide as cutoff polarizer for integrated optics," *IEEE J. Quantum Electron.*, vol. QE-13, pp. 141-145, Apr. 1977.

[12] T. E. Batchman and K. A. McMillan, "Measurement on positive-permittivity metal-clad waveguides," *IEEE J. Quantum Electron.*, vol. QE-13, pp. 187-192, Apr. 1977.

[13] T. E. Batchman and J. R. Peeler, "Gallium arsenide clad optical waveguides," *IEEE J. Quantum Electron.*, vol. QE-14, pp. 327-329, May 1978.

[14] C. M. Lee, P. S. Mak, and A. P. DeFonzo, "Optical control of millimeter-wave propagation in dielectric waveguides," *IEEE J. Quantum Electron.*, vol. QE-16, Mar. 1980.

[15] D. E. Gray, Ed., *American Institute of Physics Handbook*, 2nd ed. New York: McGraw-Hill, 1963, ch. 6, pp. 103-122.

[16] M. H. Brodsky, Ed., "Amorphous semiconductors," in *Topics in Applied Physics*, vol. 36. New York: Springer-Verlag, 1979, pp. 1-7.

[17] R. Fischer, "Luminescence in amorphous semiconductors," in *Amorphous Semiconductors, Topics in Applied Physics*, vol. 36. New York: Springer-Verlag, 1979, pp. 176-180.

[18] R. G. Smith and G. C. Mitchell, "Calculation of complex propagating modes in arbitrary plane-layered complex dielectric structures," Univ. of Washington, Seattle, EE Tech. Rep. 206, Nat. Sci. Foundation Grant Eng. 76-09937, Dec. 1977.

[19] D. E. Carson, "Photo voltaics V: Amorphous silicon cells," *IEEE Spectrum*, pp. 39-41, Feb. 1980.

[20] D. E. Ackley and J. Tauc, "Silicon films as selective absorbers for solar energy conversion," *Appl. Opt.*, vol. 16, pp. 2806-2809, Nov. 1977.

[21] O. S. Heavens, *Optical Properties of Thin Solid Films*. New York: Academic, 1955, pp. 170-172.

[22] J. D. Stratton, *Electromagnetic Theory*. New York: McGraw-Hill, 1941, pp. 515-516.

[23] A. L. Jones, "Coupling of optical fibers and scattering in fibers," *J. Opt. Soc. Amer.*, vol. 55, pp. 261-271, Mar. 1965.

[24] T. K. Lim, B. K. Garside, and J. P. Marton, "An analysis of optical waveguide tapers," *Appl. Phys.*, vol. 18, pp. 53-62, Jan. 1979.

[25] R. B. Smith, "Analytic solutions for linearly tapered directional couplers," *J. Opt. Soc. Amer.*, vol. 66, pp. 882-892, Sept. 1976.

[26] D. P. Gia Russo and J. H. Harris, "Electrooptic modulation in a thin film waveguide," *Appl. Opt.*, vol. 10, pp. 2786-2788, Dec. 1971.

[27] W.S.C. Chang and K. W. Loh, "Theoretical design of guided wave structure for electrooptical modulation at 10.6 μm," *IEEE J. Quantum Electron.*, vol. QE-8, pp. 463-470, June 1972.

[28] J. M. Hammer, R. S. Bartolini, A. Miller, and C. C. Neil, "Optical grating coupling between low index fibers and high index film waveguides," *Appl. Phys. Lett.*, vol. 28, pp. 192-193, Feb. 1976.

[29] D. G. Dalgoutte, R. B. Smith, G. Achutaramayya, and J. H. Harris, "Externally mounted fibers for integrated optics interconnections," *Appl. Opt.*, vol. 14, pp. 1860-1865, Aug. 1975.

T. E. Batchman (S'61-M'66) was born in Great Bend, KS, on March 29, 1940. He received the B.S.E.E., M.S.E.E., and Ph.D. degrees in electrical engineering from the University of Kansas, Lawrence, in 1962, 1963, and 1966, respectively.

From 1966 to 1970 he was an Engineering Scientific Specialist with LTV Missiles and Space Division. In 1970 he joined the faculty of the University of Queensland, Brisbane, Australia, as a Senior Lecturer. Among his research activities at the University of Queensland were integrated optics and dynamic modeling of telecommunications systems. Since 1975 he has been on the faculty of the Department of Electrical Engineering at the University of Virginia, Charlottesville, where he is an Associate Professor. His current research activities include integrated optical devices and microwave sensors.

Dr. Batchman is a member of Eta Kappa Nu, Sigma Tau, Tau Beta Pi, and Sigma Xi.

Glen M. McWright (S'81) was born in Washington, DC, on July 6, 1958. He received the B.S. and M.E. degrees in electrical engineering from the University of Virginia, Charlottesville, in 1980 and 1981, respectively.

He is currently pursuing the Ph.D. degree, also at the University of Virginia.

Measurement and Analysis of Periodic Coupling in Silicon-Clad Planar Waveguides

GLEN M. MC WRIGHT, STUDENT MEMBER, IEEE, T. E. BATCHMAN, MEMBER, IEEE, AND
M. S. STANZIANO, STUDENT MEMBER, IEEE

Abstract—Computer modeling studies indicate that planar dielectric waveguides clad with silicon exhibit a damped periodic oscillation in their attenuation and phase characteristics. The effect is due to a periodic coupling between the lossy, guided modes in the silicon film and the TE_0 mode of the dielectric waveguide. Experimental confirmation of the periodic coupling for a wavelength of 632.8 nm is presented. Propagation characteristics for a wavelength of 1150 nm were investigated for application in integrated optical modulators. Frequency filtering properties of silicon-clad waveguides are also examined and it is shown that the silicon thickness controls the filter response curve.

Manuscript received March 1, 1982; revised May 13, 1982. This work was supported by the NASA Langely Research Center.

The authors are with the Department of Electrical Engineering, University of Virginia, Charlottesville, VA 22901.

I. Introduction

METAL-clad optical waveguides have been studied extensively and have found considerable application in electrooptic and magnetooptic modulators [1]-[5]. Semiconductor-clad or positive permittivity metal-clad waveguides are characterized by high attenuations which have severely limited their application, although they may be useful as cutoff polarizers or attenuators [6], and more recently, for optical control of millimeter wave propagation [7], [8]. We discuss further applications for these semiconductor-clad waveguides [9] and report, in this paper, the experimental confirmation of the predicted characteristics. Frequency filtering is also suggested as an application for these clad guides in the optical propagation region based on predictions presented here.

0018-9197/82/1000-1765$00.75

The permittivity of a semiconductor is given by

$$\epsilon_R = \epsilon' - j\epsilon'' = \epsilon' - \frac{j\sigma}{\omega\epsilon_o} \tag{1}$$

where σ is the conductivity of the material at frequency ω. This can also be expressed in terms of the refractive index of the semiconductor as

$$\hat{n} = \epsilon^{1/2} = n - jk \tag{2}$$

where n and k are the real and imaginary parts of the refractive index, respectively. Values for the thin amorphous semiconductor films of interest are highly dependent on the preparation technique used [10].

Lee *et al.* [7] have shown that both the real and imaginary portions of the permittivity vary with incident light; however, the variation in the real part is small compared to the imaginary portion. It is assumed, then, that if light is incident on the semiconductor film, electron-hole pairs are created and only the conductivity varies according to

$$\sigma = \sigma_o e \Delta n(\mu_e + \mu_h)$$

where μ_e and μ_h are the electron and hole mobilities, respectively, and Δn is the number of generated electron-hole pairs. The imaginary portion of the permittivity is thus changed proportional to the number of generated pairs.

As previously reported [9], planar waveguide structures utilizing this externally induced conductivity change have been analyzed and it was shown that the attenuation and mode index of the propagating mode are significantly altered by conductivity changes in the semiconductor cladding. An amplitude modulator and phase modulator were proposed using these results. Furthermore, it was noted that the planar waveguide structures exhibit a periodic coupling between modes in the dielectric waveguide and semiconductor cladding. The experimental confirmation of the periodic coupling from the waveguide modes to the semiconductor cladding is discussed in Section II for propagation at 632.8 nm. Section III examines the waveguide characteristics at a wavelength below the bandgap of the silicon cladding (1150 nm). Based on the previous analysis of the characteristics of the guide at 632.8 nm and the results of Section III, it was observed that the silicon film could be used as a frequency filter. The frequency characteristics are investigated in detail in Section IV and these results suggest the use of such clad waveguides as coarse frequency filters.

II. Theory and Experimental Verification

Computer modeling studies of four-layer, silicon-clad, planar optical waveguides indicate that the attenuation behaves as a damped sinusoid with increasing semiconductor thickness [9]. Experimental confirmation of this predicted effect is presented after a brief review of previous predictions.

The four-layer planar waveguide structure under consideration is shown in Fig. 1 where the guided light is propagating in the z direction in the dielectric (N_3), and it is assumed there is no variation in the y direction. All materials are lossless except for the silicon (N_2). The dispersion relations for this structure are well known and two methods of solution

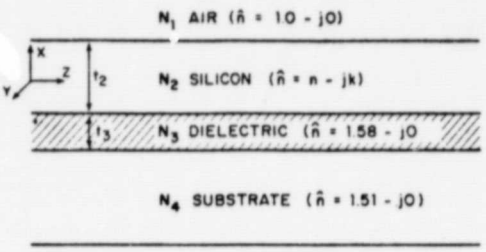

Fig. 1. Four-layer planar waveguide structure.

for the complex mode propagation constant ($\alpha + j\beta$) have been described previously [11], [12].

The waveguide consists of a semi-infinite glass substrate, a dielectric core of thickness 1 μm, a silicon cladding varying from 0.01 to 10 μm in thickness, and a semi-infinite layer of air. A free-space wavelength of 632.8 nm was assumed and all material parameters shown in Fig. 1 are for this wavelength. It should be noted that permittivity values for thin amorphous semiconductor films depend on the method of deposition and any impurities deliberately or accidentially added to the semiconductor [13], [14]. Thus, values assumed in these calculations may vary from those of the experimental films since no attempts were made to measure the permittivity of the experimental films at optical frequencies.

Silicon was investigated as a semiconductor cladding and the attenuation curve of Fig. 2 was generated by varying the cladding thickness from 0.01 to 10 μm. All other parameters were held constant in the calculations and results were confirmed using the two computer solution techniques [11], [12]. It was initially expected that decreasing the lossy cladding thickness to 0.01 μm would reduce the attenuation to zero in a well-behaved manner; however, the results were not as expected below a silicon thickness of 1.0 μm.

Experimental confirmation of the oscillatory behavior of the attenuation versus silicon thickness curve was subsequently attempted. Low-loss, single-mode optical waveguides were diffused into soda-lime glass from a sodium nitrate/silver nitrate melt using an ion-exchange fabrication technique [15]-[18]. Uniform silicon films 1 mm wide and extending across the waveguide were deposited using a radio-frequency sputtering system [19]-[21]. For each run, the system was prepumped to a base pressure less than 5×10^{-6} torr and all sputtering was performed in an argon atmosphere at a pressure of 10^{-2} torr. A number of uniform silicon films with thicknesses in the range of 0.02-0.4 μm were fabricated. High predicted attenuations in the silicon-clad guide along with severe experimental inaccuracies in either the fluid coupler or the sliding-prism attenuation measurement technique [3] has made quantitative confirmation difficult. Thus, a photographic technique was employed for confirmation of the behavior shown in Fig. 2.

As Fig. 3 indicates, qualitative confirmation of the damped oscillatory behavior of the attenuation versus silicon thickness curve has been successful. A 5 mW He-Ne (632.8 nm) laser was coupled into the silicon-clad guide using a prism coupler. Fig. 3 is a top view of the coupler and silicon-clad planar waveguide with propagation from left to right. In each of the three photographs, the coupling into the waveguide was

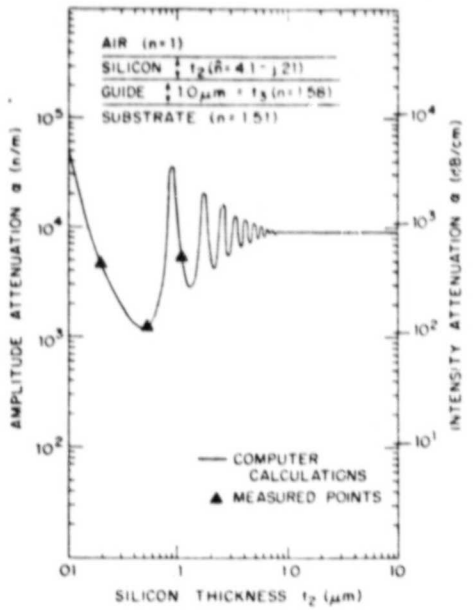

Fig. 2. Attenuation characteristics of silicon-clad waveguide (TE_0 mode, wavelength = 632.8 nm).

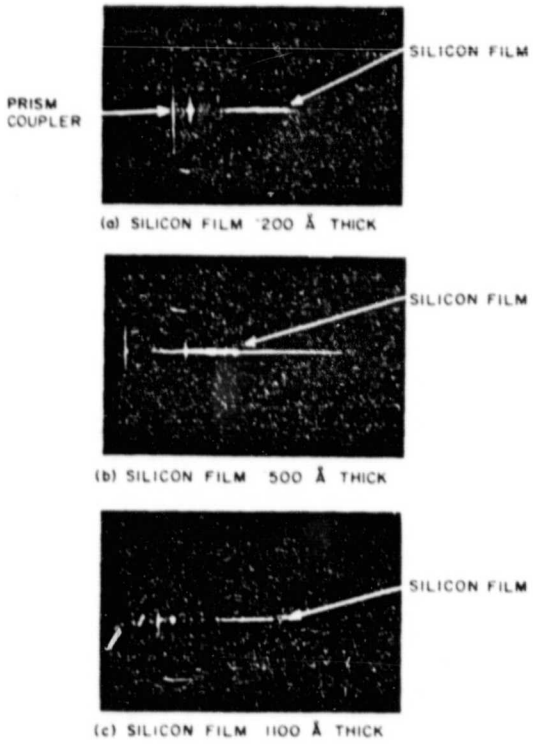

Fig. 3. Experimental measurements of waveguide attenuation.

maximized. All photographic exposures are 5 s, f2, ASA 400 film. Uninterrupted propagation occurs until the beam encounters the 1 mm wide silicon film at which point it may suffer a large attenuation. Slight differences in the beam intensity to the left of the silicon film are due to differences in coupling efficiency and scattering in the individual waveguides. For a silicon film 200 Å thick [Fig. 3(a)], the beam is clearly attenuated as computer calculations predict. For a film 500 Å thick (a predicted minimum on the attenuation thickness curve of Fig. 2) nearly uninterrupted propagation occurs [Fig. 3(b)], and for a film 1100 Å thick (a predicted region of high attenuation), the beam is again attenuated [Fig. 3(c)]. The three points labeled "measured" in Fig. 2 correspond to the film thicknesses at which the photographic exposures were taken and are not quantitative amplitude measurements. The principal conclusion which can be drawn from the data is that there is at least one minimum in attenuation which occurs in the thickness range 200–1100 Å. The existence of this local minimum between 200 and 1100 Å was similarly verified with a different set of silicon-clad waveguides. It should be noted that accurate thickness measurements are difficult for silicon films less than 200 Å and that the values for the refractive indexes used in the computer calculations may differ from those of the actual silicon-clad waveguides. Furthermore, predicted high attenuations for subsequent peaks and valleys of the attenuation versus silicon thickness curve make confirmation of the oscillatory behavior for thicker silicon films extremely difficult (i.e., the attenuation for subsequent peaks is greater than 1000 dB/cm). Additional measurements will be required to confirm the absolute attenuation levels observed.

III. Calculations and Analysis at 1150 nm

It has been predicted that the attenuation and mode index of the four-layer silicon-clad guide are significantly altered by conductivity changes in the silicon, and amplitude and phase modulators have been proposed using these results [9]. Calculations were presented for a wavelength of 632.8 nm, and modulation would be accomplished as a result of a change in the semiconductor conductivity via an incident light beam with photon energy above the bandgap of the silicon. It is evident, however, that the 632.8 nm guided wave will inadvertently excite the silicon cladding since it is above the bandgap. To circumvent this problem the wavelength was changed to 1150 nm and the amplitude and phase characteristics of the guide were analyzed. This wavelength is such that the absorption coefficient of amorphous silicon is minimal [22], [27] and appreciable excitation of the silicon cladding due to the 1150 nm guided wave is unlikely. Direct optical modulation, however, would still be realized by altering the conductivity of the silicon with a light beam with photon energy above the bandgap of silicon (in the visible region). Computer predictions of the propagation characteristics of the four-layer silicon-clad planar waveguide at 1150 nm are presented in this section.

The attenuation and phase constant curves of Figs. 4 and 5 were generated by varying the silicon cladding thickness from 0.01 to 1.0 μm (the phase constant β has been normalized by $k_o = 2\pi/\lambda_o$ so that all curves show the mode index). Material parameters shown in Figs. 4 and 5 are for a 1150 nm wavelength. The curves are again similar to exponentially damped sinusoids with extreme values of the mode index (β/k_o) coresponding to the median values (maximum slope) in the attenuation (α) curves. Extreme values of the α curve correspond to median values in the β/k_o curves and the oscillations in both curves approach a median value at 10 μm. Similar behavior was observed for a wavelength of 632.8 nm and results were described as a periodic coupling be-

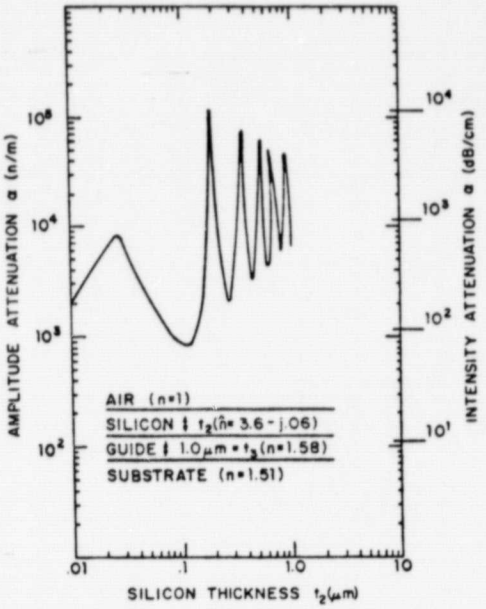

Fig. 4. Attenuation characteristics of silicon-clad waveguide (TE_0 mode, wavelength = 1150 nm).

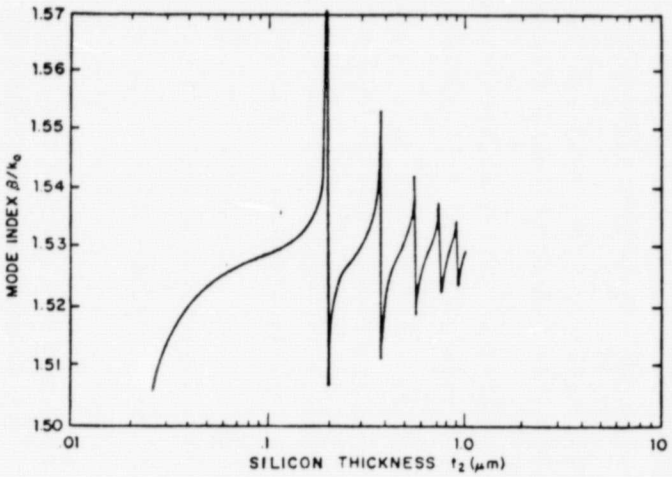

Fig. 6. Mode index characteristics of silicon waveguide (wavelength = 1150 nm).

Fig. 5. Mode index characteristics of silicon-clad waveguide (TE_0 mode, wavelength = 1150 nm).

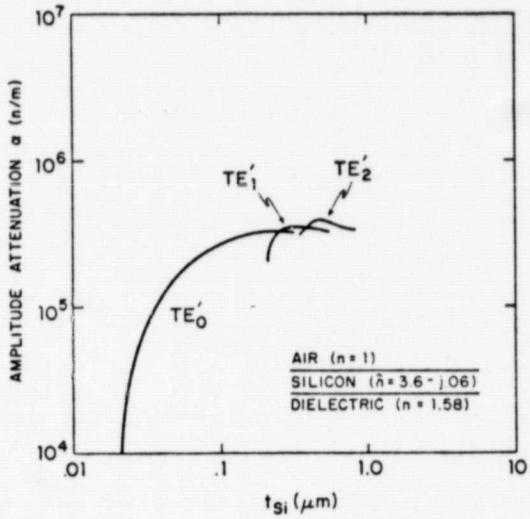

Fig. 7. Attenuation characteristics of silicon waveguide (wavelength = 1150 nm).

tween the guided mode (TE_0) in the dielectric and the lossy TE′ modes[1] of the semiconductor guide [9]. Figs. 4 and 5 show that such coupling still occurs and the amplitude of the oscillations has increased.

This coupling (or lack thereof) has a profound effect on the attenuation and phase characteristics of the original four-layer waveguide. Therefore, a partial structure consisting of a silicon guiding region surrounded by semi-infinite layers of air and dielectric was analyzed.

The mode index and attenuation constants for the first few low order TE′ modes in the silicon waveguide are shown in Figs. 6 and 7. All modes (except, perhaps the lowest order TE'_0 mode) are very lossy and the attenuation increases for the higher order modes. In Figs. 5 and 6, note that a phase match condition occurs between the TE_0 mode in the waveguide and the TE'_1 mode in the partial structure (air-silicon-dielectric) at $t_{Si} = 0.2$ μm. This phase match is present at each of the successively higher order TE′ mode cutoff thicknesses and corresponds to the respective attenuation peaks in Fig. 4 for the total structure. The sharp nulls in the attenuation curve, indicating very low coupling efficiency, occur at thicknesses midway between the cutoff value of two adjacent lossy TE′ modes. Note, however, that the first peak on the four-layer attenuation curve (Fig. 4) is considerably lower than the subsequent peaks. This behavior is unlike that of the attenuation curve presented at 632.8 nm (Fig. 2). Observe that the TE'_0 mode of the three-layer guide (Fig. 7) is reasonably low-loss, and that, although nearly complete transfer of energy between the guide and the silicon occurs for $t_{Si} = 0.25$ μm, coupling is into a low-loss mode. For the subsequent peaks on the attenuation curve (Fig. 4), coupling is into high-loss modes of the partial structure and the attenuation of the four-layer guide is thus greater. For large silicon thickness, however, the four-layer attenuation curve (Fig. 4) exponen-

[1] TE'_i denotes guided modes in the semiconductor and TE_i denotes guided modes in the dielectric.

tially approaches that of the three-layer structures previously analyzed [23], where the semiconductor layer is considered semi-infinite. Similarly, the abrupt transitions on the mode index curve of the complete structure (Fig. 5) occur when the phase match condition is satisfied and the guided waves couple into successively higher order modes of the partial structure. These results are similar to the power transfer calculations for linearly tapered directional couplers [24]-[26]. Finally, note that the period and amplitude of the attenuation characteristics of the silicon-clad guide are a function of the material permittivities for a given wavelength as Fig. 2 ($\lambda = 632.8$ nm) and Fig. 4 ($\lambda = 1150$ nm) indicate.

Calculations presented in this section demonstrate that the attenuation and mode index of the four-layer silicon clad planar dielectric waveguide behave as exponentially damped sinusoids for a wavelength of 1150 nm. The effect may be explained as a coupling between the basic TE_0 mode of the dielectric waveguide and the high loss TE′ modes of the semiconductor guide. The oscillatory behavior of the attenuation and mode index curves, a necessary prerequisite for the direct modulation of the guided beam, is still apparent and detailed calculations of a direct optical modulation scheme at 632.8 nm are presented elsewhere [9]. These calculations at 1150 nm demonstrate that the required modulation technique is still feasible without inadvertent excitation of the silicon cladding by the guided light wave.

IV. Selective Frequency Filtering

The attenuation characteristics of silicon-clad waveguides are a function of the material permittivities for a particular wavelength as Fig. 2 ($\lambda_o = 632.8$ nm) and Fig. 4 ($\lambda_o = 1150$ nm) indicate. Based on the observed change in period and amplitude of the attenuation curve oscillations as the material parameters vary with wavelength, it is evident that selective frequency filtering can be realized with a silicon-clad waveguide. In particular, for a given silicon-cladding thickness, the attenuation will vary drastically as the material permittivities vary with wavelength, and through optimization of the semiconductor cladding thickness, a particular frequency filtering response may be obtained with the clad guide. For example, note that a silicon thickness $t_{Si} = 0.10$ μm lies in a range of high attenuation ($\alpha > 10^4$ n/m) on Fig. 2 ($\lambda = 632.8$ nm), while it is in a region of low attenuation ($\alpha < 10^3$ n/m) on Fig. 4 ($\lambda = 1150$ nm). It is this effect which will be used for frequency filtering. The permittivities of all four materials (air, silicon, guide, substrate) in the planar waveguide structure of interest vary with wavelength; however amorphous silicon is particularly sensitive to frequency variations as Table I indicates [27]. The predicted frequency filtering effect is due almost solely to a change in silicon permittivity. It should be again noted that the permittivity of amorphous silicon is highly dependent upon the method of preparation.

Attenuation versus silicon thickness curves similar to those of Figs. 2 and 4 were generated as the wavelength was allowed to change from 0.35 to 1.55 μm and the permittivities of the four layers consequently varied [10], [27]. All attenuation curves retained their characteristic oscillations; however, the amplitude and period of the oscillations were significantly altered. Similarly, the mode index versus silicon thickness curves retained their characteristic oscillatory behavior although the frequency and amplitude of the oscillations changed.

TABLE I
AMORPHOUS SILICON PARAMETERS AS A FUNCTION OF WAVELENGTH

Wavelength (microns)	Refractive Index		Relative Permittivity	
	n	K	ϵ'_R	ϵ''_R
0.35	3.63	2.860	5.0	20.80
0.42	4.53	1.470	18.4	13.40
0.52	4.43	0.900	18.8	8.00
0.57	4.21	0.660	17.3	5.60
0.62	4.11	0.388	16.8	3.20
0.65	4.04	0.289	16.3	2.35
0.69	3.97	0.188	15.8	1.50
0.74	3.88	0.155	15.0	1.20
0.89	3.67	0.068	13.5	0.50
1.00	3.65	0.062	12.3	0.45
1.15	3.59	0.056	12.9	0.40
1.24	3.55	0.039	12.6	0.28
1.55	3.52	0.028	12.4	0.20

Figs. 8-10 were obtained by assuming a given silicon thickness in the four-layer planar structure and allowing the wavelength to vary (and consequently, the material permittivities). The resulting attenuation (dB) for a 1 mm wide silicon bar is plotted vertically in Figs. 8-10.

A high-pass frequency filter is realized in Fig. 8. Insertion loss is less than 7 dB for a wavelength greater than 1.0 μm for the three silicon thicknesses considered ($t_{Si} = 0.09, 0.10, 0.11$ μm), and the extinction for wavelengths less than 0.7 μm is more than 50 dB. The particular filter characteristics in the wavelength region of 0.7-1.0 μm may be adjusted by changing the thickness of the silicon cladding.

Filters with passband wavelengths of 0.7-0.9 μm are shown in Fig. 9. Note that the exact location of the passband may be varied for the three silicon thicknesses of interest ($t_{Si} = 0.15$, 0.17, 0.19 μm) and that high attenuation (>100 dB) occurs immediately outside of this passband region. Insertion loss, however, is approximately 20 dB.

Even relatively short sections of silicon-clad waveguides are lossy, and for a practical device the insertion loss must be reduced significantly. Thin dielectric buffer layers have been used to lower the attenuation losses of metal-clad dielectric waveguides [28]. These layers are placed between the dielectric core and the metal and act as buffers to remove a large portion of the field from the metal cladding. The effect of a silicon dioxide (SiO_2) buffer layer on the filter response curve was investigated. The results are shown in Fig. 10. A silicon thickness $t_{Si} = 0.13$ μm was assumed and the attenuation versus wavelength was calculated for a four-layer structure. Note that an insertion loss of approximately 40 dB is apparent in the passband region of 632.8 nm, although rapid extinction is evident (>400 dB) immediately outside of the passband region. A silicon dioxide buffer layer ($t_{Si} = 0.2$ μm) of refractive index $n = 1.46$ was then added, and the filter response curve for the five-layer structure was calculated. Insertion loss is now less than 9 dB at a wavelength of 632.8 nm while rapid extinction (>200 dB) is still evident immediately outside of this passband. Further reduction of the passband attenuation may result from optimization of the buffer layer and silicon thicknesses. Although no attempt has been made to optimize the filter characteristics, Figs. 8 and 9 indicate the low fre-

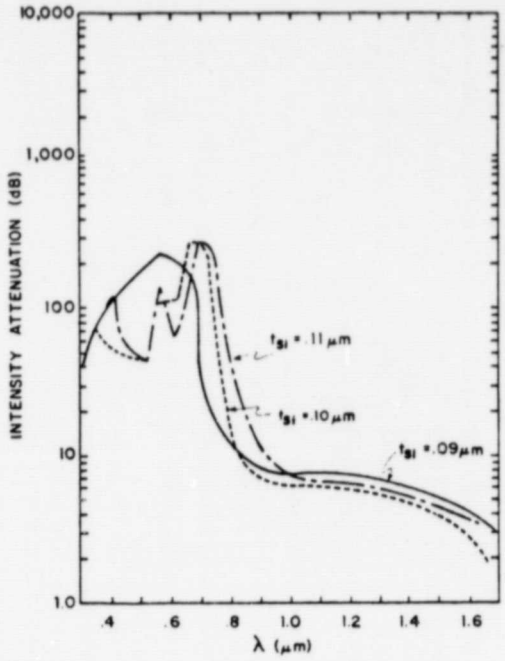

Fig. 8. Frequency response of silicon-clad waveguide (t_{Si} = 0.09, 0.10, 0.11 μm).

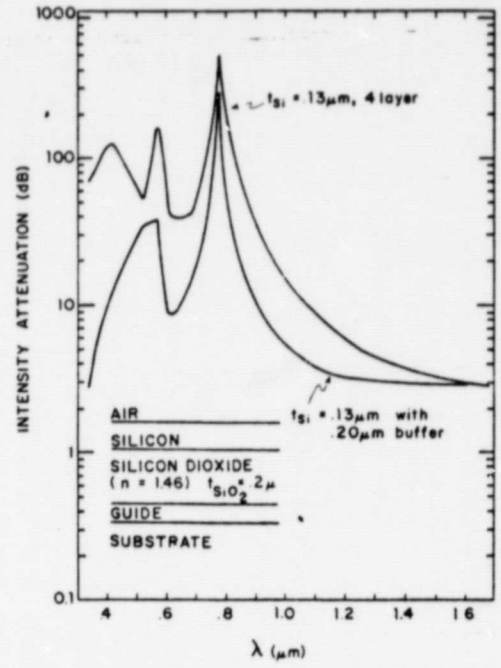

Fig. 10. Reduction in attenuation of filter with SiO_2 buffer layer (n = 1.46, t_{SiO_2} = 0.2 μm).

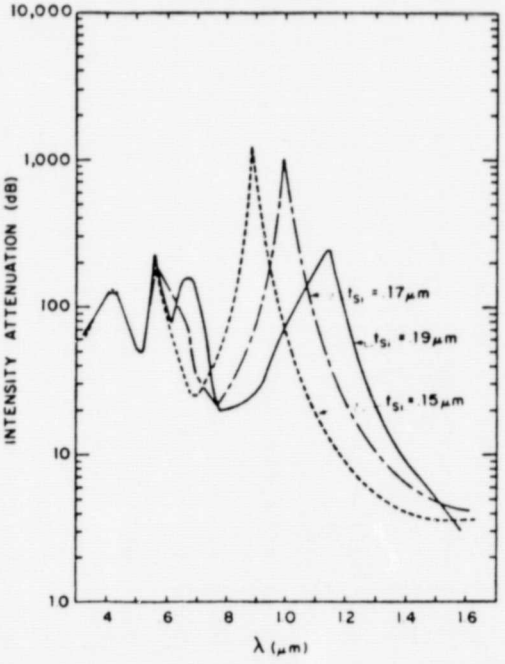

Fig. 9. Frequency response of silicon-clad waveguide (t_{Si} = 0.15, 0.17, 0.19 μm).

quency cutoff and the attenuation peaks may be adjusted by proper choice of cladding thickness.

V. Conclusions

It has been shown that planar dielectric waveguides clad with silicon exhibit a damped periodic oscillation in their attenuation and phase characteristics. The effect is due to a periodic coupling between the lossy guided modes in the silicon film and the TE_0 mode of the dielectric waveguide. Experimental confirmation of this periodic coupling for a wavelength of 632.8 nm has been achieved. Calculations for a wavelength of 1150 nm indicate that the attenuation and mode index still retain their oscillatory behavior. Thus, a direct optical modulation scheme through excitation of the silicon cladding is still applicable without inadvertent excitation of the cladding by the guided wave. The silicon-clad guide may also be used as a frequency filter, and the characteristics may be adjusted through optimization of the silicon thickness and through control of a buffer layer. Practical devices are currently being constructed to confirm their predicted characteristics.

References

[1] J. N. Polky and G. L. Mitchell, "Metal-clad planar dielectric waveguide for integrated optics," *J. Opt. Soc. Amer.*, vol. 64, pp. 274–279, Mar. 1974.

[2] S. C. Rashleigh, "Four-layer metal-clad thin film optical waveguides," *Opt. & Quantum Electron.*, vol. 8, pp. 49–60, Jan. 1976.

[3] I. P. Kaminow, W. L. Mammel, and H. P. Weber, "Metal-clad optical waveguides: Analytical and experimental study," *Appl. Opt.*, vol. 13, pp. 396–405, Feb. 1974.

[4] T. Takano and J. Hamasaki, "Propagating modes of a metal-clad dielectric-slab waveguide for integrated optics," *IEEE J. Quantum Electron.*, part II, vol. QE-8, pp. 206–212, Feb. 1972.

[5] E. M. Garmire and H. Stoll, "Propagation losses in metal-film-substrate optical waveguides," *IEEE J. Quantum Electron.*, vol. QE-8, pp. 763–766, Oct. 1972.

[6] T. E. Batchman and J. R. Peeler, "Gallium arsenide clad optical waveguides," *IEEE J. Quantum Electron.*, vol. QE-14, pp. 327–329, May 1978.

[7] C. H. Lee, P. S. Mak, and A. P. DeFonzo, "Optical control of millimeter wave propagation in dielectric waveguides," *IEEE J. Quantum Electron.*, vol. QE-16, pp. 277–288, Mar. 1980.

[8] C. H. Lee and V. K. Mathur, "Picosecond photoconductivity and its application," *IEEE J. Quantum Electron.*, vol. QE-17, pp. 2098–2112, Nov. 1981.

[9] T. E. Batchman and G. M. McWright, "Mode coupling between dielectric and semiconductor planar waveguides," *IEEE J. Quantum Electron.*, vol. QE-18, pp. 782–788, Apr. 1982.

[10] D. E. Gray, Ed., *American Institute of Physics Handbook*, 2nd ed. New York: McGraw-Hill, 1963, ch. 6, pp. 103–122.

[11] T. E. Batchman and S. C. Rashleigh, "Mode-selective properties of a metal-clad dielectric-slab waveguide for integrated optics," *IEEE J. Quantum Electron.*, vol. QE-8, pp. 848-850, Nov. 1972.

[12] R. B. Smith and G. L. Mitchell, "Calculation of complex propagating modes in arbitrary plan-layered complex dielectric structures," E. E. Tech. Rep. 206, University of Washington, National Science Foundation Grant Eng 76-09937, Dec. 1977.

[13] D. E. Carson, "Photo voltaics V: Amorphous silicon cells," *IEEE Spectrum*, pp. 39-41, Feb. 1980.

[14] D. E. Ackley and J. Tauc, "Silicon films as selective absorbers for solar energy conversion," *Appl. Opt.*, vol. 16, no. 11, pp. 2806-2809, Nov. 1977.

[15] G. Stewart, C. A. Miller, P.J.R. Laybourn, C.D.W. Wilkinson, and R. M. DeLaRue, "Planar optical waveguides formed by silver-ion migration in glass," *IEEE J. Quantum Electron.*, vol. QE-13, pp. 192-200, Apr. 1977.

[16] G. Stewart and P.J.R. Laybourn, "Fabrication of ion-exchanged optical waveguides from dilute silver nitrate melts," *IEEE J. Quantum Electron.*, vol. QE-14, pp. 930-934, Dec. 1978.

[17] T. G. Giallorenzi, E. J. West, R. Kirk, R. Ginther, and R. A. Andrews, "Optical waveguides formed by thermal migration of ions in glass," *Appl. Opt.*, vol. 12, no. 6, pp. 1240-1245, June 1973.

[18] A. Gedeon, "Formation and characteristics of graded-index optical waveguides buried in glass," *Appl. Phys.*, vol. 6, pp. 223-228, Mar. 1975.

[19] R. C. Ross and R. Messier, "Microstructure and properties of rf-sputtered amorphous hydrogenated films," *J. Appl. Phys.*, vol. 52, pp. 5329-5339, Aug. 1981.

[20] W. T. Pawlewicz, "Influence of deposition conditions on sputter-deposited amorphous silicon," *J. Appl. Phys.*, vol. 49, no. 11, pp. 5595-5600, Nov. 1978.

[21] J. C. Bruyere, A. Deneuville, A. Mini, J. Foutenilie, and R. Danielou, "Influence of hydrogen on optical properties of a-Si:H," *J. Appl. Phys.*, vol. 51, no. 4, pp. 2199-2205, Apr. 1980.

[22] M. H. Brodsky, Ed., "Amorphous semiconductors," *Topics in Appl. Physics*, vol. 36. New York: Spring-Verlag, 1979, pp. 1-7.

[23] T. E. Batchman and K. A. McMillan, "Measurement on positive-permittivity metal-clad waveguides," *IEEE J. Quantum Electron.*, vol. QE-13, pp. 187-192, Apr. 1977.

[24] A. L. Jones, "Coupling of optical fibers and scattering in fibers," *J. Opt. Soc. Amer.*, vol. 55, pp. 261-271, Mar. 1965.

[25] T. K. Lim, B. K. Garside, and J. P. Marton, "An analysis of optical waveguide tapers," *Appl. Phys.*, vol. 18, pp. 53-62, Jan. 1979.

[26] R. B. Smith, "Analytic solutions for linearly tapered directional couplers," *J. Opt. Soc. Amer.*, vol. 66, pp. 882-892, Sept. 1976.

[27] D. T. Pierce and W. E. Spicer, "Electronic structure of amorphous Si from photoemission and optical studies," *Phys. Rev. B*, vol. 5, pp. 3017-3029, Apr. 15, 1972.

[28] Y. Yamamoto, T. Kamiya and H. Yanai, "Characteristics of optical guided modes in multi-layer metal-clad planar optical guide with low-index dielectric buffer layer," *IEEE J. Quantum Electron.*, vol. QE-11, pp. 729-736, Sept. 1975.

Glen M. McWright (S'81), for a photograph and biography, see p. 788 of the April 1982 issue of this JOURNAL.

T. E. Batchman (S'61-M'66), for a photograph and biography, see p. 788 of the April 1982 issue of this JOURNAL.

M. S. Stanziano (S'79) was born in Washington, DC, on March 28, 1957. He received the B.S. degree in electrical engineering from the University of Virginia, Charlottesville, in 1980.

During the summer he has been employed with the Hazeltine Corporation, Electro-Acoustics Systems Laboratory, and with the Submarine Signal Division, Raytheon Company. He is currently completing studies towards the M.E. degree at the University of Virginia.